ISTANBUL TECHNICAL UNIVERSITY ★ GRADUATE SCHOOL OF SCIENCE ENGINEERING AND TECHNOLOGY

MODELLING OF PHYSICAL AND NUMERICAL BEHAVIORS OF UNDERSEA PE NATURAL GAS PIPES AGAINST WAVE AND CURRENT EFFECTS

Ph.D. THESIS

Uğur ÇALIŞKAN

Department of Civil Engineering

Hydraulics and Water Resources Engineering Programme

AUGUST 2014

ISTANBUL TECHNICAL UNIVERSITY ★ GRADUATE SCHOOL OF SCIENCE ENGINEERING AND TECHNOLOGY

MODELLING OF PHYSICAL AND NUMERICAL BEHAVIORS OF UNDERSEA PE NATURAL GAS PIPES AGAINST WAVE AND CURRENT EFFECTS

Ph.D. THESIS

Uğur ÇALIŞKAN
(501062504)

Department of Civil Engineering

Hydraulics and Water Resources Engineering Programme

Thesis Advisor: Prof. Dr. İlhan AVCI

AUGUST 2014

İSTANBUL TEKNİK ÜNİVERSİTESİ ★ FEN BİLİMLERİ ENSTİTÜSÜ

AKIM VE DALGA KOŞULLARI ALTINDA DENİZALTI PE DOĞALGAZ BORULARININ DAVRANIŞLARININ NÜMERİK VE FİZİKSEL MODELLENMESİ

DOKTORA TEZİ

Uğur ÇALIŞKAN
(501062504)

İnşaat Mühendisliği Anabilim Dalı

Hidrolik ve Su Kaynakları Mühendisliği Programı

Tez Danışmanı: Prof. Dr. İlhan AVCI

AĞUSTOS 2014

Uğur ÇALIŞKAN, a **Ph.D.** student of ITU **Graduate School of Science Engineering and Technology** student ID **501062504**, successfully defended the **thesis/dissertation** entitled **"Modelling of Physical and Numerical Behaviors of Undersea PE Natural Gas Pipes Against Wave and Current Effects"**, which he prepared after fulfilling the requirements specified in the associated legislations, before the jury whose signatures are below.

Thesis Advisor :	**Prof. Dr. İlhan AVCI** İstanbul Technical University	.....
Jury Members :	**Prof. Dr. Şevket ÇOKGÖR** Istanbul Technical University	.....
	Yrd. Doç. Dr. Ali UYUMAZ Istanbul Technical University	.....
	Doç. Dr. C. Melek KAZEZYILMAZ ALHAN Istanbul University	.....
	Prof. Dr. M. Emin KARAHAN Beykent University	.....

Date of Submission : 27 June 2014
Date of Defense : 27 August 2014

To my family,

FOREWORD

I would like to thank my thesis adviser Prof. Dr. İlhan AVCI for his very kind help, support and guidance in every stage of my phd study. Without Prof. Dr. İlhan AVCI's help I couldn't have completed my study.

I would like to thank my family for their support.

In this thesis and in scope of a R&D (AR-GE) project, a certain part of the preparation of test channel and supplying the PE pipes which were used in the Istanbul Technical University Civil Engineering Faculty Hydraulics Laboratory were provided and contributed by FIRAT Plastik Kaucuk San. ve Tic. A.Ş., pressurizing the test specimens in the ITU Hydraulics laboratory, test specimens and various gauge and measurement devices for "Kartal-Adalar undersea PE Natural Gas Pipeline" were provided by IGDAS; material tests for the specimens which were taken from existing Kartal-Adalar undersea pipeline and from ITU Hydraulic laboratory tests were carried out by UGETAM A.Ş. materials laboratory and in addition to these organizations, this research project was supported by Istanbul Technical University Research Fund. I would like to thank above organizations for their very kind help and support.

A certain part of the computing resources used in this study were provided by the National Center for High Performance Computing of Turkey (UYBHM) under grant number 4002032012.

August 2014

Uğur ÇALIŞKAN
(Civil Engineer, M.Sc)

TABLE OF CONTENTS

Page

ABBREVIATIONS

a : Amplitude of the motion
a : Accelaration
A : Cross section area of the body
CAE : Computer Aided Engineering
CFD : Computational Fluid Dynamics
CSD : Computational Structural Dynamics
$\mathbf{C_D}$: Drag Coefficient
$\mathbf{C_m}$: Hydrodynamic mass coefficient
$\mathbf{C_M}$: Inertia coefficient
$\mathbf{C_L}$: Lift coefficient
$\mathbf{C_{Lmax}}$: The max lift force coefficient
$\mathbf{C_{Lrms}}$: r.m.s lift force coefficient
$\mathbf{c_p}$: Pressure coefficient
CPU : Central Processing Unit
D : Diameter of the cylinder
DNS : Direct Numerical Simulation
e : Gap between cylinder and bottom wall
e/D : Gap-ratio
EN : European Norms
$\mathbf{E_0}$: Modulus of elasticity at time zero
$\mathbf{E_{50}}$: Modulus of elasticity after 50 years
$\mathbf{F_D}$: Drag force
$\mathbf{F_L}$: Lift force
$\mathbf{F_{Lmax}}$: The maximum lift force
$\mathbf{F_{Lrms}}$: r.m.s value of the lift force
$\mathbf{F_p}$: Form Drag per unit length of structure
$\mathbf{F_f}$: Friction drag per unit length of structure
FIV : Flow-Induced Vibrations
FSI : Fluid-Structure Interaction
$\mathbf{f_v}$: Vortex-shedding frequency
$\mathbf{f_w}$: Frequency
FVM : Finite Volume Methods
GPU : Graphics Processing Unit
HPC : High Performance Computing
HDPE : High Density Polyethylene
ISO : International Organization for Standardization
ν : Kinematic viscosity
KC : Keulegan-Carpenter number
LES : Large Eddy Simulation
m : Mass of body
$\mathbf{m^l}$: Hydrodynamic mass
ODE : Ordinary Differential Equation

RANS : Reynolds Averaged Navier Stokes Simulation
$\overline{\mathbf{p}}$: Pressure on the cylinder surface
PE : Polyethylene
p : Pressure
$\mathbf{p_0}$: Hydrostatic pressure
Re : Reynolds Number
St : Strouhal Number
$\mathbf{T_w}$: The period of the oscillatory flow
TS : Turkish Standarts
U : Flow velocity
$\mathbf{U_b}$: Velocity of the body in the in-line direction
$\mathbf{U_c}$: Velocity of the current
$\mathbf{U_m}$: Maximum velocity
$\dot{U}$: Flow velocity
V : Volume of cylinder
VIV : Vortex-Induced Vibrations
ν : Poisson ratio
α : Avearage coefficient of thermal expansion
ω : Angular frequency of the motion
ρ : Fluid density
$\overline{\boldsymbol{\tau}_0}$: Wall shear stress on the cylinder surface

LIST OF TABLES

Page

LIST OF FIGURES

Page

MODELLING OF PHYSICAL AND NUMERICAL BEHAVIORS OF UNDERSEA PE NATURAL GAS PIPES AGAINST WAVE AND CURRENT EFFECTS

SUMMARY

Natural gas plays an important role and an increasing use in cities because of its very unique properties as being environmentally friendly and overall sustainability concerns. Transfering natural gas from one location to another with an easy to build and cheap pipeline system is essential and especially overcoming the natural obstacles such as sea has a vital importance. Using HDPE pipes for these type of applications could be the solution to all.

Undersea pipelines and their design principles have great importance in hydrodynamics. In design of these types of engineering structures, pipe material properties, flow characteristics and fluid-structure interaction properties have key importance on the overall behavior of the system. In this study, physical and numerical behaviors of HDPE pipes were investigated in order to determine their performance in undersea natural gas pipelines. Because of the highly elastic material properties of the HDPE, the system was considered as elastic pipe with fixed supports.

The physical lab model were set up in Istanbul Technical University Civil Engineering Faculty Hydraulics lab, and by using this lab model, long term hydrodynamic tests were carried out. After completion of hydrodynamic loadings, test specimens were tested in an accredited lab. and material test results were analyzed.

The prototype model, Kartal-Adalar Undersea Natural Gas pipeline, was analyzed based on its long term performance. Pipe specimens were taken from Kartal-Adalar Natural Gas Pipeline in two different dates. Test specimens were sent to the material lab in order to perform the required tests. Material test results for pipe specimens which were taken from the prototype pipeline were investigated and their performance were evaluated.

To analyse the system numerically, relevant components of ANSYS software package were used to prepare the numerical (computer) model. ANSYS software package components (ANSYS Fluent and others) were used for modelling required part of the system and relevant solvers were used to solve the numerical model.

As a result of this study, overall properties of the such system were investigated and pipes that are made of HDPE material performance under current and wave loads were evaluated. In addition to these, usability of HDPE pipe for natural gas pipelines in undersea applications were evaluated and its performance was analyzed.

AKIM VE DALGA KOŞULLARI ALTINDA DENİZALTI PE DOĞALGAZ BORULARININ DAVRANIŞLARININ NÜMERİK VE FİZİKSEL MODELLENMESİ

ÖZET

Doğal gazın çevreye zarar vermemesi ve sürdürülebilir sistemin önemli bir parçası olması sebebiyle şehirlerde kullanımında artış gözlenmektedir. Doğal gazın merkez noktalardan diğer noktalara transferi açısından görece ucuz ve kolay imal edilebilir bir çözüm bulunması ve uygun çözüm yöntemleri ile deniz ve benzeri doğal engellerin ötesine iletilebilmesi kritik bir öneme sahiptir. HDPE boru hatlarının bu tip uygulamalarda kullanılması tüm problemlere çözüm olabilecek niteliktedir.

Denizaltı boru hatları ve bu hatların tasarım prensipleri hidrodinamik bilim dalı açısından son derece önemlidir. Bu tip mühendislik yapılarının tasarımında, boru hattının yapımında kullanılan boruların malzeme özellikleri, akım karakteristikleri ve yapı-akışkan etkileşimi tüm sistemin davranışının anlaşılması açısından anahtar bir öneme sahiptir. Bu çalışma içerisinde kullanılan boruların PE boru olması nedeniyle, tüm sistem mesnetlerden ankastre bağlanmış olan elastik boru sistemi olarak alınmıştır.

Bu çalışmada, farklı akım ve dalga koşulları altında denizaltı PE boru hatlarının davranışları, fiziksel ve nümerik olarak incelenmiştir. Ayrıca, bu çalışma için prototip boru hattı olan Kartal-Adalar Denizaltı Doğal Gaz boru hattı incelenmiş ve uzun süreli hidrodinamik yüklemeler karşısındaki davranışı analiz edilmiştir.

Bu çalışma temel olarak 3 parçadan oluşmaktadır. Bunlar, fiziksel laboratuvar modelleri, prototip model ve nümerik (bilgisayar) modelleridir.

Fiziksel laboratuvar modeli İstanbul Teknik Üniversitesi İnşaat Fakültesi Hidrolik laboratuvarı içerisinde hazırlanmıştır. Bu laboratuvar modelinde uzun süreli hidrodinamik testlerin etkitilmesi için boru örnekleri deney düzeneğine yerleştirilerek akım ve dalga yüklemeleri yapılmıştır.

Sistem içerisinde farklı çapta borular ayrı ayrı deney düzeneğine yerleştirilerek hidrodinamik yüklemeler yapılmıştır. Farklı çapta borular için, ilgili boru çapı için belirlenmiş olan mesnet açıklığı kullanılmıştır. PE 80 ve PE 100 serisi borular için deneyler ayrı ayrı yapılmıştır.

Fiziksel deneylerde, akım, dalga ve akım + dalga koşulları sisteme uygulanmıştır. Bu deneylerde, her bir deney koşulu için, hidrodinamik yüklemeler 6 hafta boyunca yaklaşık olarak günlük 7 saat süresince sisteme uygulanmıştır.

Hidrodinamik yükleme testleri tamamlandıktan sonra, test sistemi uzerinden boru örnekleri alınarak akredite malzeme laboratuvarına gönderilmek suretiyle malzeme testleri yapılmış ve malzeme laboratuvarından gelen test sonuçları analiz edilmiştir.

Prototip model olarak Kartal-Adalar Denizaltı Doğal Gaz boru hattı incelenmiştir. Bu boru hattı İGDAŞ tarafından 2006 yılında projelendirilmiş ve yapılmış olan yaklaşık olarak 4000 m uzunluğunda bir boru hattıdır. Kartal-Adalar Denizaltı Doğal Gaz boru hattı, uzun süreli performans kriterleri gözönünde bulundurularak analiz edilmiştir. Kartal-Adalar Doğal Gaz Boru hattı üzerinden 2 ayrı zaman diliminde boru örnekleri alınmıştır. Alınan bu örnekler malzeme laboratuvarına gönderilerek ilgili malzeme testleri yapılmıştır. Bu boru hattından alınan boru örneklerinin malzeme test sonucları incelenmiş ve bu örneklerin performansları değerlendirilmiştir.

Sistemin nümerik (bilgisayar) modelleri ANSYS paket programının bileşenleri kullanılarak hazırlanmıştır. Akışkan modellemesi, CFD analizi ve diğer sistem bileşenlerinin modellenmesinde ilgili program bileşenleri (ANSYS Fluent ve diğer) ve çözüm elemanları, nümerik modelin hazırlanması ve çözülmesi aşamalarında kullanılmıştır.

Nümerik modeller için, öncelikle sistemin geometrik modeli oluşturulmuştur. Bu geometrik modelde, akışkan hacmi tanımlanmış ve boru yapısı bu akışkan hacmi içerisinde her iki ucundan ankastre mesnetli olacak sekilde tanımlanmıştır. Borunun dış yüzeyi yapı-akışkan etkileşim yüzeyi olarak tanımlanmıştır.

Nümerik modeller hazırlanırken sistemin elastik özelliklerini yansıtacak şekilde uygun model elemanları seçilmiş ve yapı-akışkan etkileşiminin yansıtılması sağlanmıştır. Hazırlanmış olan bu sistemlerde, hidrodinamik etkiler nedeniyle oluşan yükler yapı sistemine iletilip, bu yükler altında yapı sisteminde oluşan yer değiştirmeler akışkan sistemine iletilerek akışkan hacminin ağ yapısı dinamik olarak tekrar düzenlenmek suretiyle sistemin belirlenen iterasyon sayısı altında çözüm yapması sağlanmıştır.

Hazırlanmış olan çalışmada, ilgili sistem için 3 kısımda (fiziksel laboratuvar modelleri, prototip model ve nümerik modeller) inceleme yapılmış ve sonuçlar analiz edilmiştir. Bu çalışmamız, hazırlamış olduğumuz modeller sistemin nümerik ve fiziksel özelliklerini başarıyla analiz etmemizi sağlamıştır.

Fiziksel modellerde kullandığımız farklı çap ve mesnek açıklığındaki boru sistemi örnekleri benzer sonuçlar vermiş olup birbirine uyumlu sonuçlar ortaya çıkmıştır.

Çalışmamıza konu olan sistemin nümerik modellemesinde karşılaşılacak en büyük zorluklardan bir tanesi yapı-akışkan etkileşiminin eksiksiz olarak modellere yansıtılmasıdır. Hazırlamış olduğumuz nümerik modeller, sistem içerisinde yapı ve akışkan bileşenlerinin uyumlu şekilde çözüm yapmasını sağlamıştır. Sonuçlar kullanılarak hazırlanmış olan grafik ve diyagramlar sistemin temel akım ve yapı koşullarını ifade edebildiğini göstermiştir.

Prototip boru hattı sisteminin (Kartal-Adalar Doğal Gaz boru hattı) uzun süreli hidrodinamik yükler altındaki davranışının analizi başarıyla tamamlanmıştır. İki ayrı tarihte (2008 ve 2010) alınmış olan boru numuneleri sistemin performansını anlamak açısından yeterli bilgiyi sunmaktadır. İki ayrı derinlikten alınan (9 m ve 15 m) numunelerin malzeme dayanıklılık test sonuçları benzer doğrultuda yönelim göstermektedir.

Fiziksel laboratuvar modellerinden ve prototip sistemden alınan numunelerin malzeme test sonuçları, şartnamelerde tanımlanmış olan kabul edilen minimum değerlerden daha yüksek çıkmıştır. Normal şartlarda PE malzeme için kopma-uzama değerleri zaman içerisinde azalan bir yönelim izlemektedir. İlave olarak gelen

hidrodinamik yükler altında da bu azalma değerlerine ilave etkiler olduğu belirlenmiştir. Analizler sonucunda kopma-uzama değerleri şartnamelerde belirlenen minimum istenen değerlerden yüksek çıkmıştır.

Bu çalışmayı oluşturan 3 ana kısım (fiziksel modeller, nümerik modeller ve prototip sistem) birbirini tamamlayıcı niteliktedir. İncelenen sistemin davranışını tam olarak anlayabilmek için 3 kısım birarada kullanılmalı ve değerlendirilmelidir.

Bu çalışmanın sonucunda, boru hattı sisteminin temel özellikleri incelenmiş ve HDPE tipi malzemelerden imal edilen boruların akıntı ve dalga koşulları altındaki performansları değerlendirilmiştir. Bu konulara ek olarak HDPE boruların doğalgaz iletim boru hatlarının deniz altı geçişleri açısından performansları ve kullanılabilirlikleri değerlendirilmiştir.

1. INTRODUCTION

Undersea pipelines (also known as submarine, subsea, marine or offshore pipeline) are pipelines that are laid on the seabed or below it inside a trench. Undersea pipelines are used to carry gas, water or oil.

The pipeline characteristics depends on the medium which the pipeline is designed to transport and pipe material. Pipe material might be steel or composite material such as PE (polyethylene, HDPE, high-density polyethylene).

PE (Polyethylene) material is commonly used and recognized thermoplastic material. This material was discovered in 1930s and after then, it is used for different purposes and in different application areas. PE pipes have very broad range of applications and their application areas continue to grow in recent years. Because of their beneficial properties, more and more new application areas are added to the list. Having highly elastically material properties, modeling flow around undersea PE pipes requires a bit more attention than conventional flow around cylindrical structure problems. It is necessary to model these types of pipe systems to represent their highly elastical material properties and their possible behavior against hydrodynamics loads and effects.

In design phase of any project, designers and project owners try to find materials which provide reliability, usability in the long term, easily serviceability and cost-effectiveness. For pipe systems, PE pipes provide all these aforementioned properties and in addition to them, they provide relatively easy construction and installation process.

Some of the specific benefits of PE pipes are follows (PPI, 2005);

- Life cycle cost savings
- Lightweight
- Flexibility
- Leak free, fully restrained joints

- Corrosion resistance
- Chemical resistance
- High tensile resistance
- Fatigue resistance
- Seismic resistance
- Construction advantages
- Durability
- Hydraulically efficiency
- Temperature resistance
- Ductility
- Not affected by marine ecosystem.

Briefly, PE pipes are durable, tough, flexible, providing important performance advantages and relatively easy to construct. These advantages have great importances in real world engineering problems.

Polyethylene material has numerous use areas. Below list highlights main application areas of PE pipes:

- Chemical resistant piping systems
- Water pipes (for domestic water supply and agricultural uses)
- Corrosion protection for steel pipelines
- Natural Gas pipelines
- Plastic bags, bottles and similar items
- Telecom ducts
- Electrical and plumbing boxes
- Storage sheds
- Pressurized air pipelines
- Waste water disposal pipelines

HDPE material's density ranges from 0.93 to 0.97 g/cm^3. In spite of the fact that, the density of HDPE is only marginally higher than the ordinary polyethylene, HDPE material has little branching and this gives it stronger intermolecular forces and tensile strength.

In this research, PE and HDPE terms have been used interchangeably and both are referring to the high-density polyethylene material.

Table 1.1 briefly listed common engineering properties of the HDPE material.

Table 1.1: Common engineering properties of HDPE material.

Property		Unit	PE 80	PE 100
Density	ρ	kg/m^3	950	960
Modulus of elasticity at time zero	E_0	MPa	800	1050
Modulus of elasticity after 50 years	E_{50}	MPa	150	200
Elongation at yield		%	10	10
Elongation at break		%	>350	>350
Tensile strength at Yield		N/mm^2	21	24-25
Tensile strength at break		N/mm^2	30-33	37
Poisson ratio	ν		0.4-0.5	0.4-0.5
Average coefficient of thermal expansion	α	°C^{-1}	0.2 x 10^{-3}	0.2 x 10^{-3}
Oxidation Induction Time		Min	>20	>20
Temperature range		°C	-40 to 80	-40 to 80

There are numerous examples of HDPE usage in different areas and Figure 1.1 shows submerging process of PE submarine pipeline.

Energy is one of the main concerns in recent years. One of the usable sources of energy is natural gas. Moreover, natural gas plays an important role and has increasing use in large cities in Turkey because of environmental, economical and sustainability concerns. Natural gas should be transported with high care due to its dangerous material classification and important problems occur in the sea crossing cases for pipelines. The construction, maintenance and repair of classical steel pipes are expensive, difficult and require special techniques and long time. Because of aforementioned reasons, investigating economical and practical methods for supplying natural gas is a very important necessity.

Figure 1.1 : During submerging process of PE submarine pipeline (Pipelife Norge, 2002).

In this content, as a transportation medium, PE pipe systems could be used for natural gas pipelines. Natural gas is a practical energy source for residential and medium level industrial areas. For constructing supply lines in sea crossings more easily, PE pipes could be used, however, in this situation, it is very important to understand the physical behaviors of these pipes against flow effects.

To present day, there are limited number of projects that used PE pipes for sea crossings. One of the example projects is "Kartal-Adalar natural gas pipeline" project, which was constructed in 2006. This project was planned and constructed by IGDAS (Istanbul Gas Distribution Industry and Trade Incorporated Company). This particular project serves as prototype in our study.

Undersea pipelines and their engineering design principles have great importance in hydrodynamics. Flow around undersea pipe networks have been studied by many researchers and have been investigated in different perspectives. In these researches, in most of them main objective was to find out stability problems of pipes and near range local changes (scouring and deposit) on the bottom.

In these types of problems (flow around bodies, for example cylindrical structure, pipe lines), the system can be assumed as rigid with fix supported, rigid with elastic supported or elastic with fix supported based on system's configuration or the materials which are used. In most situations, pipes can be assumed as rigid bodies so

system can be modeled as rigid cylinder with fix or elastic supports. To use these configurations, the pipe or structure material should be suitable. The main material should not deform under given loads and should maintain its shape. If the pipe's material has highly elastical properties such as PE, the pipe should be taken as elastic structure and it should be modeled to represent its elastical properties in order to model the overall system correctly.

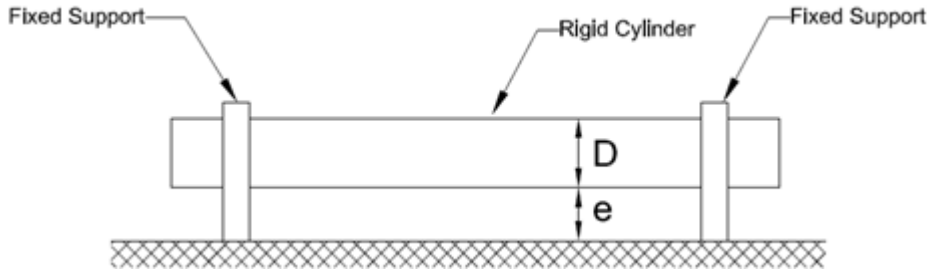

Figure 1.2 : Schematic representation of rigid cylinder with fixed supports.

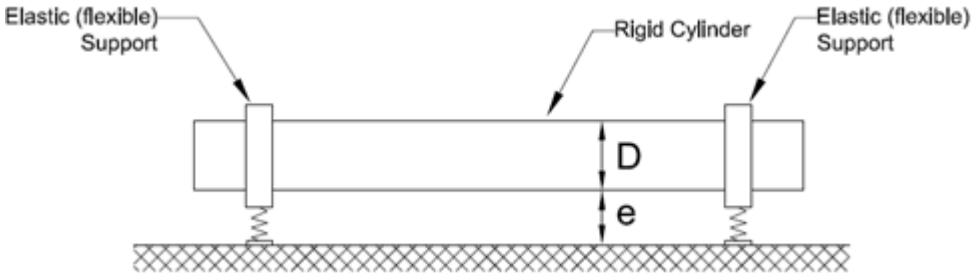

Figure 1.3 : Schematic representation of rigid cylinder with elastic supports.

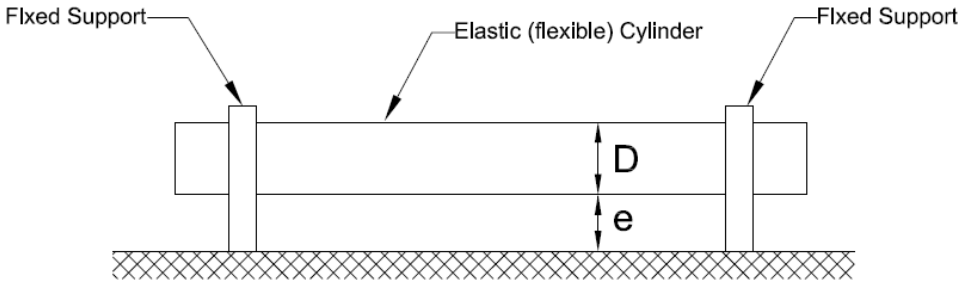

Figure 1.4 : Schematic representation of elastic cylinder with fixed supports.

To understand the flow effects around PE pipes, physical and numerical models should be prepared and carefully investigated. In numerical models because of the elastical properties of PE material, system needs to be prepared as elastical pipes with fix supports and Fluid – Structure Interaction should be taken into account. In addition, to represent Fluid – Structure Interaction correctly and accurately the prepared model should be a fully coupled one.

1.1 Literature Review

In hydrodynamics, flow around basic shapes (primitive shapes such as cylinder, rectangular etc.) are used for as a reference system and base point for more complex shapes and situations. Moreover, flow around cylindrical structures is a well-known and deeply researched subject in last decades. However, most of the studies investigated flow around rigid bodies and flow around elastically supported rigid bodies. In recent years, flow around elastic structures has attracted many researchers. Flow around elastic cylindrical elements (beams, pipes etc.) is a very important research field due to its primitive shape. To understand physical behaviors of these systems, analyses should be carried out in hydrodynamic and structural perspective all together.

In researches, main focus areas are "Flow around Cylindrical Structures", "Fluid-Structure Interaction", "Flow-Induced Vibrations (Vortex-Induced Vibrations)" and "Computational Fluid Dynamics Models".

1.1.1 Flow induced vibrations (vortex induced vibrations)

Flow-Induced Vibrations (Vortex-Induced Vibrations) is one of the fundamental engineering problems. Many engineering disciplines are studying this subject in order to understand their systems. In this particular field, there are many researches.

Williamson and Govardhan (2008) reviewed the recent result in vortex-induced vibrations research area. In their review, they summarized fundamental results and discoveries concerning vortex-induced vibrations. Wu et al. (2012) also reviewed the recent studies on vortex-induced vibrations of long slender cylinders. They gave a brief outline of numerical methods used in VIV of long slender cylinders research fields.

Gabbai and Benaroya (2005) reviewed the literature on the mathematical models used to investigate vortex-induced vibration (VIV) of circular cylinders. In their study, Wake-oscillator models, single-degree-of freedom, force decomposition models, and some other modeling techniques and approaches were studied and explained in some degree of detail. They also gave an overview of numerical methods used in solving the fully coupled fluid-structure interaction problems briefly.

Bearman (2011) reviewed the recent researches on vortex-induced vibrations of isolated circular cylinders. As a result, they concluded that, the response of a flexible cylinder with a low product of mass ratio and damping was highly susceptible to Reynolds number changes.

We can classified researches, which cover Vortex Induced Vibration behavior of the cylindrical or similar structures, as experimental or numerical based on their methodologies. We present important researches in Vortex Induced Vibration behavior of the cylindrical or similar structures in following paragraphs.

Khalak and Williamson (1999) experimentally investigated vortex-induced vibrations at low mass damping. Experiments in during their research showed that two distinct type of response of an elastically mounted rigid cylinder exists.

Elastic circular cylinder's vortex-induced vibrations were studied by Zhou et al. (1999) numerically. They chose the Reynolds number as 200 for all calculations in their research. Their results showed that fluid damping is responsible for a limit-cycle oscillation behavior. They obtained reasonable agreement with previous experimental computational data.

Wang and Zhou (2005) studied Vortex-Induced vibration characteristics of an elastic square cylinder experimentally. In their study, elastic square cylinder were fixed supported at both ends and they were in a uniform cross flow. They concluded that, when the vortex-shedding frequency coincides with the third-mode natural frequency of the fluid-structure system, a violant vibration occurs.

Cheng et al. (2006) experimentally studied on the closed-loop control of the vortex induced vibrations of a flexible square cylinder. They fixed the cylinder at both ends and placed them in a setup that only cross-flow effects existed. They found that the control effect altered the nature of the fluid-structure interactions, changing the in-phased fluid-structure synchronization into anti-phased interactions. Because of that effect, the damping of the fluid-structure system significantly enhances and it effects vortex shedding and structural vibrations.

Bourdier and Chaplin (2012) experimentally investigated vortex-induced vibrations of a rigid cylinder on elastic supports. Blevins (2009) modeled vortex-induced vibration of cylinders. Someya et al. (2010) studied flow-induced oscillating cylinders that have two degree-of-freedom experimentally.

Pasto (2008) experimentally investigated vortex-induced vibrations of a circular cylinder in laminar and turbulent flows. In his study, he carried out various wind tunnel tests. As a result, he concluded that, both mass-damping parameter and Reynolds number play important roles influencing the response.

Lin and Yu (2005) carried out an experimental study, which is about cross-flow vibration of a flexible cylinder in cylinder arrays. In their experiment, they monitored cylinder equipped with two accelerometers and was flexibly mounted in a water tunnel, surrounded by one to six identical cylinders elastically mounted in rotated triangular pattern. As a result, they found that if the monitored cylinder having different natural frequency from the surrounding cylinders, the difference between natural frequencies of the cylinders has insignificant effects on the critical velocity, and on the other hand, they have strong influence on the vibration amplitude above the critical velocity.

Zhu et al. (1995) investigated vortex-induced vibrations of an elastic circular cylinder in the wake of another circular cylinder. In their study, fluid damping and fluid stiffness coefficients for cylinder in the wake of another one were measured. They found that their technique was sufficient for characterization of the fluid effects for cylinders in the wake of another one. In their study, they also explained flow-induced vibration effects of elastic cylinder in some detail.

Someya et al. (2010) investigated flow induced oscillating cylinder with two-degrees-of-freedom experimentally. They analyzed the flow by using image-processing techniques and PIV technique to obtain the velocity field. Inline vibrations of the cylinder and cross flow direction vibration of the cylinder were analyzed separately. They found that these vibrations were anisotropic, and the anisotropy was not dependent of the diameter of the cylinder, the reduced dumping factor and the blockage ratio.

Okajima et al. (2007) studied flow induced streamwise oscillation experimentally. They used two cylinders in tandem arrangement in their experimental setup and they carried out the tests in a wind tunnel. They mounted one of the cylinders in the experimental setup as elastically supported and that cylinder could move in the flow direction elastically. The second cylinder in the arrangement was mounted to the

system as fixed supported. They used smoke-wire method to visualize the flow around cylinders.

So et al. (2000) investigated free vibrations of an elastic cylinder in a cross flow and its potential effects on the near wake experimentally. They used different velocities in the experimental setup. They concluded that, cylinder vibrations had little or no effect on the mean drag and the normalized mean field. On the other hand, they quoted that cylinder vibrations enhance turbulent mixing, and this causes substantial increase in the turbulent intensities.

So et al. (2008) experimentally investigated the effect of free-stream turbulence on vortex-induced vibration of an elastic cylinder in a cross-flow and the associated fluid forces. The chosen range of Reynolds number was 5000-41000. As a result, they concluded that, free-stream turbulence feeds energy to the cylinder as energy analysis showed, and the increment of the energy of the cylinder reaches its maximum at the lock-in point. Therefore, when at the approach flow is turbulent, the lock in region is main concern.

Nishihara et al. (2005) investigated characteristics of fluid forces and wake patterns of circular cylinders (which were in the streamwise direction) in a cross flow experimentally. They used subcritical Reynolds numbers. Their results agreed with previous studies and reduced-ranges with negative added damping exist. They also noted that the added mass coefficient varies greatly, depending on the reduced velocity, and gradually decreases as the reduced velocity increases.

Wang et al. (2003) investigated vortex-induced vibrations of two side-by-side elastic cylinders. In their research, they placed the cylinders as fixed at both ends. They investigated them in cross-flow experimentally using fiber-optic Bragg grating sensors. They examined interrelationships between the vortical structures that were generated by the two cylinders. They concluded that the combined systems (fluid-cylinders) natural frequencies, associated with each cylinder, might exhibit some differences (up to 5%).

Bando and Otsuka (2008) tried to estimate hydrodynamic forces on an irregularly oscillating cylinder in their research. They used a symmetrical vortices model to achieve their research objectives. Their results demonstrated that, vortex formations are independent of both previous and present KC numbers, is possible to give these

as a function (which has the parameter as displacement of each swing). They also noted that, their results and the results of force measurements agreed.

Galvao et al. (2008) studied on employing passive flow control using two-dimensional hydrofoils to reduce vortex-induced vibrations and drag on a cylinder of circular cross-section experimentally. They concluded that, properly positioned foils could significantly alter the flow around a circular cylinder to eliminate vortex-induced vibrations and reduce drag.

Kang and Jia (2013) was performed an experimentally study on vortex induced vibrations of a horizontal cylinder with two degrees for freedom. Their sample was 5 cm in diameter and had a 120 cm in length. Their experimental model was composed of a cylinder model and a VIV experimental apparatus. The cylinder was PVC plastic. They concluded that the vibration of the cylinder in in-line direction appeared to be multi-frequency. They also found that, the various forms of cylinder's vortex vibration trajectories depended primarily on the combination of natural vibration frequency and reduced velocity.

Pham et al. (2010) numerically studied the two dimensional laminar flow past a circular cylinder to oscillate transverse to the free-stream. They performed their simulations for various range of cylinder oscillation frequencies (0.8 to 1.2). They concluded that when the exciting frequency exceeds the natural vortex shedding frequency, the secondary vortex shedding frequency appeared with the value less than the natural shedding frequency.

Zhao et al. (2012) investigated vortex-induced vibration of a circular cylinder in transverse direction in oscillatory flow numerically. They used a one-degree-of-freedom system in their research. They studied variation of amplitudes and frequencies of the vibration with reduced velocities. In their research, they chose KC numbers in range of 10 to 20. Their one the most notable conclusion was that the vibrations were in single-frequency mode if the reduced velocity was smaller than 3 for both KC=10 and 20.

Wanderley et al. (2008) investigated vortex-induced vibration of an elastically mounted circular cylinder and they tried to predict amplitudes of the VIV oscillations. In their investigation, they used k-ε turbulence model to simulate the turbulent flow. They concluded that, numerical results for the fixed cylinder agreed

well with previous studies and numerical formulations were able to capture the amplitudes of oscillation and vortex shedding modes of elastically mounted cylinder.

Xie et al. (2011) investigated vortex-induced vibrations of a flexible cylinder at a constant Reynolds number of 1000. They used moving meshes technique (with finite volume method as an application domain) and Euler-Bernoulli beam theory to model the dynamic behavior and responses of the structure (the flexible cylinder). They confirmed that reduced velocity and the amplitude response relationships agreed well with experimental results. In addition, they concluded that, vortex patterns comparison for five vibrating modes (which they observed in their study) showed that three-dimensional wake patterns were able to alter greatly. In addition to that, vortical intensities in the wake were associated to the vibrating modes.

Sha (2008) studied vortex induced vibration of finned cylinders at low Reynolds number (Re = 50 – 200). They modeled cylinders as a mass spring system in fluid flow. They analyzed vortex structures and response amplitudes with different arrangements of pins. They found that when compare with bare cylinder, Triangle60 fins and Quadrangle45 fins response amplitude had remarkable decreases.

Bollo and Baranyi (2011) studied on two-dimensional flow around a circular cylinder that oscillated in one of two directions (in-line or transverse directions) or following an orbital path. They carried out their investigation for Reynolds number of 140. Their findings showed that computational methods they use (two different methods) had similar results for in-line, transverse and orbital cylinder motions.

Zhang et al. (2009) studied on numerical simulation of vortex-induced vibration of a two dimensional elastic circular cylinder with the two degree of freedom, and it was under uniform flow with Reynolds number was chosen as 200. They concluded that similar trends in characteristics between the results of the one degree of freedom cylinder model and the streamwise vibrations had certain effects on the lateral vibrations.

Mittal and Kumar (2001) studied light circular cylinder's flow-induced vibration characteristics at Reynolds number ranging from 10e3 to 10e4. In their research, fluid-structure interaction shows a significant dependence on the Reynolds number. They also observed several mechanisms of the non-linear oscillator for self-limiting its vibration amplitude.

Zhao et al. (2013) performed a study on vortex-induced vibrations of a circular cylinder under combined effects of steady and oscillatory flow. They investigated numerically by solving the two-dimensional Reynolds-Averaged Navier-Stokes equations. Their focus was on investigating the flow ratio, which is percentage of the steady flow velocity component in the total fluid velocity. They concluded that, the lock-in regime in the combined steady and oscillatory flow is wider than both the one in the pure steady flow and the one in the pure oscillatory flow.

Some researchers studied vortex-induced vibrations of Euler-Bernoulli beams. Wang et al. (2001) investigated flow-induced vibration of a fixed-fixed elastic cylinder. They considered a large aspect ratio (≈58). They modeled structural vibration with Euler-Bernoulli beam theory. They compared their finding with experimental measurements and discrete-parameter model. Their findings mainly correlated the compared systems. So and Wang (2003) studied vortex induced vibrations of two side-by-side beams in cross flow numerically. Their results had a good agreement with experimental measurements and another numerical study.

Yamamoto et al. (2004) studied the hydroelastic interactions that take place between oscillating flexible cylinders and fluid forces. In their research, cylinders were subject to currents and shear flows. They estimated the hydrodynamic forces with using discrete vortex method. They concluded that, for shear flows quasi-steady theory gave a very good agreement. Moreover, they noted that lagrangian scheme for the calculation of hydrodynamic force was efficient.

Huera Huarte et al (2006) investigated force distribution along the axis of a flexible cylinder. They investigated the cylinders under multimode vortex induced vibrations effects. The Reynolds number was between 2800 and 28000. They concluded that with large cross flow responded the drag distributions along the riser to be quite variable; on the other hand, it was in contrary to low cross-flow responses.

Huera-Huarte and Bearman (2009) investigated vortex-induced vibrations of a long flexible cylinder and wake structures in their research. In their experimental model, they used cylinder with 16 mm in external diameter and 1.5 m in total length and it was pin jointed. They chose Reynolds number as 1200 to 12000. They observed that when the lowest tensions were applied to the model, its dynamic response was very similar to rigid body's responses. On the other hand, as the tension increase, it started

to behave like cable or a tension dominated structure. Another finding of their result was that, vortex modes in the wake of the oscillating cylinder to be dependent on the amplitude distribution along the length of the model.

Zhao and Cheng (2011) studied vortex induced vibrations of a circular cylinder close to a plane boundary numerically. The cylinder they modeled had two-degree-of-freedom and they used k-ε turbulence model for simulating turbulent flow around cylinders. They investigated to gap ratios (e/D) and these ratios were between 0.002 and 0.3. They chose Reynolds number ranging from 1000 to 15000. As a result, they concluded that vortex induced vibrations occurred even if the initial gap ratio was as small as e/D=0.002. In addition, they noted that, initial condition of current velocity had an effect on VIV and the resonance range for increasing velocity initial condition was wider than constant velocity initial condition.

Srinil et al. (2013) performed an experimental and numerical investigation on circular cylinder's VIV characteristics under variable natural frequency ratios. They used a mechanical spring-cylinder system to achieve a low equivalent mass ratio in both in-line and cross-flow directions. In their system, they placed the cylinder vertically. They found good qualitative agreements between numerical and experimental models.

1.1.2 Flow around cylinders and their modelling techniques

Modelling flow around cylindrical or similar structures numerically is crucial for finding optimized solutions for engineering problems in hydrodynamics and related disciplines. Many researchers studied in these problems and possible design techniques.

In such a complex system like flow around cylinder or similar immersed bodies, computer models and simulations demand high amount of computer resources (computational resources). In the case of elastic cylinders and flow around them, total required computational resources are relatively higher than rigid models.

With the recent developments in computer technologies, especially in areas such as CPU, GPU, parallel programming and HPC, numerical research projects that are about flow around elastically deformed structures are more feasible then before.

These types of structures and flow around them can be modelled numerically by using different computational approaches. It is possible to use commercial CFD packages or in-house numerical algorithm (mainly in DNS (Direct Numerical Simulation)) to prepare numerical models.

Blackburn and Henderson (1999) investigated flow around oscillating cylinder in two-dimension. Their main objective was to study the effect of variations in frequency ratio F on entrainment phenomena produced by forced cross-flow oscillation within the primary synchronization regime. Their simulation was for Re=500 and a fixed motion amplitude for 0.25. They used spectral element discretization with second-order time-splitting scheme in order to solve the two dimensional incompressible Navier-Stokes equations. Their research showed that phase-switching behavior observed in number of experiments, and demonstrated that the switch was associated with a change in sign of mechanical energy transfer between the cylinder and the flow.

Dong and Karniadakis (2005) investigated direct numerical simulations (DNS) of flow past stationary and oscillating cylinders at specific Re number value. Their research successfully captured the flow physical quantities such as drag and lift coefficients, and the statistics of cylinder wake reasonably well. They also showed that high order based DNS is an effective tool for studying the VIV phenomena at close realistic values of Reynolds Number.

Evangelinos et al. (2000) investigated turbulent flow past rigid and flexible cylinders subject to vortex-induced vibrations and use direct numerical simulation (DNS) based on spectral method to simulate them. All simulations were performed at Re=1000. They presented their DNS results very clearly to help other researchers.

Baranyi et al. (2010) studied flow around a cylinder forced to oscillate in line with the main flow. They considered relatively low-Reynolds numbers, Re=60-350 (they used nine Reynolds number in that range) and two different frequency ratios in their research. They carried out computations in this study using tested finite-difference code and they compared some of the results with a commercial CFD code.

Fluid damping is another important concept in hydrodynamics. Zhou and So (2000) studied fluid damping of an elastic cylinder in a cross flow. They used a numerical technique and ARMA (auto-regressive moving-average) technique. Zhang et al.

(2003), also studied on fluid damping of an elastic cylinder in a cross flow. Their study was an experimental one and they studied of a long slender cylinder with fixed at both ends. Their experimental research results showed that fluid damping values varied significantly at resonance when the vortex-shedding frequency coincided with one of the natural frequencies of the fluid-structure system.

So et al. (2003) studied a numerical technique for mesh shape preservation. They described a technique that could prevent the mesh from severe distortion in flow induced vibration calculations. They compared the predictions between with or without mesh prevention. They concluded that mean transverse displacements of the cylinder could be 25% larger between these two systems.

Hemon and Santi (2002) investigated aeroelastic behavior of rectangular cylinders in cross flow. Their investigation was both experimental and numerical. The experiments were performed with flexible rectangular cylinder clamped at both ends. As a result of their study, they mainly concluded that, comparison between the static case and forced oscillations, in the galloping range, the secondary vortices inside the shear layer became symmetrical and their effects on the forces was cancelled.

Lau (2004) investigated elastic airfoil's flow induced vibrations, which were caused by upstream cylinder at a Reynolds number of 10000. They used laser vibrometer to measure the bending and torsional vibration displacements at the mid-span of the airfoil and the cylinder. They used dimensionless gap size (which was between two structures) as a governing parameter. They concluded that assuming the structures in any fluid-structure interaction problem to be rigid was not appropriate regardless of their stiffness degree.

Baranyi et al. (2010) studied on low Reynolds number flow around a cylinder forced to oscillate in-line. They used Reynolds number as 60 to 350. Moreover, they did computations for two frequency ratios for 0.8 and 0.9. Their analysis provided details on the transition of the dominant wake modes in response to the symmetry bifurcation underlying the vortex switches observed in the simulations.

In flow around a cylindrical structure type of problems, cylinder position respect to wall (or canal bed) is important as well. Dipankar and Sengupta (2005) investigated flow past a stationary cylinder in the vicinity of wall. They used two different gap ratios, and studied flow characteristics and their changes in these two gap ratios.

Shah and Lu (2008) numerically investigated oscillating flow past a circular cylinder in the vicinity of a plane wall. Their investigation was two-dimensional and they investigated gap ratio (between cylinder surface and the wall) on the flow behavior. They concluded that, for gap ratio smaller than or equal to 0.25, the periodicity in the flow is attributed to both the outer shear layer and the oscillating frequency, for gap ratio greater than 0.25, there was proper vortex shedding in the flow and the periodicity in the flow was mainly due to mean flow.

Presence of a free surface is also important for some cases. Carberry et al. (2001) studied the effect of a free surface for both stationary and oscillating cylinders. They concluded that for both the stationary and oscillating cylinders, the wake to become non-symmetric because of presence of the free surface and a net negative lift force on the cylinder occurs.

Sumner (2010) reviewed current understandings of the flow around two circular cylinders in cross flow. They summarized the literature on the flow around two circular cylinders, which had equal diameter. Liu et al. (2001) investigated two side-by-side elastic cylinders in a cross flow numerically. In their research, two cylinders were supported at both ends and they considered two cases, first rigid case where structural stiffness of the cylinder was assumed infinite and second one elastic case where the cylinders undergo oscillations. They concluded that, for different spacing ratios flow patterns are found to be consistent previous experimental observations. Zhao et al. (2007) studied on turbulent flow past two circular cylinders (the cylinders were different diameter) numerically. They used k-ε turbulence model to simulate turbulent flow. As a result, they concluded that, the small cylinder relative position had significant effects on the hydrodynamics force and vortex shedding characteristics of the cylinders.

Lam et al. (2003) studied the measurements of force coefficients and strouhal numbers (St) on four cylinders in a square configuration. They used a laser-induced fluorescence visualization technique. They concluded that the downstream cylinders were usually subjected to more serious fluctuating forces under the influence of unsteady wake vortices. They also noted that, the upstream cylinders normally experienced larger mean drags than the downstream ones.

For recent years, several researchers carried out some 3D (Three-dimensional) numerical studies. Lam and Zou (2010) investigated 3D laminar flow around four circular cylinders in an in-line square configuration. Their investigation's focus areas were effects of spacing ratios, aspect ratio on 3D flow characteristics, and the force and pressure coefficients of the cylinders. They chose the Reynolds number as 200. As a result, they concluded that spacing ratio, aspect ratio, and the no-sli end wall condition had important combined effects on free shear layer development of the cylinders. They also concluded that effects had strong influences on the pressure fields and force characteristics. Zhao et al. (2010) investigated combined steady and oscillatory flow past a circular cylinder numerically with using three-dimensional Direct Numerical Simulation (DNS). They tried to investigate how existent steady current influenced flow regime and hydrodynamic forces. They found good agreement when comparing lift coefficient and in-line force coefficient in pure oscillatory flow case with experimental data. Lazarkov and Revstedt (2008) studied flow-induced oscillation of an elastically supported circular cylinder subject to a fluid flow at Reynolds number 100 and 400. They created three-dimensional simulations. They concluded that, for very strong confinement (in the case of short cylinder) cylinder's motion was governed by cylindrical structures' natural frequency even beyond synchronization range. They also noted that the upper boundary of the synchronization range showed no dependency on the confinement, only on Reynolds number.

1.1.3 Fluid structure interaction

When the structural behavior is important in any given problem, Fluid-Structure interaction mechanisms between these two domains (structure and fluid) need to be identified.

Fluid-Structure Interaction consists of many different design elements and components. Fluid and Structure components need to be initialize separately and their coupling mechanism shall be designed and optimized by using many parameters. Gluck et al. (2001) studied numerical approach of a time-dependent fluid-structure coupling for membrane and thin shell structures with large displacements. They used finite volume based CFD code for computing flows and finite element based structural code to perform structural simulations. In addition,

they used MpCCI coupling system to connect these two solvers and interoperate both of them. Their research was one of the earliest attempts to design a coupled system (their system was partitioned – fully implicit coupling algorithm) and they successfully verified their system setup. Their system showed stable convergent behavior and satisfactory result in different perspectives.

Wang (2008), proposed a new idea for solving aeroelastic problems numerically. His technique combined CFD and CSD packages for fluid-structure interactions. His study's results showed that coupling method was very accurate and logical. In addition, his method can be used to solve fluid-structure interaction problems. Wang (2008) idea was mainly same with Gluck et al. (2001) but with different solver and coupler participants. Ansys Fluent (as CFD solver) and ABAQUS (as structural solver) were used in the system and UDF function based connection system was employed as coupling mechanism. Test cases showed that his approach was also effective and accurate.

As we highlighted above, modeling of Fluid-Structure Interaction (FSI) system consist of three main components and they are fluid solver, structural solver and coupling mechanism. In all related research and engineering activities, these three main components shall be defined and optimized accordingly. Another example for these types of studies is Abdullah et al. (2005). They presented a method for a simulating wind-structure interaction by using commercial software packages. (In addition, with the nature of the system, their proposed method was time dependent.) They used Fluent as a CFD program (fluid solver component) to find the wind induced forces acting on a structure and used Matlab (as structural solver) for determining the structural responses and specially coded coupling component for enable these two different systems to interoperate and interact with each other. Their model was rather basic, a cylinder shape structure and flow around it. As a result, the method that they proposed successfully described the dynamic interaction between wind and structure and low Reynolds number vortex shedding around a circular cylinder (but it is important to note that, their method was not capable of capturing lock-in phenomena.)

It is also possible to model and numerically analyzed the fluid structure interaction problems with specially designed and developed numerical methods. Yang et al. (2008) studied on fluid – structure interaction of elastically mounted rigid bodies by

using embedded-boundary method. They adopted a strong coupling scheme (defined as a system in which the fluid and the structure are treated elements of a single dynamical system. Within their system, all governing equations (fluid and structural) were integrated simultaneously and solved interactively in the time domain) over a predefined 2D Cartesian coordinate system. Their results were in good agreement with reference data. Their method also had the basic FSI components, which are ODE solvers (as fluid solver and structural solver) and strong-coupling scheme (as coupling algorithm).

As we see in the above very well studied examples, different FSI system approaches can have different main components and overall FSI systems performance is tightly depend on them.

Fluid Structure interaction is also very important in Bridge design. Design of bridges against aerodynamic forces and understand their interaction between bridge structures is very important. Mazzilli et al. (2000) investigated aeroelastic behavior of a cable-stayed bridge by using simple numerical model. Their research limited to structural behavior of the bridge under wind loads and did not include any coupled effects. Szabo and Gyorgyi (2009) studied three dimensional fluid structure interactions between bridge and wind. In their study, they performed three-dimensional coupled CSD-CFD simulation.

1.1.4 Other related studies

Adli and Ibrahim (2011), studied on dynamic characteristics of the offshore riser pipeline due to vortex flows. In their research Glass-fiber reinforced plastic (GRP) pipe was used and they implemented two dimensional finite element computational method. They concluded as their proposed model showed dynamic responses of GRP pipe correctly and its vortex induced vibrations characteristics.

Choi (2001) studied on offshore pipelines and analyzed free spanning length. In the study, new improved procedure introduced, and concluded that new calculations could allow increasing free span lengths of offshore pipelines. Liu et al. (2012) investigated single flexible cylinder's behavior in axial flow. They numerically investigated fluid-structure interaction for elastic cylinder in an axial flow. They used Lagrange-Euler (ALE) Navier-Stokes equations and vibration equation of Euler-

Bernoulli beam as dynamic equation. They concluded that, loading, induced by the turbulent flow, was one key factor to induce the dynamic instability.

Chen and Zha (2005) investigated flow-induced vibration of elastically mounted cylinder and they used fully coupled fluid-structure interaction methodology (They used previously proposed high-resolution upwind scheme). They concluded that technique they used, can be used accurately and efficiently for calculating flow-induced vibrations based on fully coupled fluid-structure interaction problems.

Belver et al. (2012) investigated fluid-structure interaction for steel chimney under vortex-induced vibrations to analyze its dynamic behavior. In their study, for each period, the fluid problem was solved and with these, aeroelastic analysis was carried out. Geometry of the mesh updated according to the structural displacements. They concluded that their model successfully captured the theoretical and experimental behavior of slender structures and their results matched with the theoretical results.

Hydrodynamic forces acting on undersea (submarine) pipelines were studied by various researches. Avci et al. (1996) prepared a detailed report on forces acting on undersea tunnel structures. In this report, hydrodynamic forces were investigated in detail and their effects in various conditions were highlighted. Cokgor (1997) studied hydrodynamic forced on the circular cylinders under current, wave and coexisting flows. In his experimental research, pressure distributions on the cylinder were measured in order to determine the forces. Cokgor and Avci (2002) investigated hydrodynamic forces on partly buried cylinder experimentally. In their research, waves and currents effects were existed together.

Hatipoglu and Avci (2003) studied flow around a partly buried cylinder shaped structure. In their research, flow cylinder was in a steady current and in selected flow conditions Reynolds numbers were 13000 and 26000. Their research was experimental and numerical, and they used Fluent to model their system numerically. Their results indicated that the lengths of the separation regions near the upstream and downstream of the cylinder decreased with the increasing burial ratio.

1.2 Objective and Scope of This Study

Researchers studied flow around cylindrical structures in different perspectives over the time and until recent years; most of the researchers were interested in flow

around rigid cylinder and forces acting to the system. When we consider elastical deformations of the cylinders (cylindrical beam or pipe), systems behave different from the rigid one and it is difficult to prepare a computational and experimental system to represent elastical behavior.

After recent developments in computational engineering (with advances in CPU, GPU and HPC technologies) and software packages (fluid, structural solvers and coupling algorithms), modelling and calculating elastical behaviors of such systems are more feasible. The latest improvements in computer technology give engineers new opportunities to solve and understand complex problems with more accuracy in less computational time-frame.

In this study, main aims are to prepare a physical and a mathematical model (computer model) to represent elastical behavior of cylinder, which is subject to current and wave effects. Prepared laboratory model has elastic properties due to pipe material (PE pipes). Therefore, the difficulty is to reflect this physical property (elastic material property) in our computer model. To achieve this, overall system designed as FSI (Fluid-Structure Interaction) system. After preparing aforementioned computer models, main effects due to flow field that acting to cylinder was determined respect to time.

For the computer model, ANSYS Fluent CFD software system (as fluid solver) was used for modeling fluid behavior and ANSYS Mechanical (as structural solver) was used for modeling structural behavior. To achieve a coupled behavior, these two solvers connected to each other by using ANSYS System Coupling component (as coupling algorithm).

In the physical model (laboratory model), test specimens (PE pipes) were subject to hydrodynamic forces (long term- 1.5 months 7 hour every day) that were caused by current and wave effects. During these tests, three different conditions were applied. In the first one only current existed, in second one only wave effects existed and in the last one current and wave effects were applied together. After these long term hydrodynamic loading, the pipes were sent to material laboratory to find out change in their material properties because of these long-term hydrodynamic loading. Using laboratory results total change in material properties can be determined and by using these laboratory results the final conditions of these pipes can be estimated.

For understanding the behavior of such a system in real world applications, the prototype system, “Kartal-Adalar natural gas pipeline” project, was investigated closely. The specimens that were taken from this pipeline may give us unique information about such systems behavior. The specimens material test results may give us a starting point for understanding the system’s overall performance capacity.

Using mathematical model (which is prepared to represent Fluid – Structure Interaction system in fully coupled mode), hydrodynamic effects could be determined accordingly. After determining these effects respect to time, it could be possible to estimate current conditions of pipes numerically.

We can list main objectives of our study as below:

a) Preparing a physical model (laboratory model) to test specimens (PE pipes) which are subject to hydrodynamic forces (long term- 1.5 months 7 hour every day) which are caused by current and wave effects.

b) Evaluating changes in material properties of PE pipes, after long-term lab-tests, and using material test results to investigate their performance against such hydrodynamic forces.

c) Analyzing and investigating the prototype system (Kartal-Adalar PE Natural Gas pipeline system) material test results and determining pipelines performance over the long term. (Evaluating the usability of HDPE pipe in such systems.)

d) Preparing mathematical models (computer models) in order to investigate flow characteristics in this problem domain. (Flow around PE elastic cylindrical structures). Analyzing mathematical model results to understand behavior of such systems.

e) Creating a roadmap and a starting point for future studies in this particular subject for more detailed results.

f) Creating a roadmap and starting point for numerical approximation methodology to estimate conditions of such pipe systems without long-term physical laboratory experimental tests.

As a result, our proposed method is a starting point for fully implemented methodology. In our research, we are aiming to create a roadmap and direction to the full implementation.

2. FLOW AROUND A CYLINDER AND HYDRODYNAMIC FORCES

2.1 Flow Around a Cylinder and Forces in Steady Current

Flow around a circular cylinder is a one of the base model for hydrodynamic research and technical studies. Flow around cylinder depends on the cylinder Reynolds number, which is a dimensionless quantity and describes the flow characteristics.

$$\mathrm{Re} = \frac{DU}{\nu} \tag{2.1}$$

D: Diameter of the cylinder

U: Flow velocity

ν: Kinematic viscosity

When Reynolds number increases flow characteristics changes dramatically. In Figure 2.1, the flow regimes experienced with increased Re are summarized (Sumer and Fredsoe (2006)).

2.1.1 Vortex shedding

Vortex shedding is a fundamental concept for flow regimes. Vortex shedding regimes can be classified based on the flow's Re number. For Re > 40, vortex shedding starts to occur for all flow regimes. If Re > 40, one vortex grows larger than other, which is formed in up and down side of the cylinder. For Reynolds number greater than 40, the boundary layer over the cylindrical bodies' surface will separate because of the fact that adverse pressure gradient. In addition, because of these effects, over cylinder surface, a shear layer is formed. (Figure 2.2)

Vortex shedding mechanism can be briefly explained as strong vortex draws the opposite vortex. As we see in the Figure 2.3 larger vortex (vortex A) that is clockwise direction draws the other vortex (vortex B) that is counter-clockwise direction.

Vortex B cut off vorticity supply of Vortex A from its boundary layer and this is the where Vortex A is shed (which means being a free vortex and convected

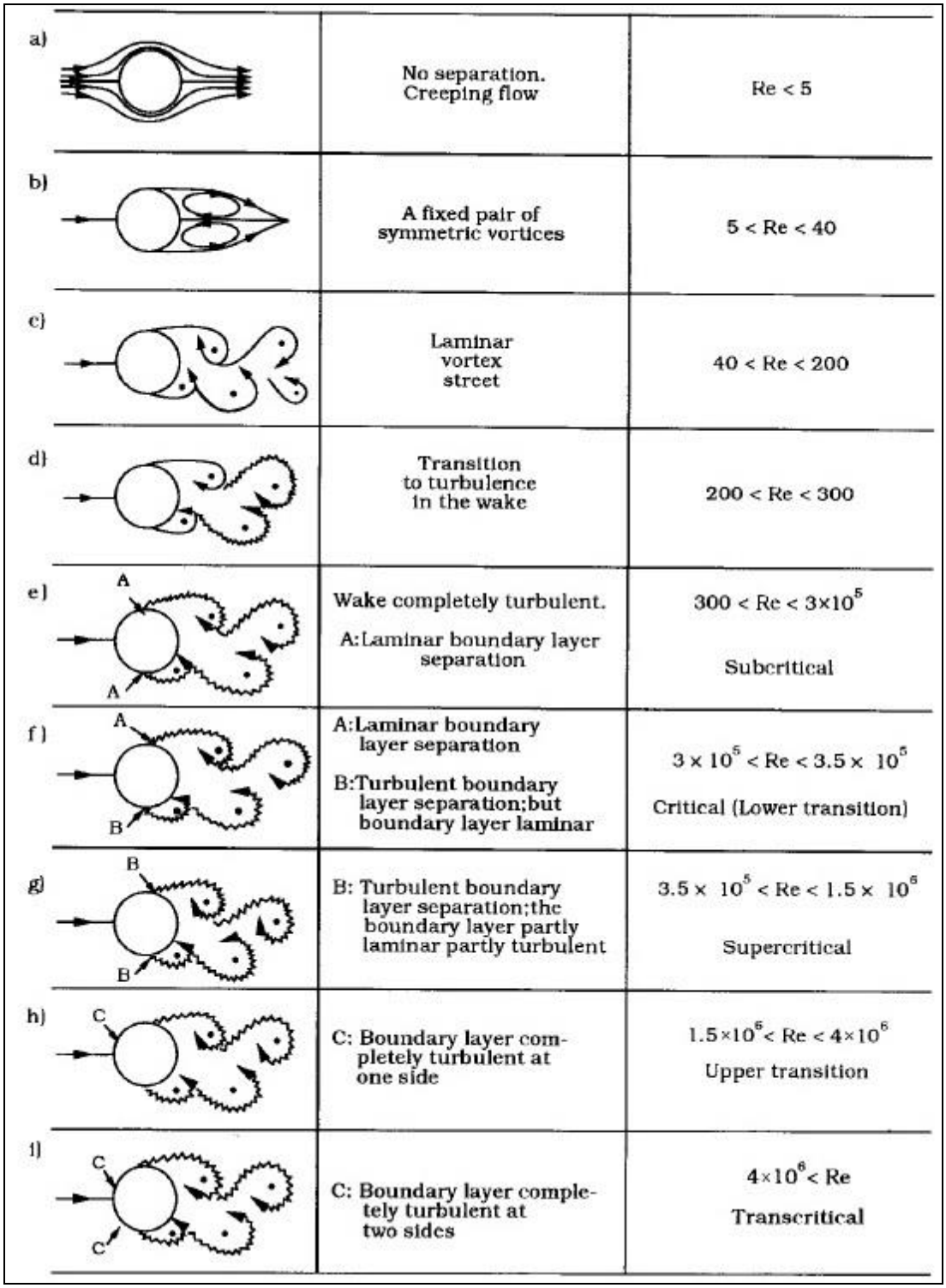

Figure 2.1 : Flow around a circular cylinder in steady current (Sumer and Fredsoe (2006)).

downstream by the flow). And this mechanism continues with opposite site, Vortex C cut of Vortex B and vortex B is free in the end of that.

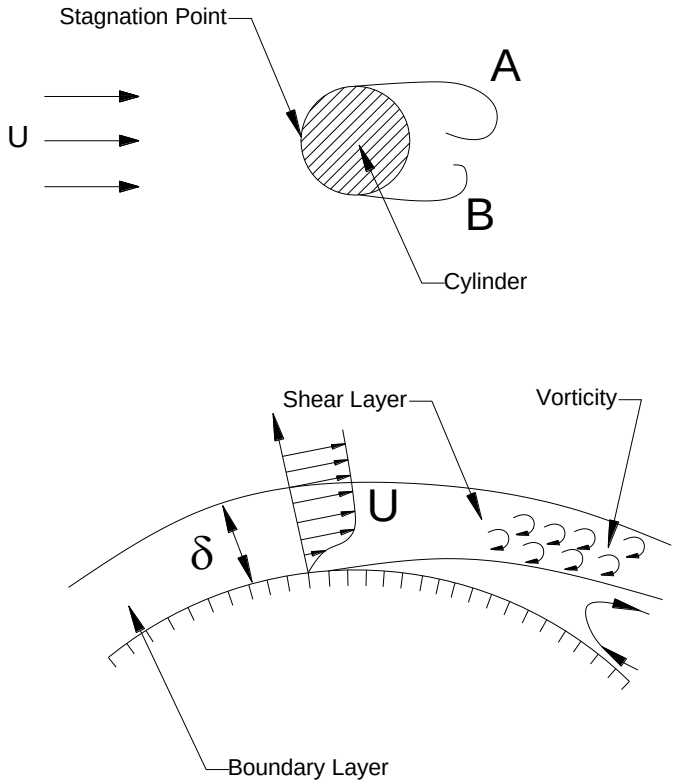

Figure 2.2 : A and B vorticies and shear layer around the cylinder surface.

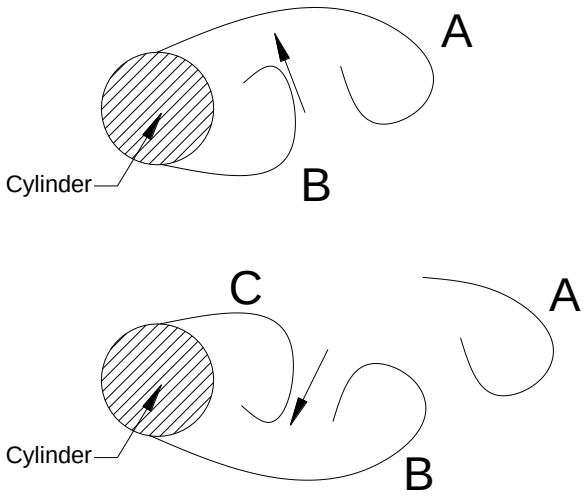

Figure 2.3 : Vortex sheding mechanism.

2.1.2 Vortex shedding frequency and strouhal number

In many engineering and science discipline, special indicators are necessary for classification and measurement purposes. Dimensionless numbers are one of them and in hydrodynamic, Strouhal number is one of them. It is possible to define

Strouhal number as that normalized vortex-shedding frequency. When we normalized vortex-shedding frequency with flow velocity (U) and cylinder diameter D, we reach a dimensionless number and this number called Strouhal number.

$$St = St(\mathrm{Re}) \tag{2.2}$$

Where

$$St = \frac{f_v D}{U} \tag{2.3}$$

f_v: vortex-shedding frequency

D: Cylinder diameter

U: Flow velocity

Figure 2.4 shows how the Strouhal number changes with Reynolds number (Re) (Sumer and Fredsoe (2006)).

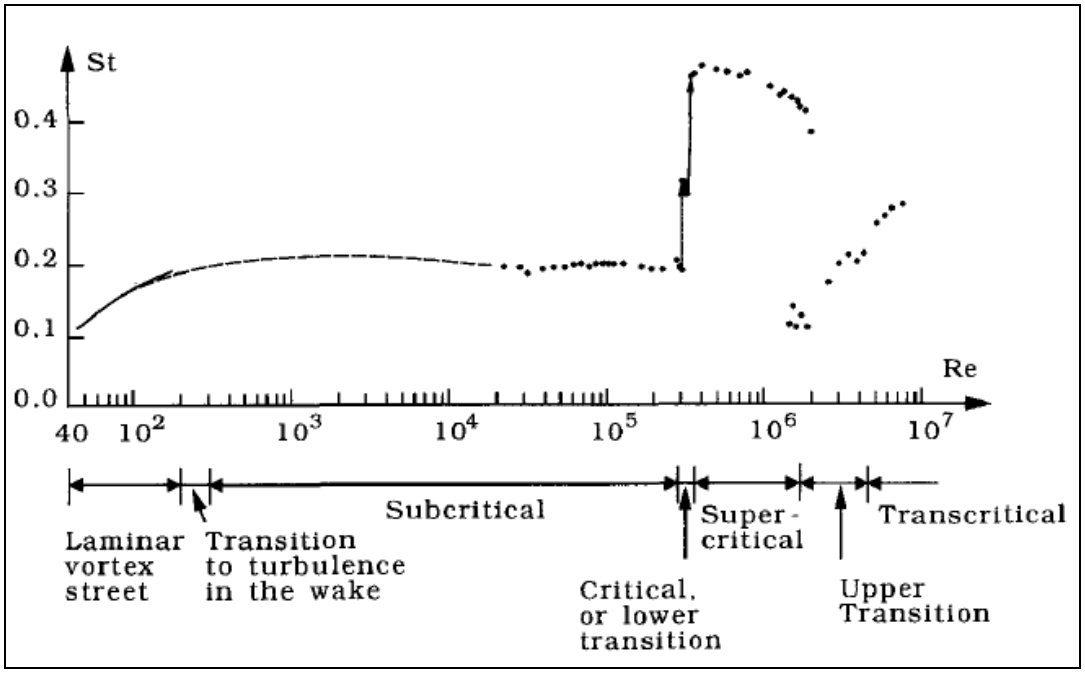

Figure 2.4 : Strouhal number for a smooth circular cylinder (Sumer and Fredsoe (2006)).

As we mentioned earlier, vortex shedding starts to appear at Reynold number equals to 40 and for this case Strouhal number is approximately equal to 0.1. When Reynold number increases, Strouhal number also increases and for Re=300 it reaches the

value of 0.2. For the subcritical regimes (Re < 10e5) Strouhal number nearly equal and has the value of 0.2. (Sumer and Fredsoe (2006)).

2.1.3 Wall proximity effect to flow

In hydrodynamics, boundary conditions have critical importance for flow characteristics. Changes in the boundary conditions directly changes the flow. Effects caused by certain boundry condition changes depends on the type of the boundary and its degree of modification.

For cylinders placed near wall or canal beds (this is a usual practice for pipelines), significant number of changes occur in the flow around the cylinder. Sumer and Fredsoe (2006) summarized these changes as following (Figure 2.5);

1. For the gap-ratio values smaller than e/D=0.3, vortex shedding is suppressed.
2. For the gap-ratio, e/D = 1 stagnation point is located about $\varphi=0^{o}$ and for the gap-ratio, e/D=0.1 stagnation point is located about $\varphi=-40^{o}$.
3. Angular position of the separation points changes with gap-ratio. The separation point at the free-stream side of the cylinder moves upstream and that at the wall side moves downstream.
4. On the free-stream side of the cylinder suction is larger that on the wall side of the cylinder. (When cylinder moves away from wall, this effect disappears and symmetry between two sides is restored.

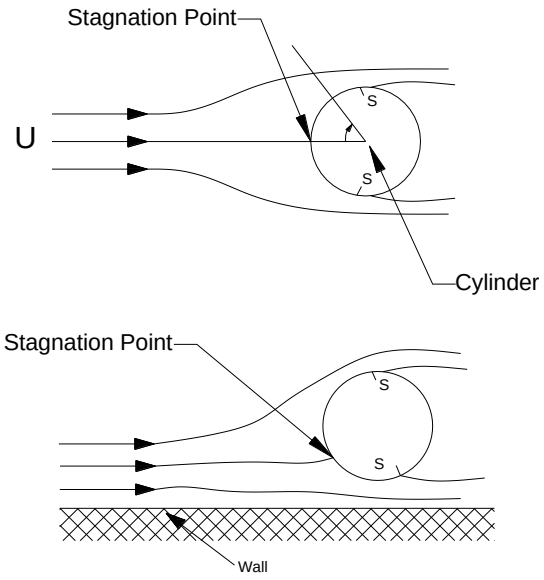

Figure 2.5 : Flow field around a free cylinder and a cylinder near-wall.

2.1.4 Forces on a cylinder in steady current

Cylinders, which are subject to flow effects, are acted by resultant forces. These forces have two components, first component is pressure component and the second one is friction components.

Resultant force's inline component due to pressure per unit length of the cylindrical object can be formulized as (and is termed the form drag):

$$\overline{F}_P = \int_0^{2\pi} \overline{p}\cos(\phi) r_0 d\phi \qquad \textbf{(2.4)}$$

And because of friction effects, it could be formulized as (and is termed the friction drag);

$$\overline{F}_f = \int_0^{2\pi} \overline{\tau}_0 \sin(\phi) r_0 d\phi \qquad \textbf{(2.5)}$$

In this equations $\overline{p}$ is symbolize the pressure and $\overline{\tau}_0$ is symbolize the wall shear stress on the cylinder surface. They are time-averaging ones, so they are marked with overbar to emphasize that.

The sums of these two forces, which are defined below, are called mean drag and that is total in-line force.

$$\overline{F}_D = \overline{F}_P + \overline{F}_f \qquad \textbf{(2.6)}$$

2.1.5 Drag and lift effects

As explained before, except for very small Reynolds numbers (Re < 40), the vortex shedding feature is common to all flow regimes.

The pressure distribution around the cylinder is changing periodically as the vortex shedding progress and because of these, force components that are acting to cylinder changes periodically.

As clearly seen in Figure 2.6 pressure distributions are changing with time and resulting force calculated by integrating the pressure distributions over the cylinder surface. In addition, Figure 2.7 is showing the force traces according to the same experimental research as Figure 2.6.

As Figure 2.6 and Figure 2.7 shows, changes occur to drag force in in-line direction with time in periodical nature and in the transverse direction, the lift force, changes periodically with time, even though the flow is symmetric; there is still a force component on the cylinder in the transverse direction.

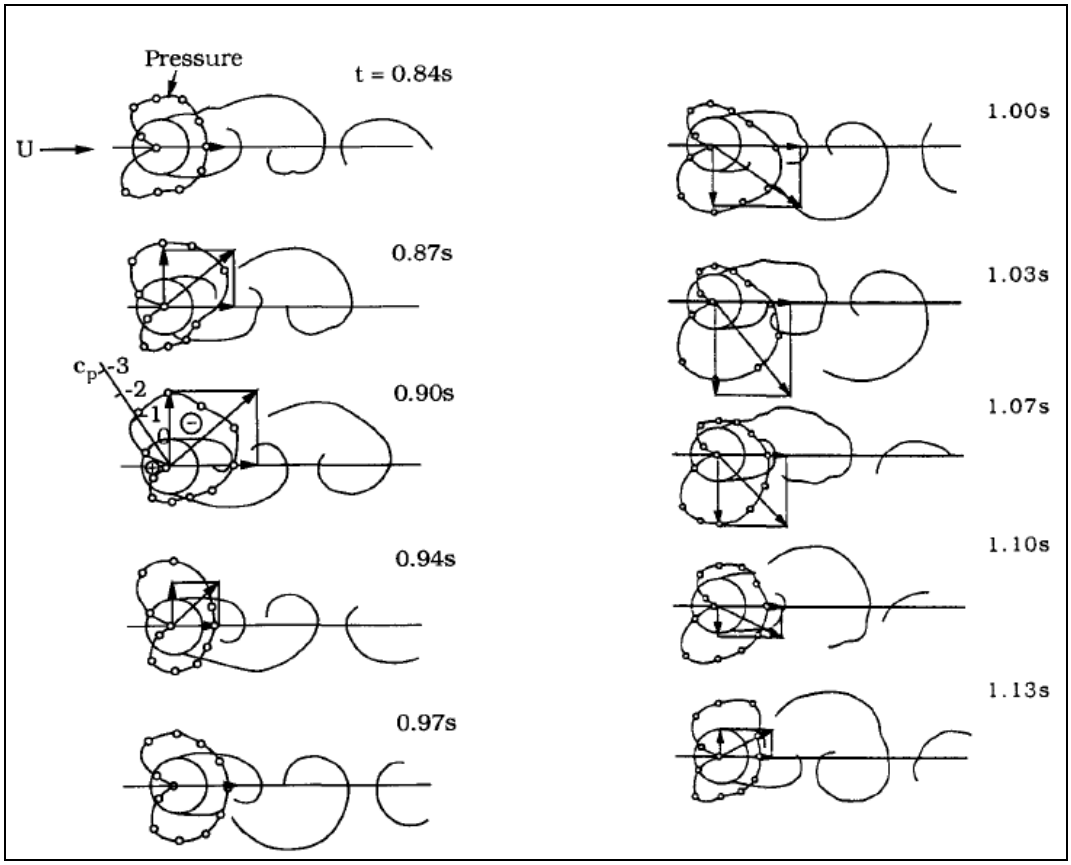

Figure 2.6 : Time development of pressure distribution and the force components, as the vortex shedding progress. ($Re=1.1x10^5$, D=8 cm and U=1.53 m/s. $c_p=(p-p_0)/(1/2\rho U^2)$) (Sumer and Fredsoe (2006)).

The periodic change of the vortex shedding causes the pressure distribution of the cylinder due to the flow will change periodically, so generating a periodic variation in the force components on the cylinder. Force components can be divided into cross-flow and in-line directions. The force of the cross-flow direction and in-line direction, lift force (F_L) and drag force (F_D) respectively.

The lift force appears when the vortex shedding starts to occur and it fluctuates at the vortex shedding frequency. Similarly, the drag force also has the oscillating part due to the vortex shedding, but in addition to this, it also has a force component as a result of friction and pressure differences and this part is called the mean drag force. Lift and drag forces can be formulated as equation 2.7 and 2.8.

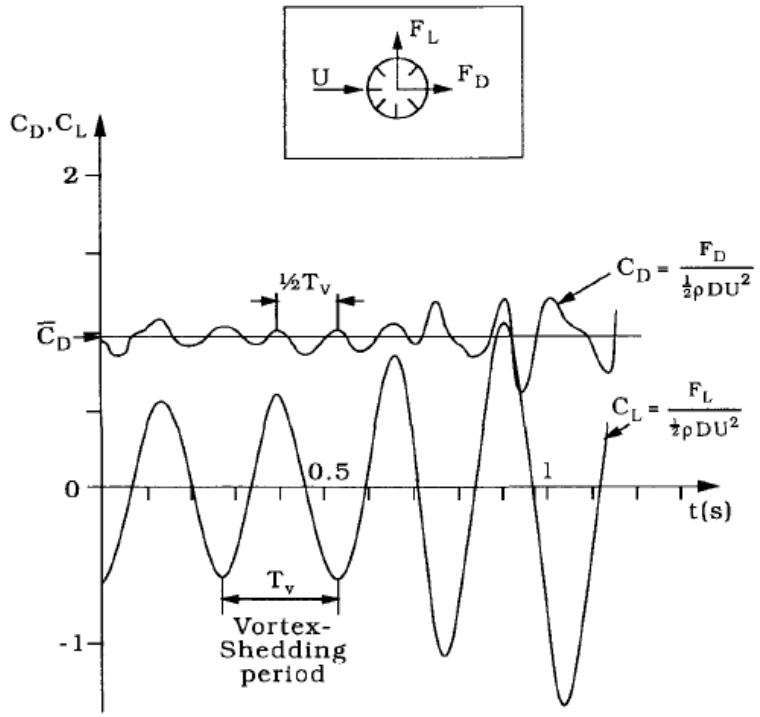

Figure 2.7 : Drag and lift force traces obtained from the measured pressure distribution in the Figure 2.6. ($C_D=F_D/(½\rho DU^2)$ and $C_L=F_L/(½\rho DU^2)$ (Sumer and Fredsoe (2006)).

When we place a cylinder in a steady current, two forces act to the cylinder; drag force and lift force (Figure 2.8).

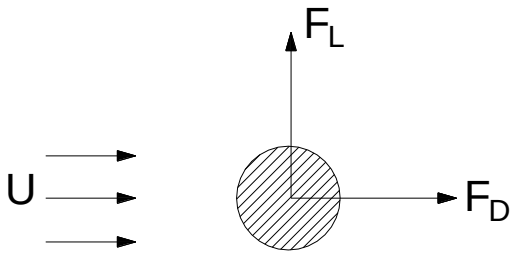

Figure 2.8 : Forces acting to a cylinder in steady current.

These two forces could be simply defined as;

$$F_D = \overline{F}_D + \hat{F}_D \sin(2\omega_s t + \phi_s) \qquad \textbf{(2.7)}$$

And

$$F_L = \hat{F}_L \sin(\omega_s t + \phi_s) \qquad \textbf{(2.8)}$$

Where;

$\hat{F}_D$: The amplitudes of the oscillating drag

$\hat{F}_L$: The amplitudes of the oscillating lift

$\overline{F}_D$: The mean drag

C_D and C_L are the dimensionless parameters for drag and lift forces, and they are shown in equation 2.9, 2.10 and 2.11.

$$\hat{C}_L = \frac{\hat{F}_L}{\frac{1}{2}\rho LDU^2} \quad \textbf{(2.9)}$$

$$\hat{C}_D = \frac{\hat{F}_D}{\frac{1}{2}\rho LDU^2} \quad \textbf{(2.10)}$$

$$\overline{C}_D = \frac{\overline{F}_D}{\frac{1}{2}\rho LDU^2} \quad \textbf{(2.11)}$$

Where;

L: Cylinder length

ρ : Fluid density

D: Cylinder diameter

U: Flow velocity

2.1.6 Forces on a cylinder near wall or a wall type boundary

As explained before, changes in the flow characteristics which are mainly caused by wall proximity are obviously have a strong influence to the forces acting on the cylindrical object. In this respect, e/D value is the main parameter in these influences. For values greater than e/D = 0.3 effects have minor influence to the forces and in some cases (depends on the problem and case objectives) wall boundary condition could be neglected.

2.1.6.1 Changes on drag force

In the research, which was done by Bearman and Zdravkovich (1978), cylinders were placed in there different from a plane wall and pressure distribution around cylinders had been measured. In Figure 2.9 shows the resulting pressure distributions.

According to Bearman and Zdravkovich (1978), research and similar experiments showed that drag coefficient decreases with decreasing gap ratio near the wall boundary.

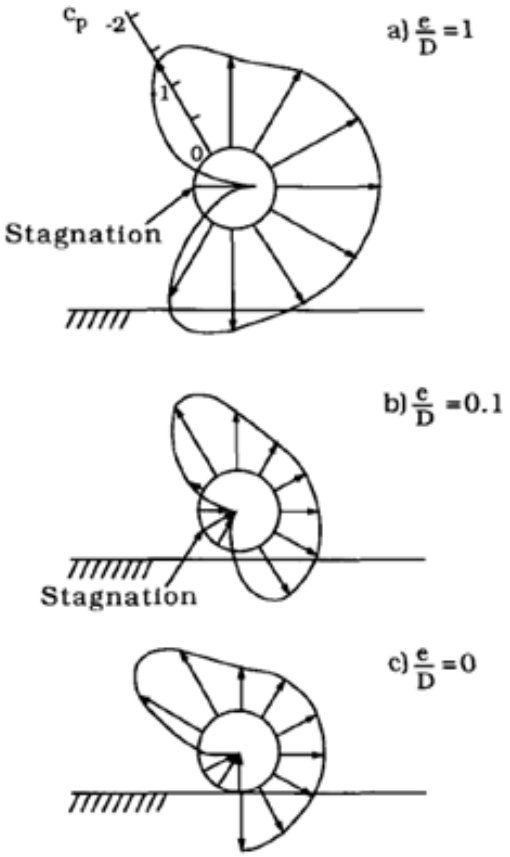

Figure 2.9 : Pressure distribution on a cylinder near a wall as a function of gap ratio e/D. $c_p=(p-p_0)/(1/2\rho U^2)$ where p_0 is the hydrostatic pressure. (Bearman and Zdravkovich (1978)).

2.1.6.2 Changes on lift force

Because of the fact that non-symmetrical nature of the mean flow around a near wall cylinder, non-zero lift effect should be exist. As clearly seen on Figure 2.9, for gap ratios e/D=0.1 and 0 non-symmetric pressure distribution causes lift effects on the cylinder.

For gap ratios such as e/D=0.2-0.3 and above, lift effects are fairly small. But when gap ratios are getting smaller, lift effects increases tremendously.

2.1.6.3 Oscillating drag and lift forces acting on a cylinder near wall

The vortex shedding is suppressed for the gap ratios which are smaller than 0.3, so in the situation when gap ratio is smaller than 0.3, the vortex-induced oscillating lift and drag will cease to exist.

2.2 Flow Around a cylinder and forces in oscillatory flows

When the cylinder is exposed to an oscillatory flow an additional parameter, which is called Keulegan-Carpenter number, appears. The Keulegan-Carpenter number (KC number) is defined by:

$$KC = \frac{U_m T_w}{D} \tag{2.12}$$

U_m: Maximum velocity

T_w: The period of the oscillatory flow

D: Diameter of the cylinder

When the flow has a sinusoidal characteristic with the velocity given by:

$$U = U_m \sin(\omega t) \tag{2.13}$$

From these equations maximum velocity will be:

$$U_m = a\omega = \frac{2\pi a}{T_w} \tag{2.14}$$

a: the amplitude of the motion

ω: the angular frequency of the motion

And in the sinusoidal case, KC number will be:

$$KC = \frac{2\pi a}{D} \tag{2.15}$$

And angular frequency of the motion:

$$\omega = 2\pi f_w = \frac{2\pi}{T_w} \tag{2.16}$$

f_ω: the frequency

Small KC numbers means that water particles orbital motions are small relative to the total width of the cylinder and when KC number is very small, separation behind the cylinder may not even occur.

On the other hand, Large KC numbers mean that, the water particles travel large distances (relative to the total width of the cylinder), resulting in separation behind the cylinder and possible vortex shedding. In addition to these, in case of very large KC number (KC $\rightarrow \infty$), it can be expected that the flow for each half period of the motion resembles that experienced in a steady current (Sumer and Fredsoe (2006)).

2.2.1 Flow regimes as a function of KC number and Re number

Flow regimes change when Keulegan-Carpenter number changes. Fig 2.10 below shows the flow around a cylinder while KC number is increased from zero. In this example, Reynolds number (Re) is $10e^3$.

When Re changes, the flow regimes may also change and upper and lower limits of the indicated KC number may change as well.

2.2.2 Wall proximity effects on flow regimes in oscillatory flows

The influence of wall proximity on the flow around cylindrical structure depends on gap to diameter ratio (e/D). For e/D = 0.3, these effects has minor influence for general behaviors and in some cases these effects could be neglected (Sumer and Fredsoe (2006)).

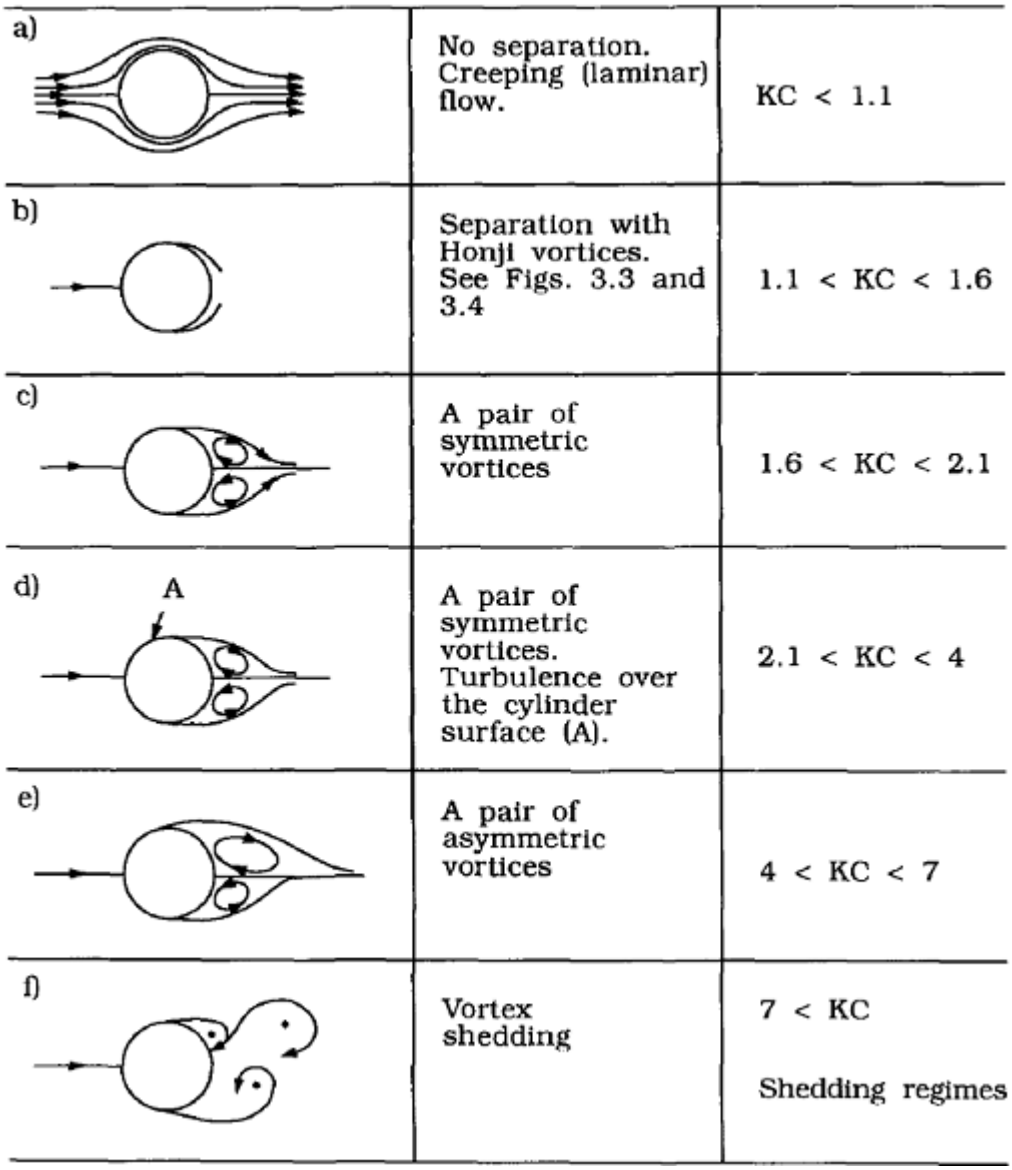

Figure 2.10 : Regimes of flow around a smooth, circular cylinder in oscillatory flow. Re = 10e3. Source for KC < 4 is Sarpkaya (1986a) and for KC > 4 Williamson (1985).

2.2.3 Forces acting on a cylinder in regular waves

Cylindrical structures that are subject to an oscillatory flow may experience two kinds of forces, the in-line and the lift forces.

2.2.3.1 In-line force

There are two main forces acting to body in oscillatory flows and these are In-force and Lift force (Figure 2.11).

In the case of oscillatory flows, there are two addition components to steady currents force per unit length formula.

These additional components are hydrodynamic-mass force and Froude-Krylov force components.

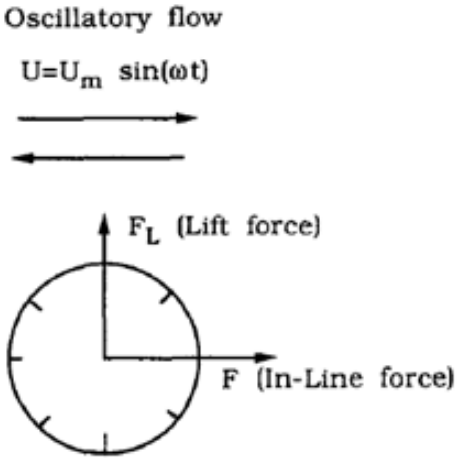

Figure 2.11 : Definition sketch for oscillatory flow force components.

$$F = \frac{1}{2}\rho C_D D U|U| + m'\dot{U} + \rho V \dot{U} \qquad \textbf{(2.17)}$$

In equation 2.17 ;

$m'\dot{U}$: Hydrodynamic-mass force

$\rho V \dot{U}$: Froude-Krylow force

m' : Hydrodynamic mass

V: Volume of cylinder

Hydrodynamic mass is defined as the mass of the fluid around the body which is accelareted with the movement of the body due to the action of pressure.

The force to accelerate the total mass (the mass of the body and hydrodynamic mass) may be written as;

$$F = (m + m')a \qquad \textbf{(2.18)}$$

Where;

a: Accelaration

In most situations, the hydrodynamic mass is calculated by neglectng friction effects, the flow is calculated by expressing fluid force equilibrium between pressure and inertia.

It is possible to summarize the procedure to calculate the hydrodynamic mass for a body placed in a still water with below steps (Sumer and Fredsoe (2006));

1. Accelerate the body in the water (this acceleration will create a pressure gradient around the body resulting in the hydrodynamic-mass force).
2. Flow field calculation with occurs around the body
3. Based on the flow information in the step 2, Calculate the pressure on the surface of the body
4. With using pressure information, determine the force on the body information.

In tradition format, the hydrodynamic mass is written as;

$$m' = \rho C_m A \tag{2.19}$$

where;

A: the cross-section area of the body

C_m: hydrodynamic-mass coefficient (for circular cylinder C_m=1)

The Froude-Krylov Force

Hydrodynamic mass force is existed when a body is moved with an accelaration a in still water. This force is caused by the fluid in the immediate sorroundings of the body. On the other hand, in the case of helding body stationary and moving the fluid with an acceleration a, there will be two effects. First effects is explained above and

second effect will be that the accelareted motion of the fluid in the outer-flow region will generate a pressure accoding to;

$$\frac{\partial p}{\partial x} = -\rho \frac{dU}{dt} \tag{2.20}$$

where;

U: the velocity far from the cylinder

This pressure gradient in turn will produce an additional force on the cylinder and this effect is named as the Froude-Krylov force.

For a cylinder with the cross-section area A and with unit length,

$$F_P = \rho A \dot{U} \tag{2.21}$$

Where;

$$\dot{U} = \frac{dU}{dt} \tag{2.22}$$

In the case when the body moves in an otherwise still water, there will be no pressure gradient created by the acceleration of the outher flow, therefore the Froude-Krylov force will not exist in the case (Sumer and Fredsoe (2006)).

The Morison Equation

For the cylinder which is held stationary, the total in-line force can be formulated for an accelerated water environment as below equation 2.23 and 2.24;

F = [Drag Force]+[Hydrodynamic Mass Force]+[Froude-Krylov Force] **(2.23)**

$$F = \frac{1}{2}\rho C_D D U|U| + \rho C_m A \dot{U} + \rho A \dot{U} \tag{2.24}$$

And Equation 2.24 could be written as;

$$F = \frac{1}{2}\rho C_D D U|U| + \rho(C_m + 1)A\dot{U} \quad \textbf{(2.25)}$$

And by defining a new coefficient, C_M,

$$C_M = C_m + 1 \quad \textbf{(2.26)}$$

And from above equations, the Morison equation defined as;

$$F = \frac{1}{2}\rho C_D D U|U| + \rho C_M A\dot{U} \quad \textbf{(2.27)}$$

In equation 2.27, the force term, $\rho C_M A\dot{U}$ is called the inertia force and the new coefficient C_M is called the inertia coefficient.

In the case when the body moves relative to the flow in the in-line direction (when body is flexibly mounted or the body has a flexible behavior this may occur), the Morison equation is written as (Sumer and Fredsoe (2006));

$$F = \frac{1}{2}\rho C_D D(U - U_b)|U - U_b| + \rho C_m A(\dot{U} - \dot{U}_b) + \rho A\dot{U} \quad \textbf{(2.28)}$$

Where;

U_b : velocity of the body in the in-line direction.

And it is important to note that; the Froude-Krylov force must be based on $\dot{U}$ rather than $(\dot{U} - \dot{U}_b)$, because of the fact that the Froude-Krylov force is associated with the absolute motion of the fluid rather than the motion of the fluid relative to the body.

2.2.3.2 Lift force

A cylinder that is exposed to an oscillatory flow, the cylinder may undergo a lift force. If the flow has very small KC numbers (flow around the cylinder is an unseparated flow), then lift force will not be generated. Figure 2.12 is briefly shows the development of the lift force as the KC number is increased from zero. As seen

from the figure 2.12, the lift force first comes into existence when KC is 4 and well-established lift-force regimes are formed after KC is 7, and beyond this value of KC number, the vortex shedding is present (Sumer and Fredsoe (2006)).

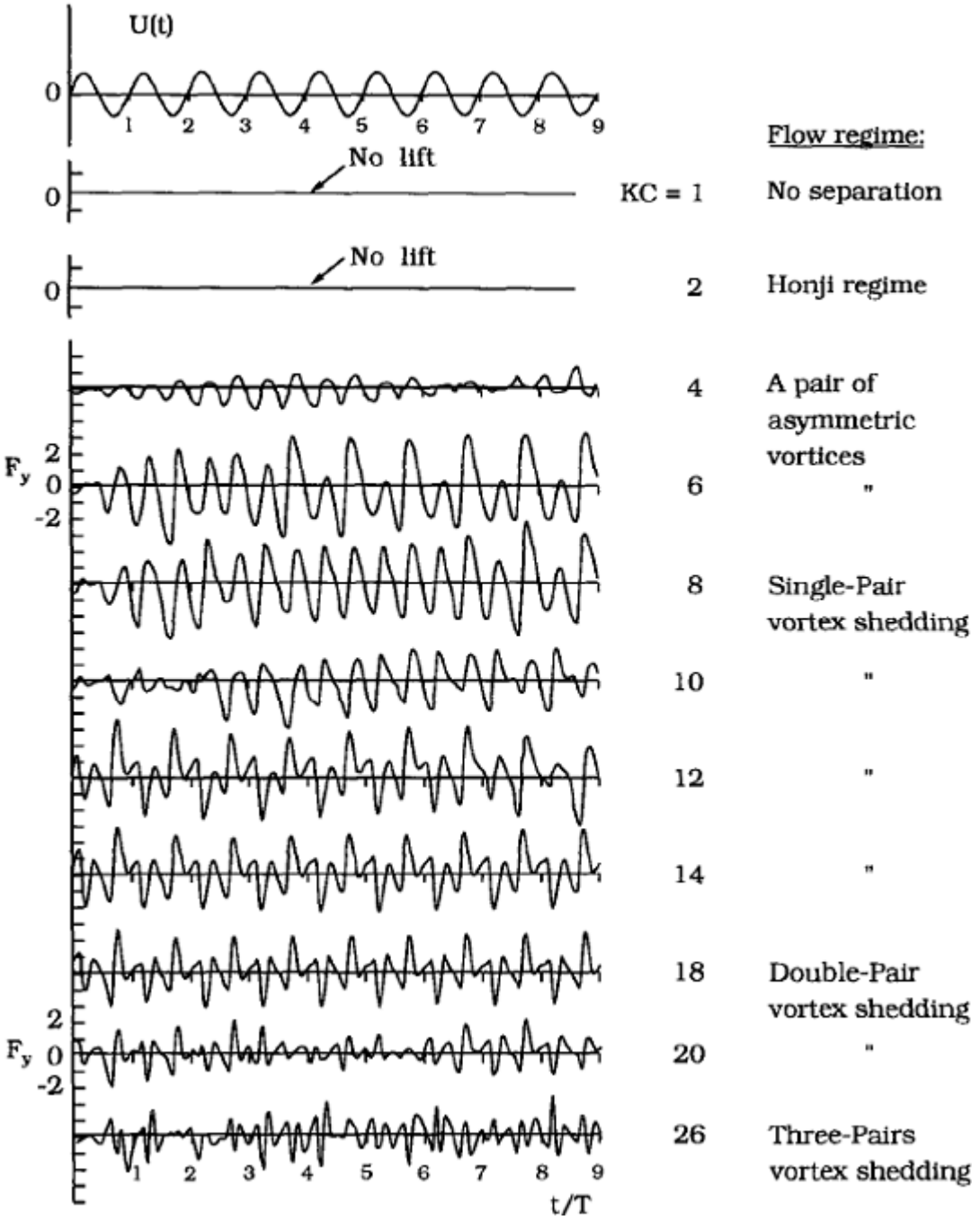

Figure 2.12 : Computed lift force traces over nine periods of oscillation at various KC – values for β(=Re/KC) = 196 (Sumer and Fredsoe (2006)).

When calculating the magnitude of the lift force, there are two acceptable approaches. In first approach, the maximum value of the lift force is considered and in second one root-mean-square (r.m.s) value of the lift force is adopted to represent

the magnitude of the lift force. These two approaches can be represented as follows (Sumer and Fredsoe (2006));

$$F_{L\max} = \frac{1}{2}\rho C_{L\max} D U_m^2 \qquad \textbf{(2.29)}$$

and

$$F_{Lrms} = \frac{1}{2}\rho C_{Lrms} D U_m^2 \qquad \textbf{(2.30)}$$

Where;

F_{Lmax} : The maximum lift force

F_{Lrms} : r.m.s value of the lift force

C_{Lmax} and C_{Lrms} : Corresponding force coefficients.

In some cases, the time variation of the lift force could be approximated by a sinusoidal variation and in these cases, the coefficients could be linked by equation 2.31 (Sumer and Fredsoe (2006)).

$$C_{L\max} = \sqrt{2} C_{Lrms} \qquad \textbf{(2.31)}$$

The both coefficients (C_{Lmax} and C_{Lrms}) are functions of KC and Re.

The figure 2.13 presents the lift-force data, showing the effect of Re number on the lift force. The figure also includes steady current data for comparison. The figure clearly shows that the effect of Re number is significant.

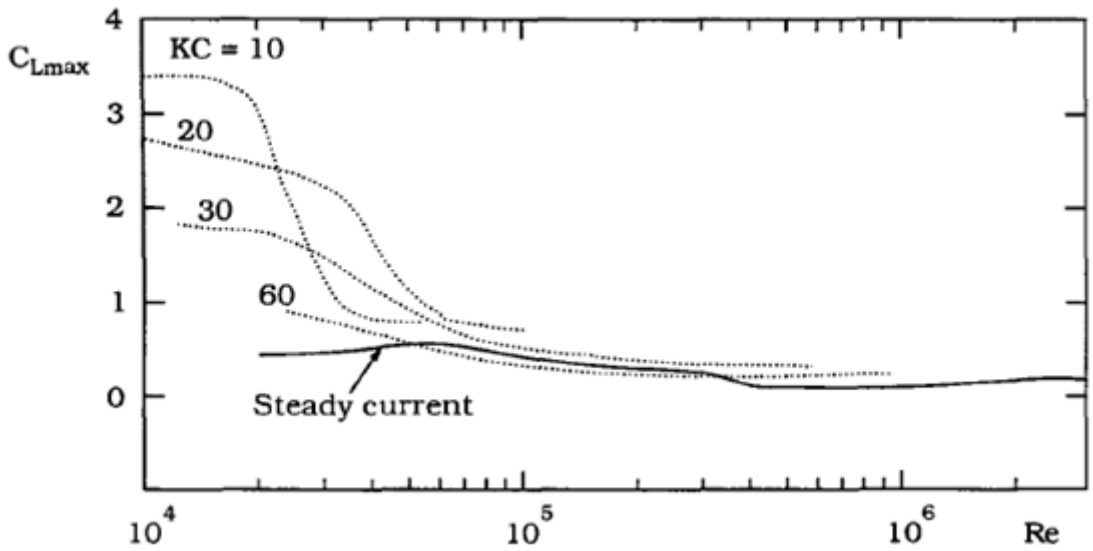

Figure 2.13 : Maximum lift coefficient for a free, smooth cylinder (Sumer and Fredsoe (2006)).

2.2.4 Current and waves coexistance effects

In most engineering applications, waves and currents are coexists. However, in some applications one of these two effects has relatively minor importance so less significant one can be omitted. On the other hand, in some applications both has strong influence and their coexistence and presence should be taken into account carefully.

In situations where current coexists together with waves, the presence of current may affect the waves.

To understand these effects and to create more understandable solution domain some simplification need to be done. To simplify the problem, oscillatory flow is considered unchanged in the presence of a superimposed current. U_c and U_m are velocity of the current and maximum value of the velocity of the oscillatory flow respectively. And let U_c/U_m is their ratio.

In addition, Re number and KC number are defined as; $Re=U_mD/\nu$ and $KC=U_mT_w/D$ respectively.

Figure 2.14 shows the coexistence effects. From the figure, below observations can be listed (Sumer and Fredsoe (2006)):

1. Flow velocity is varies with respect to time and the in-line force varies with respect to time in the same fashion as the flow velocity.

2. The way in which the lift force varies with time during the course of one flow cycle changes markedly as the parameter U_c/U_m is changed from 0 to 1. In case of $U_c/U_m=0.5$, the portion of the flow period where the flow velocity U < 0 is just enough to accommodate shedding from both the upper and the lower sides of the cylinder and this effect is characterized by one positive and one negative lift force in the lift force trace. For $U_c/U_m=1$, as seen from figure 2.14, the shedding disappears when the oscillatory component of the motion is in the direction opposite to the current.

3. When vortex shedding exists, the figure 2.14 indicates that the Strouhal number relation;

$$St = \frac{f_v D}{(U_c + U_m)} \tag{2.32}$$

is satisfied (the velocity is taken as the sum U_c and U_m, which are the current velocity and wave velocity respectively. In addition, in equation 2.32 f_v is the average vortex-shedding frequency.)

The Morison equation may be adopted in the present case but the velocity U(t) should be defined as in the equation 2.33.

$$U = U_c + U_m \sin(\omega t) \tag{2.33}$$

In Figure 2.15, C_D and C_M coefficients as functions of the parameters U_c/U_m can be seen.

The drag coefficient generally decreases with the ratio U_c/U_m. The inertia coefficient, C_M is not very sensitive to U_c/U_m except for the KC=5 (Sumer and Fredsoe (2006)).

Influence of current on the lift coefficient is illustrated in Figure 2.16. The lift coefficient is defined with the same equation (equation 2.29) but U_m is replaced by U_c+U_m.

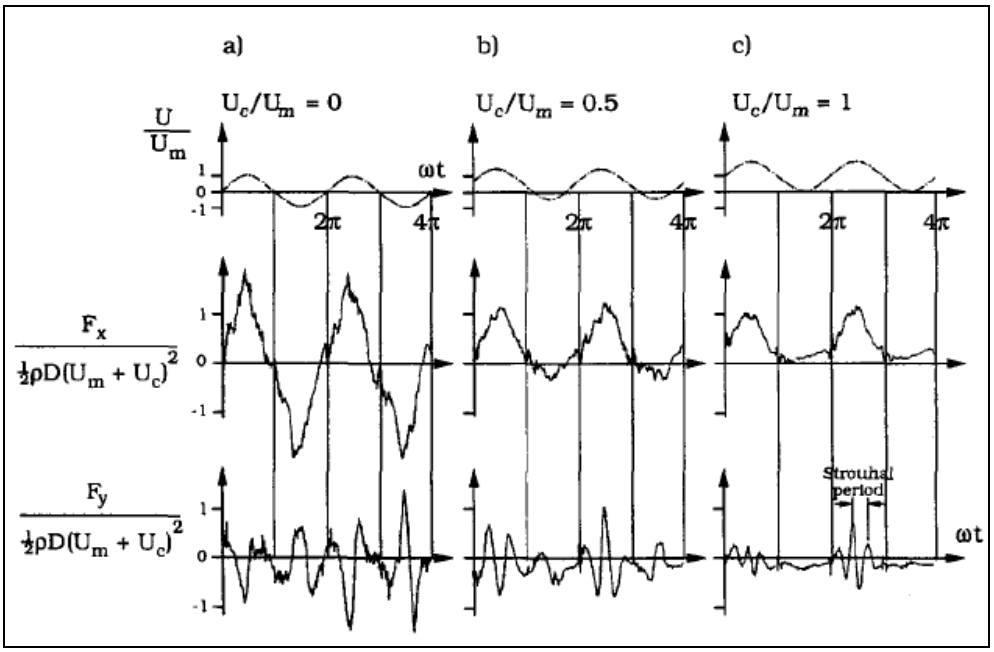

Figure 2.14 : Force time series in the case of coexisting current (KC=20) (Sumer and Fredsoe (2006)).

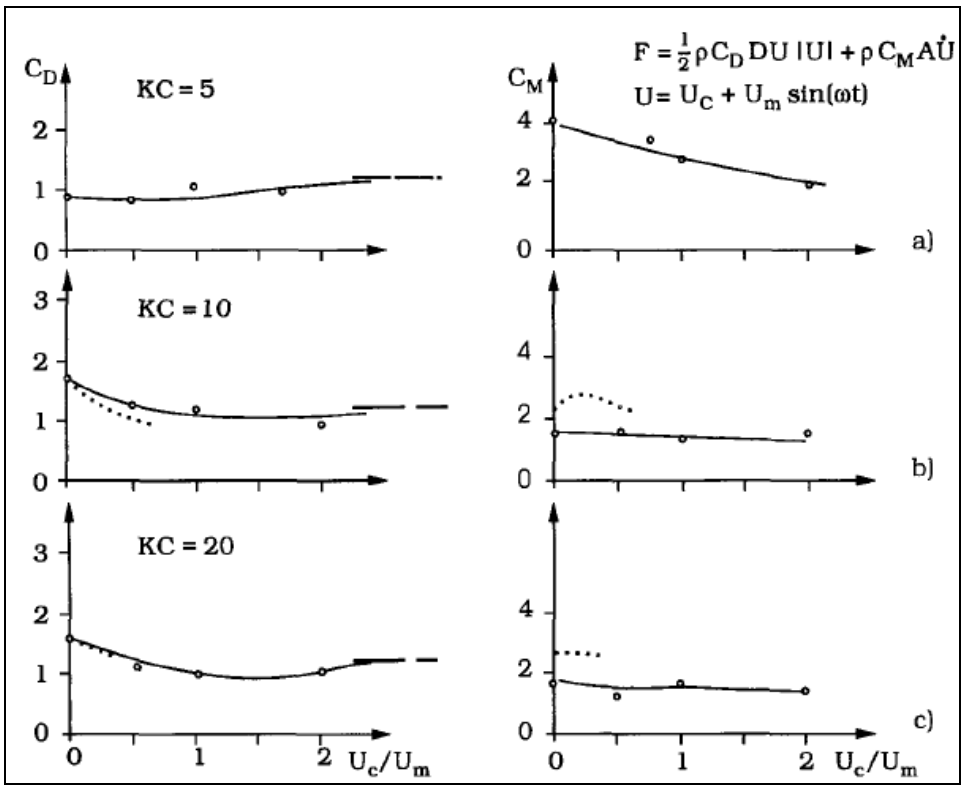

Figure 2.15 : Effect of coexisting current on in-line force coefficients (Sumer and Fredsoe (2006)).

The figure 2.16 indicates that C_{Lmax} decreases markedly when the current is superimposed on the oscillatory flow. As the ratio U_c/U_m increases, the lift

coefficient might be expected to approach its asymptotic value obtained for the current-alone case (which is indicated with dash lines in the figure 2.16) (Sumer and Fredsoe (2006)).

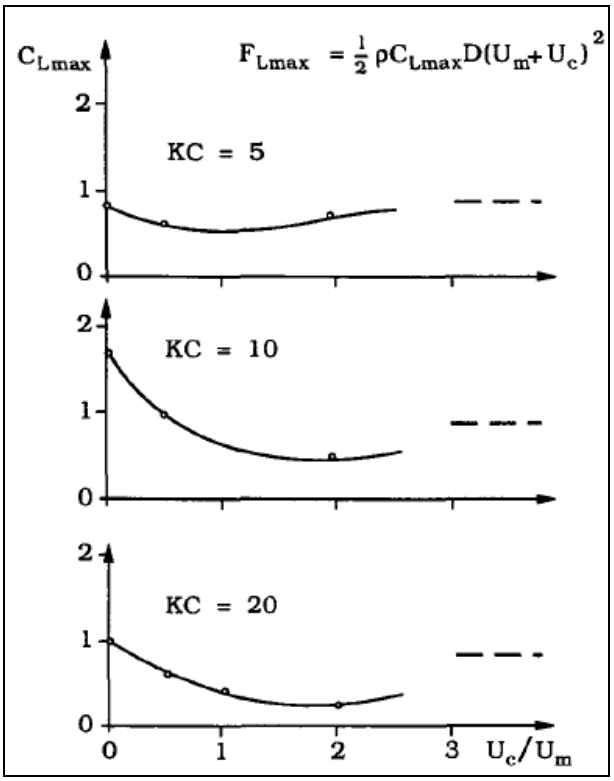

Figure 2.16 : Effect of coexisting current on lift coefficients (Sumer and Fredsoe (2006)). ($k/D = 4x10^{-3}$, $Re=3x10^4$. Dash lines are asymptotic values for steady current for $Re=3x10^4$).

It may be concluded that from the presented results that the superposition of a small current on waves may generally reduce the force coefficients. As the current component of the combined waves and current flow becomes increased, however, the force coefficient tends to approach their asymptotic values measured for the case of current alone (Sumer and Fredsoe (2006)).

3. NUMERICAL MODELLING TECHNIQUES

With the advances in Computer technology, numerical methods can be used in more and more areas of science and engineering. These design and computational methodologies are called Computer Aided Engineering (CAE). Computational Fluid Dynamics (CFD) and Computational Structural Dynamics (CSD) are two of the examples of high technology enabled numerical methodologies. With help of advance computer resources, Fluid mechanics/dynamics and structural dynamics problems can be solved with help of computer models. CFD software is very good alternative and/or support platforms to expensive and time consuming laboratory experiments.

3.1 CFD

After progress in Computer technology, engineering problems can be solved using numerical techniques with more accuracy. Computational Fluid Dynamics enable us to investigate and understand Fluid Dynamics problems in more detail and more ease. Computational Fluid Dynamics can be defined as the science of predicting fluid flow, heat and mass transfer, chemical reactions and related phenomena. To achieve these goals (to predict aforementioned physical phenomena), CFD solves equations for conservation of mass, momentum energy etc. with help of computer resources.

Computational Fluid Dynamics (CFD) is analyzing and modeling systems that contain fluid flow or fluid related elements with computers. It is possible to define CFD as the science of predicting fluid flow, head and mass transfer and chemical reactions. In industrial and academic research and application centers are using CFD software and modeling tools in growing trend. CFD techniques have several advantages over traditional experimental techniques. Some of the advantages are summarized below (Hatipoglu, 2000).

- It is possible to design and analyze systems that are very hard to model experimentally.

- In design phase of a project, CFD techniques save significant amount of time and financial resources
- With using CFD techniques, very detailed results can be obtained for the selected problem.

In the engineering design process, CFD software systems are used in below stages:

- Concept designs and preliminary design stages
- Detailed design of a proposed product and its further development process
- Optimization of the current design
- Eliminating the design faults and Troubleshooting
- Redesign of an existing system

When comparing with cost of experimental setup of a selected problem, CFD models are very inexpensive and effective. CFD models can be created easily with using available software packages in short time period. CFD analysis complements testing and experimentation by reducing total design effort (time and man-hour) and cost required for experimentation (preparing and running physical model) and data acquisition (analyzing the data that collected from physical model).

CFD techniques have very broad range of application areas. Main application areas of CFD software packages can be summarized as below.

- Aerodynamic design of vehicles
- Hydrodynamic design of ships
- Aerodynamic design of building and bridges
- Design of building ventilation systems
- Design of off-shore engineering structures

- In biomedical engineering (for examples, modeling blood and internal structure of heart)
- Design of Engines
- Design of flow around bodies and structures

In recent years, many commercial CFD software packages have been developed. A lot of academic institutions and engineering companies are using these software packages for their research and design efforts. Main CFD packages are, Fluent (ANSYS Fluent), STAR-CD, Flow-3D, CFX (ANSYS CFX) and OPENFOAM.

3.1.1 CFD softwares

CFD software systems contain several modules that are designed to solve fluid dynamic problems. These modules are developed using numerical solution techniques and algorithms. Nearly all commercial CFD software packages are several similar fundamental elements. These main elements can be listed as below. (Figure 3.1 shows these main elements and their contents.)

1. Pre-processing module
2. Calculation module (main module, solver module)
3. Post-processing module

Pre-processing module is using for defining the problem (geometrical properties and system) and inputs. In this module, inputs and geometrical properties of the systems are arranged in a format that calculation module can understand and use.

In pre-processing, geometrical properties are defined and these defined geometry meshes with selected meshing algorithm and technique. After creating meshed geometry, boundary conditions are defined. In pre-processing phase, fluid properties may be defined as well. In most of the applications, accuracy of the solution is directly connected with mesh geometry and number of cells in it. Usually, if number of cells is increase, accuracy of the solution is also increase. But after a point, increasing number of cells or grid points do not have significant effect over accuracy

of the system, so when that point have been reached increasing of the number of cells will only increase computational expenses.

In calculation module (main CFD module), with using input and geometrical values from pre-processing module, main calculations are done. Firstly, for unknown flow characteristics, with using simple functions, some values are initialized. These values are re-calculated with flow equations and compared with beginning values. These iterations are calculated systematically until selected convergence degree reached.

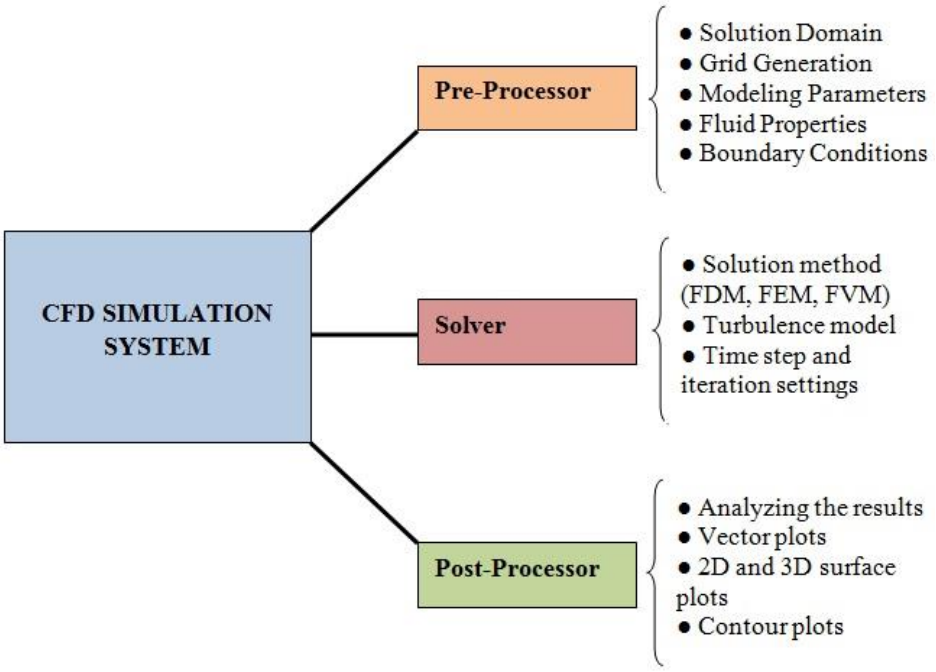

Figure 3.1: CFD simulation system overview.

CFD software packages usually use Finite Volume Methods. Some of the applications use Finite Element Methods or Finite Difference Methods as well.

Post-processing modules are used for visualize and analyze calculation module results. In this module, results can be visualized with image generation techniques, datas and results can be presented and some additional repetitive tasks can be performed on these results.

3.2 ANSYS Fluent

ANSYS Fluent is one of the most popular commercial CFD software package used by many engineering design companies and research institutes around world. With Fluent, it is possible to model fluid flow, heat transfer and chemical reactions.

3.2.1 Application areas of fluent

Fluent has very broad range of application areas. Below is a main application areas of Fluent. (ANSYS Fluent (2012))

- Modelling of steady-state or transient flows
- Modelling of compressible and incompressible flows, including all speed regimes (low subsonic, transonic, supersonic, and hypersonic flows)
- Modelling of inviscid, laminer and turbulent flows
- Newtonian or Non-Newtonian flows
- Ideal or real gases
- Heat transfer, including forced, natural, and mixed convection, conjugate (solid/fluid) heat transfer, and radiation
- Free surface and multiphase models for gas-liquid, gas-solid, and liquid-solid flows
- Cavitation model
- Phase change model for melting/solidification applications
- Porous media with non-isotropic permeability, intertial resistance, solid head conduction, and porous-face pressure jump conditions
- Acoustic models for predicting flow-induced noise
- Dynamic mesh model for modeling domains with moving or deforming mesh

3.2.2 Program's internal structure

Fluent software package is a one of the most respected commercial CFD software package around the world. It uses Finite Volume Methods (FVM) to solve the Fluid Dynamics problems.

It is possible to summarize Fluent internal structure as below (ANSYS 2012):

- Domain is discretized into a finite set of control volumes
- General conservation (transport) equations for mass, momentum, energy, spacies, etc. are solved on this set of control volumes

- Partial differential equations are discretized into a system of algebraic equations
- All algebraic equations are then solved numerically to render the solution field.

It is important to note that Fluent control volumes are cell-centered (for some other CFD codes have node-centered control volumes, such as ANSYS CFX)

3.2.3 Program's algorithm

Figure 3.2 summarizes Fluents internal solving steps (ANSYS Fluent 2012).

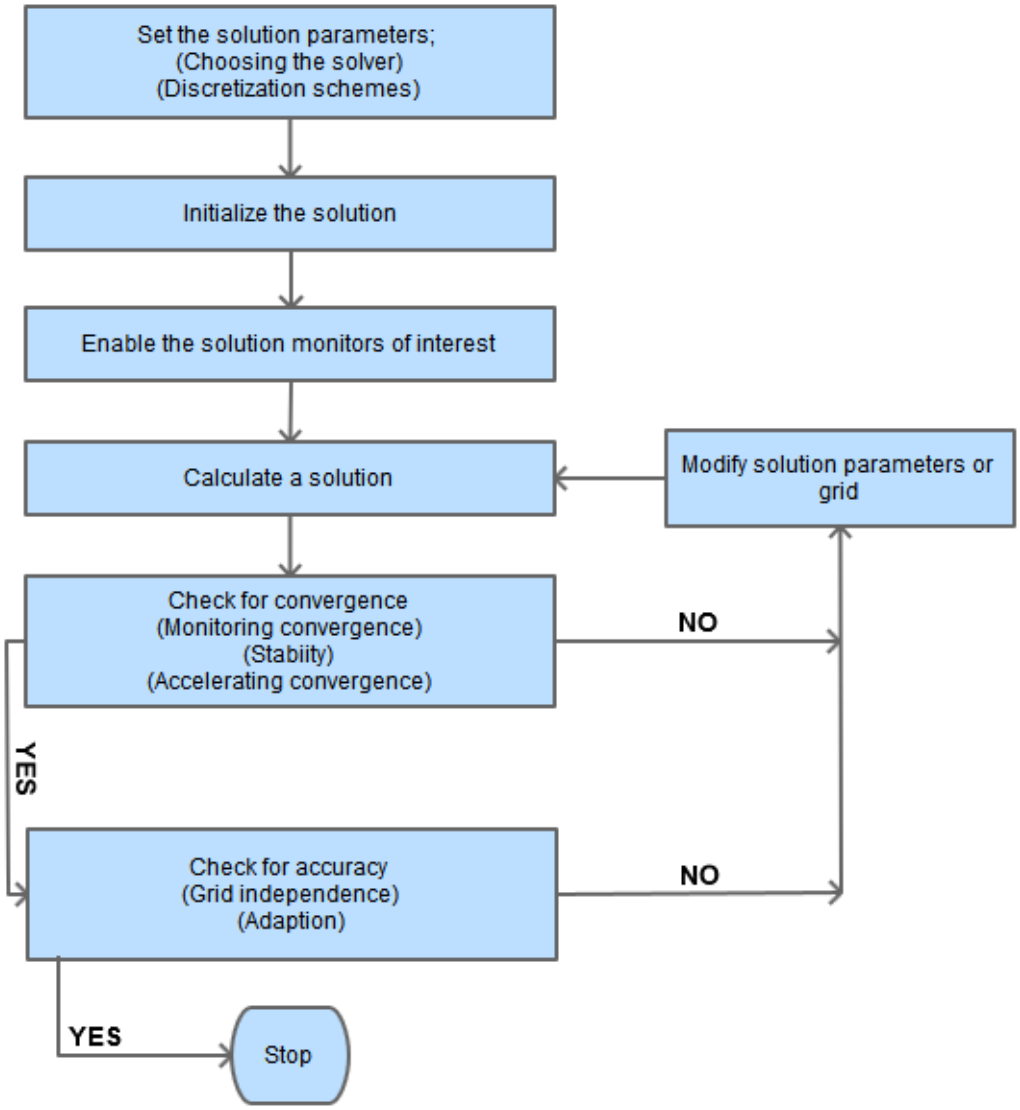

Figure 3.2: Fluent solving steps.

In fluent two solvers are available; Pressure based solver and density based solver.

3.2.4 Turbulans models

Turbulent flow characteristics can be defined as (ANSYS 2012);

- Unsteady, three-dimensional, irregular, stochastic motion in which transported quantities (mass, momentum, scalar species) fluctuate in time and space
- Enhanced mixing of these quantities result from the fluctuations.
- Unpredictability in detail
- Large scale coherent structures are different in each flow, whereas small eddies are more universal.
- Energy is transferred from larger eddies to smaller ones
- Large eddies contains most of the energy
- In the smallest eddies, turbulent energy is converted to internal energy by viscous dissipation.

There are different approaches to calculate turbulence effects; and they are DNS (Direct Numerical Simulation), LES (Large Eddiy Simulation), RANS (Reynolds averaged Navier Stokes Simulation). In these three models, RANS models are most effective and their computational costs per iteration are less expensive. (RANS models enable us to solve the system more quicker than the other two)

Main features of DNS (Direct Numerical Similation) approaches; (ANSYS 2012)

- Numerically solving the full unsteady Navier-Stokes equations
- Resolves the whole spectrum of scales
- No modelling is required
- But the computational cost is too high, so it is not practical to use.

Main features of LES (Large Eddy Simulation) approaches;

- Solves the filtered Navier-Stokes equations
- Some turbulance is directly resolved
- Computationally less expensive than DNS but the efforts and computational resources needed are still too large for most practical applications.

Main features of RANS (Reynolds Averaged Navier-Stokes Simulation) approaches;

- Solve time-averaged Navier-Stokes equations
- All turbulant motion is modeled
- For most problems the time-averaged flow (and level of turbulence) are all that needed.
- Many different models are available and this approach is the most widely used approach for industrial flows.

RANS based turbulence models which are available in Fluent are;

- One equation model (Spalat-Allmaras)
- Two equation models (standard k- ε, RNG k- ε, realizable k- ε, standard k-ω, SST k-ω)
- Reynolds Stress model
- K-kl-ω transition model
- SST transition model

To represent turbulance effects numerically, Reynolds averaged Navier-Stokes Simulation (RANS), standard K-ε turbulans model and realizable k- ε model suit in most practical applications and they serve as optimized methods.

3.3 ANSYS Mechanical

ANSYS Mechanical is a member of ANSYS product family and it uses Finite Element Analysis techniques to solve structural systems. It is one of the leading CSD (Computational Structural Dynamics) software. The software package provides a complete set of elements behavior, material models and equation solvers for a wide range of mechanical design problems (ANSYS 2012). Typical application areas for ANSYS Mechanical are:

- Structural Systems (Static and Transient) (Linear and Nonlinear structural analyses.
- Dynamic Systems (Modal analysis, random vibration, flexible and rigid dynamics)

- Heat Transfer
- Magnetostatic
- Electrical

3.4 Fluid Structure Interaction (FSI)

Fluid-Structure Interaction occurs when a fluid flow interacts with a solid structure. These interactions may cause structural deformations significant enough to change the fluid flow itself (2-way interaction).

In some application areas, deformations may be neglected on the fluid side, and in these cases 1-way Fluid-Structure Interaction technique may be used.

FSI has a critical role of understanding many engineering problems. It has application areas such as Material selection, fatigue, effect on fluid flow and structural parameters.

3.5 ANSYS System Coupling

ANSYS software package introduces a FSI solution technique called System Coupling. System Coupling provides the infrastructure to couple fields from different solvers (ANSYS (2012)). System Coupling uses ANSYS Fluent to analyze fluid behavior and ANSYS Structural to analyze structure behavior. System coupling module co-operate these two solvers in selected time frame and time steps.

ANSYS System Coupling uses the iteratively implicit approach. This approach can be briefly defined as; iteratively updating the problem until the FSI interface quantities converge. This solution technique is robust and use larger time steps.

System Coupling transfers the force and displacement quantities between the participants (in our study, ANSYS Fluent and ANSYS Structural (Mechanical)). System coupling allows fields solved in different solvers to be coupled together. For 2-way FSI analyses, iterations are typically used between the solvers within each time step so that the forces/displacements can converge at that time step.

Figure 3.3 shows schematic definition for the transient 2-way FSI simulation (ANSYS (2012)). It has three levels of iterations:

1. Time Loop: The transient loop - each loop/step moves forward in time, as in a standard CFD or FEA transient simulation.
2. Coupling Loop: Loads/displacements are updated between the FEA and CFD solvers.
3. Field Loop: The usual inner loop, used to converge the fields(s) within a solver.

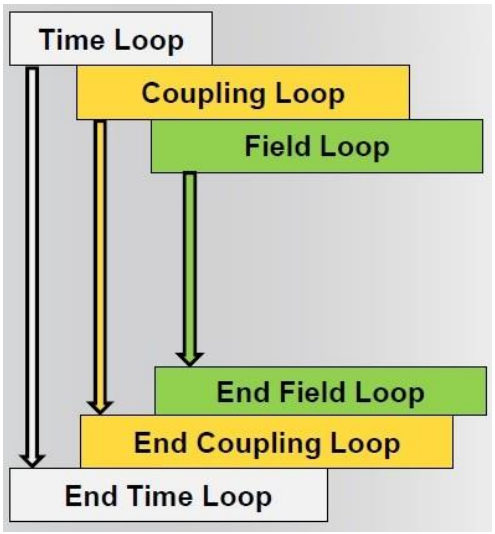

Figure 3.3: The transient 2-way FSI simulation (ANSYS (2012)).

The workflow involves identifying boundary regions in Mechanical and Fluent that will send/receive data. All coupling settings are defined in the System Coupling component. In the computer model geometry, the fluid and structural interfaces should physically match at FSI interface.

3.6 Basic Principles and Techniques of Numerical Model Preparation

Design and solution steps of the CFD models can be defined and summarized as below (ANSYS (2012)):

- Problem Identification
    1. Define design goals
    2. Identify the domain and its properties
- Pre-Processing

3. Preparing geometry
4. Creating suitable mesh
5. Physics (flow properties and related parameters)
6. Solver Settings

- Solve

7. Compute solution

- Post Processing

8. Examine the results
9. Revisions to the model (if necessary)

Below sections briefly define design and solution steps and identify required actions within these steps.

3.6.1 Defining modelling goals

In this stage following actions are taken.

- Modelling options (simplifying assumptions such as symmetry and periodicity, type of physical models to cover in the analysis)
- Degree of accuracy (required degree of accuracy)
- Calculation time frame (required time to solve the system under existing computer infrastructure)

3.6.2 Identify the domain and its properties

In this stage following actions are taken.

- Defining the computational domain (beginning and ending sections and points, boundary condition information, types)
- Investigation to find out whether or not simplified or approximated solution domain is possible (such as 2D domain, or modifying boundaries which have very little effect in the overall system to simplify the problem domain)

3.6.3 Preparing geometry

In this stage following actions are taken.

- Preparing models using built in tools or exporting the base model from CAD package and modifying it.
- Extract the fluid region from a solid model.
- Remove unnecessary features that would complicate meshing process
- Make use of symmetry

3.6.4 Creating suitable mesh

In this stage following actions are taken.

- Determining the required mesh resolution in each region of the domain
- Predicting the regions of high gradients (mesh should resolve geometric features of interest and capture gradients of concerns, e.g. velocity, pressure, temperature gradients)
- Selecting the type of mesh (the most appropriate mesh structure) based on geometry's complexity and solution requirements) (such as quad/hex mesh or tri/tet or hybrid mesh)
- Determining computer resources (number of cells/nodes and type of physical model)
- Create the mesh structure based on above stages.

3.6.5 Physics (flow properties and related parameters)

In this stage following actions are taken.

- Define material properties (for fluid, solid and mixture)
- Select appropriate physical models (such as turbulence, combustion, multiphase, etc)

3.6.6 Solver settings

In this stage following actions are taken.

- Prescribe operating conditions

- Prescribe boundary conditions at all boundary zones
- Provide initial values (or values from a previous solution)
- Set up solver controls
- Set up convergence monitors

3.6.7 Compute solution

In this stage following actions are taken.

- The computer will solve the discretized conservation equations iteratively until convergence.
- Convergence is reached when changes in solution variables from one iteration to the next are negligible.

3.6.8 Examine the results

In this stage following actions are taken.

- With using visualization tools solutions are visualized.
- Overall flow pattern, separation points, shear layer are investigated.
- Numerical reporting tools can be used to calculate quantitative results such as forces and moments, average heat transfer coefficients or surface and volume integrated quantities.

3.6.9 Revisions to the model

After examining the results, if the model is not met design goals, some revisions can be considered in the numerical model. In this stage following actions are taken.

- Revision to the physical model properties
- Revision to the boundary conditions
- Revision to mesh structure
- Revision to the solver setups

After revision to the model, new solution results will be in optimized form for the problem domain and the results will meet the design goals. (If the model is not met the design goals, revision process are carried out until the required goals are met.)

4. NUMERICAL MODELLING

In these types of problems (flow around bodies, for example cylindrical structures, pipe lines), the system can be assumed as rigid with fix supported, rigid with elastic supported or elastic with fix supported, based on system's configuration or the materials which are used. In most situations, pipes can be assumed as rigid bodies so system can be modeled as rigid cylinder with fix or elastic supports. To use these configurations, the pipe or structure material should be suitable. The main material should not deform under given loads and should maintain its shape. If the pipe's material has highly elastical properties such as PE, the pipe should be taken as an elastic structure and it should be modeled to represent its elastical properties in order to model the overall system correctly.

After recent developments in computational engineering (with advances in CPU, GPU and HPC technologies) and software packages (fluid, structural solvers and coupling algorithms), modeling and calculating elastical behaviors of such systems are more feasible. The latest improvements in computer technology give engineers new opportunities to solve and understand complex problems with more accuracy in less computational time frame.

In numerical models because of the elastical properties of PE material, system needs to be prepared as elastical pipes with fix supports and Fluid – Structure Interaction should be taken into account. Moreover, to represent Fluid – Structure Interaction correctly and accurately the prepared model should be a fully coupled one.

In this study, analyses of numerical model were carried out by using ANSYS (commercial software packages) which is introduced briefly in Section 3. Main criteria for selecting ANSYS package is its capabilities to simulate FSI mechanism and enable us to prepare a fully coupled interaction system.

For the computer model, ANSYS Fluent CFD software system (as fluid solver) was used for modeling fluid behavior and ANSYS Mechanical (as structural solver) was used for modeling structural behavior. To achieve a coupled behavior, these two

solvers were connected to each other by using ANSYS System Coupling component (as coupling algorithm).

4.1 Setup and Inputs for Numerical Models

Figure 4.1 shows the 3D physical domain of our system. The system was considered as a rectangular prism fluid domain (fluid enclosure) with a cylindrical structure (fixed at both ends). Our numerical models mainly consisted of 3 parts; fluid, solid and coupling system. These three parts were, ANSYS Fluent, ANSYS Mechanical and ANSYS System Coupling respectively.

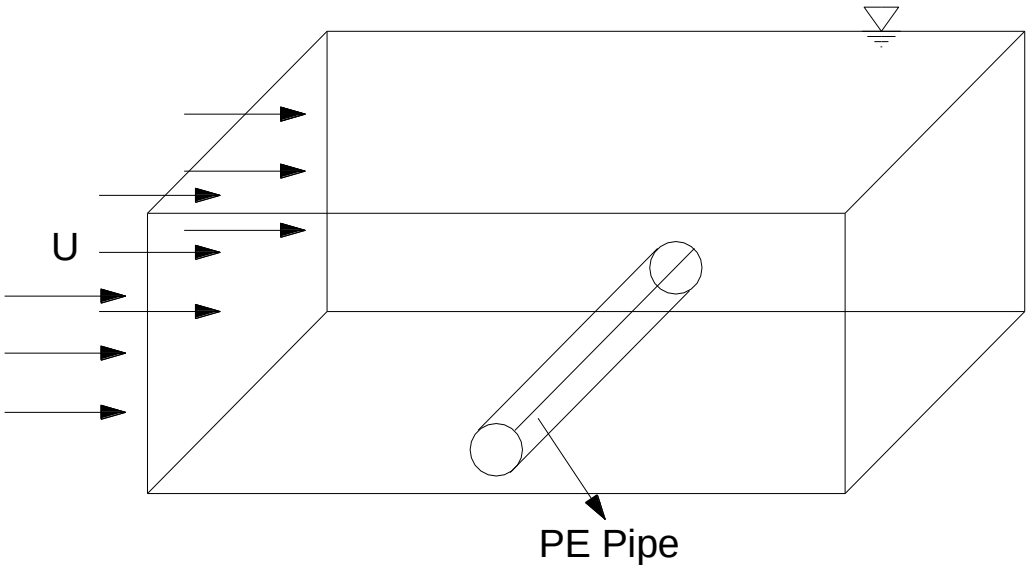

Figure 4.1: 3D physical domain of the problem.

In the beginning, geometry of our problem domain was created (based on our 3D physical domain, see figure 4.1) in the geometry module (Ansys DesignModeler) of the program.

The geometry consisted of two parts, first part was pipe and the second one was fluid enclosure. After creation of the geometry, physical and numerical domains for our problem were identified. In addition, for identified domains, boundary conditions were specified individually in the models.

The computational domain was created in ANSYS DesignModeler. Computational domain modeled as rectangular fluid enclosure with a cylindrical structure.

Figure 4.2 shows the numerical model and figure 4.3 identifies numerical model's elements. Figure 4.4 shows 2D view of computational domain of our system.

Table 4.1 presents boundary conditions that we defined in ANSYS DesignModeler.

Table 4.1: Boundary conditions for the fluid domain.

Domain	Boundaries	Type
fluid_d	Bottom_face	SYMMETRY
fluid_d	Inlet	VELOCITY-INLET
fluid_d	Left_face	SYMMETRY
fluid_d	Outlet	PRESSURE-OUTLET
fluid_d	Pipe_surface_fluid	WALL
fluid_d	Right_face	SYMMETRY
fluid_d	Top_face	SYMMETRY

Figure 4.5 shows typical pipe element. Pipe element was modeled with its diameter and thickness.

For different pipe diameters, thicknesses were taken from the pipe manufacturers catalog and the same span lengths as the physical model setup were used. For different pipe diameters and span lengths computational domains properties (geometry) were adjusted.

Boundary conditions were defined in the ANSYS DesignModeler and they were same for all numerical models.

In DesignModeler, fluid domain and pipe element were defined and pipe element was subtracted from fluid domain to create a fluid enclosure. Finally, we had a model with two main parts, fluid enclosure and pipe structure.

It is important to note that, pipe diameter, span lengths, inlet and outlet lengths were defined as parameters to create a parametric design model. In this model, changing the parameters would change the model setup and create a new geometry without requiring to model from zero point.

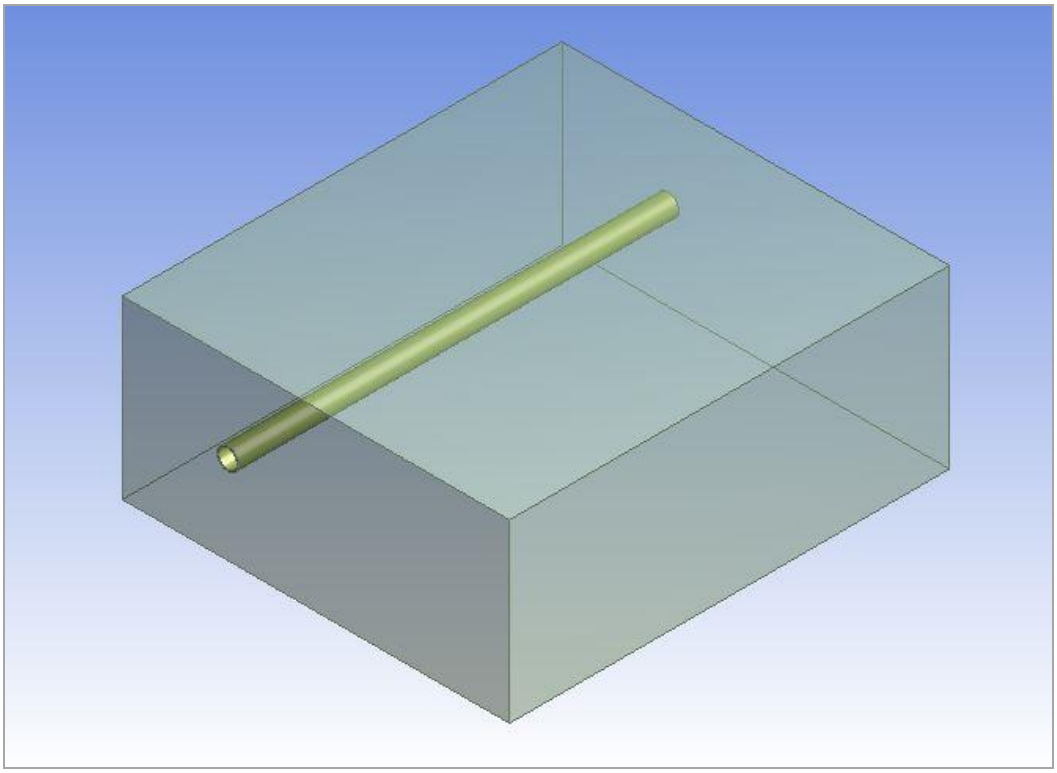

Figure 4.2: Numerical model (computational domain).

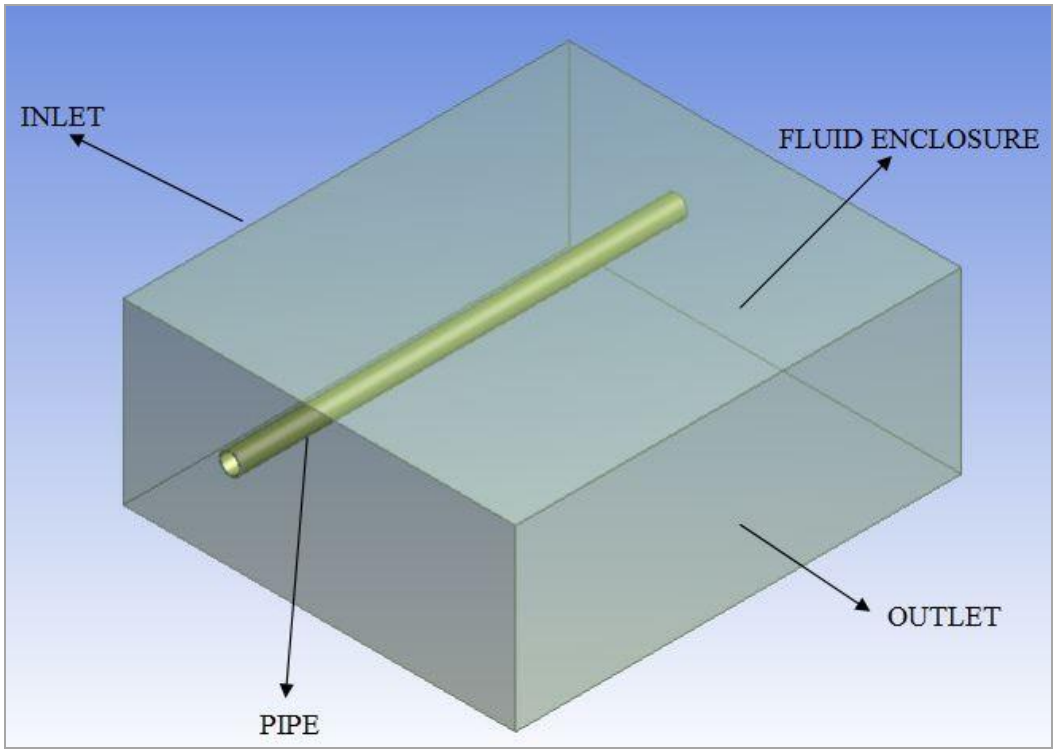

Figure 4.3: Setup elements of the numerical model.

Figure 4.4: Computational domain in 2D.

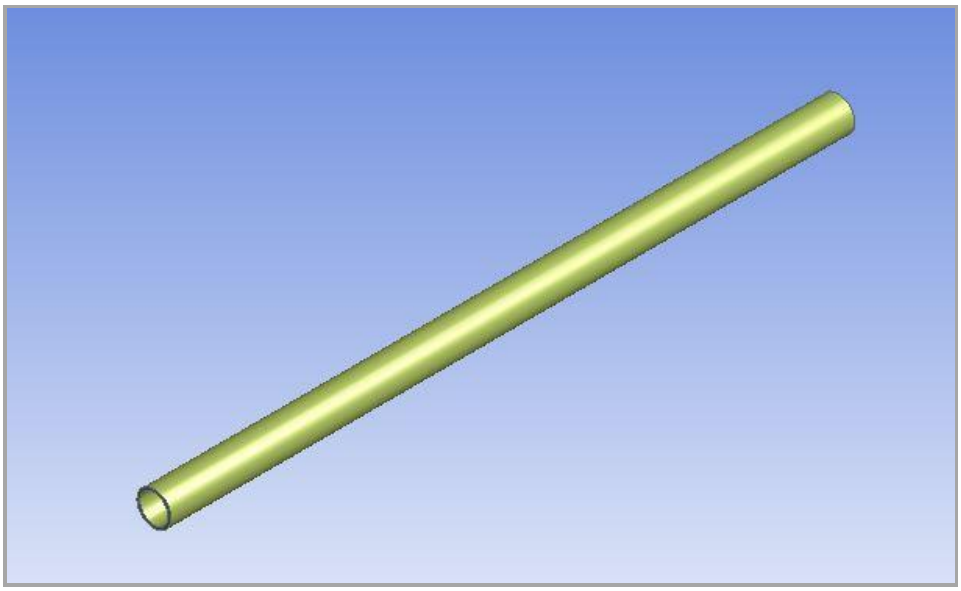

Figure 4.5: Pipe.

For defined geometry and boundary conditions, a suitable mesh structure was created.

Because of the limited software license and computational resources, only medium mesh structure was generated and run.

Around the pipe, mesh refinement was increased to capture and analyze results more clearly.

In Figure 4.6, computational domains overall mesh structure is presented. In the computational model, unstructured mesh was used. Figure 4.7 and Figure 4.8 show mesh structures from different viewpoints.

Table 4.2 summarizes mesh information for the fluid domain.

Table 4.2: Mesh information for fluid domain.

Domain	Nodes	Elements
fluid_d	33356	175393

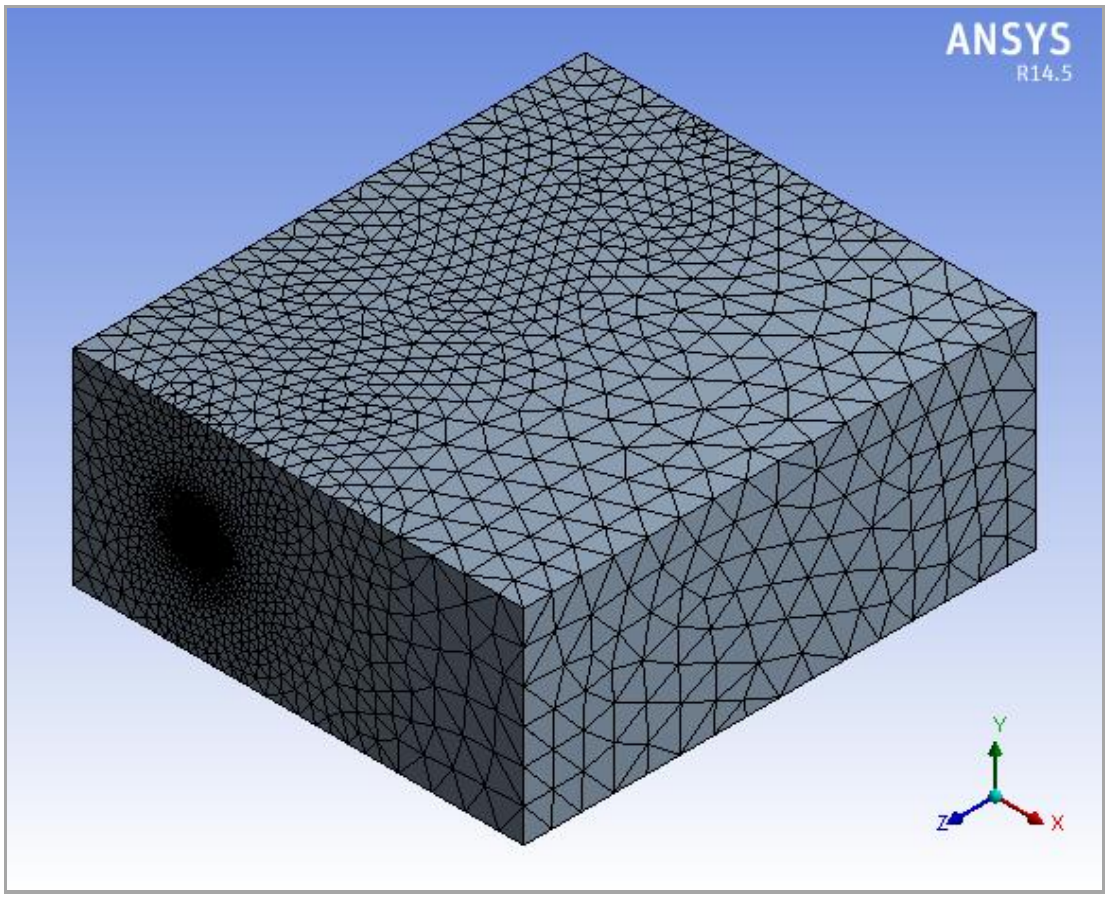

Figure 4.6: Defined mesh structure 3D.

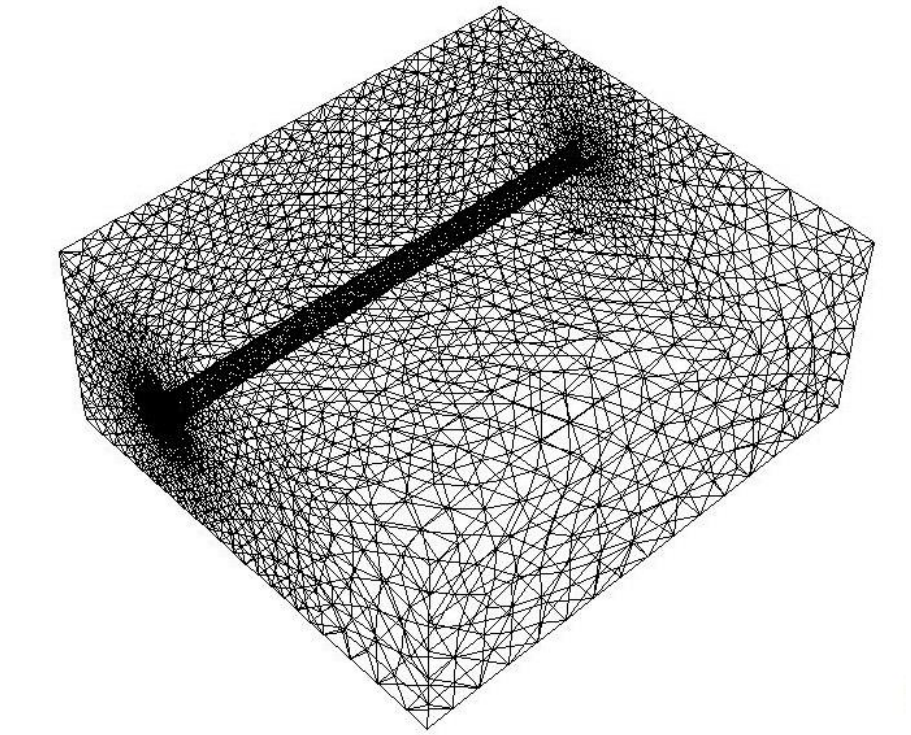

Figure 4.7: Defined mesh structure (inside view).

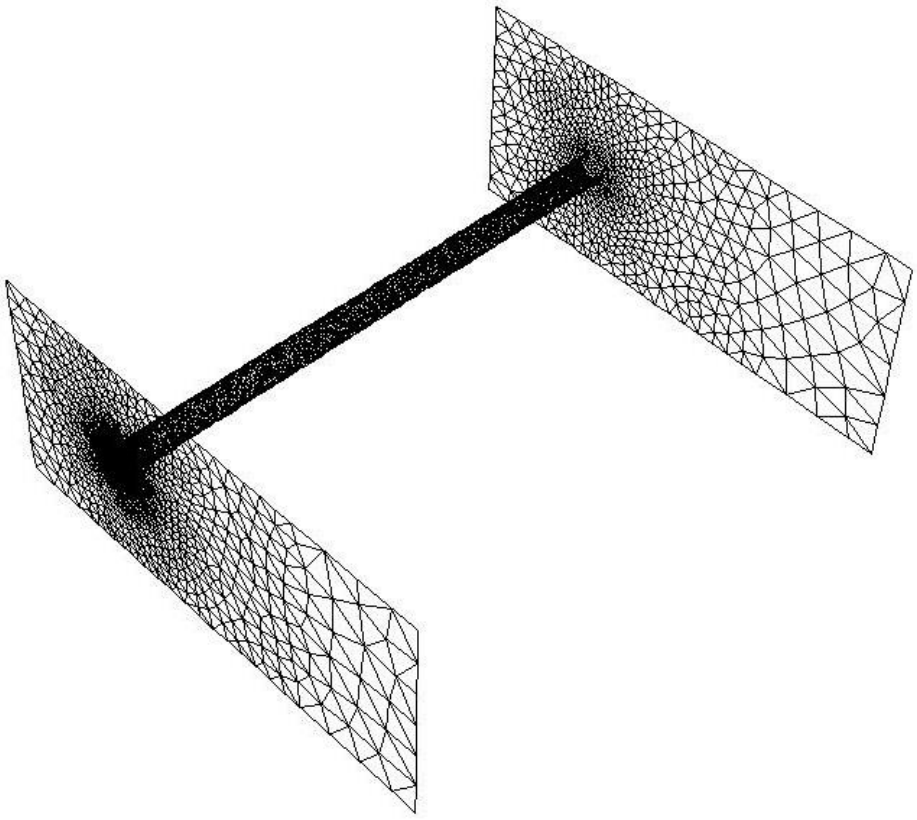

Figure 4.8: Defined mesh structure (two planes and pipe).

A symmetry plane was created in order to decrease the number of elements in numerical models and decreasing total number of elements (and nodes) enabled us to decrease total calculation time in solving stage.

Table 4.3 shows the Numerical Model Matrix below.

Table 4.3: Numerical modal matrix.

Condition	Pipe Diameters		
	D50	D63	D125
Current (Flow velocity=25 cm/s)	C50	C63	C125
Wave (Wave height=30 cm, wave period = 1.2 s)	W50	W63	W125
Current+Wave (Flow velocity=25 cm/s + Wave height=30 and wave period = 1.2 s)	CW50	CW63	CW125

As we explained in above section, all geometry preparations and preprocessing stage was completed by using ANSYS DesignModeler.

4.1.1 Setup and input for CFD solver

As CFD solver, ANSYS Fluent were used for the numerical models in this study.

For current velocity, 0.25 m/s was used, which was the same as the pyshical model conditions.

Turbulent flow characteristics and other required flow related parameters were given to CFD Solver as inputs (see appendix B for more detailed information).

K-ε turbulans model was used in ANSYS Fluent models. This turbulance model is well know and suitable for our problem domain.

K-ε turbulans model is known as robust and very widely used turbulans model. It gives reasonably acceptable results.

For flow velocity 25 cm/s was used and for wave height 30 cm was used.

Re and KC numbers were calculated for each case as well and in our study, Reynolds numbers were between ~5000 to ~31000 in our model cases.

Boundary conditions were identified to the solver and their properties were input. (Pressure inlet, pressure outlet and for cylinder surface, wall boundary conditions)

4.1.2 Setup and input for CSD solver

Pipe material properties and supports were defined in the CSD solver accordingly (see appendix B for more detailed information).

Material properties were identified, in CSD solver only HDPE materials engineering properties were input, because solver only interested in solid material properties.

In figure 4.9, material properties for pipe structure is presented.

Properties of Outline Row 3: Polyethylene

	A	B	C	D	E
1	Property	Value	Unit		
2	Density	950	kg m^-3		
3	Isotropic Secant Coefficient of Thermal Expansion				
4	Coefficient of Thermal Expansion	0.00023	C^-1		
5	Reference Temperature	22	C		
6	Isotropic Elasticity				
7	Derive from	Young's Modulus...			
8	Young's Modulus	1.1E+09	Pa		
9	Poisson's Ratio	0.42			
10	Bulk Modulus	2.2917E+09	Pa		
11	Shear Modulus	3.8732E+08	Pa		
12	Tensile Yield Strength	2.5E+07	Pa		
13	Compressive Yield Strength	0	Pa		
14	Tensile Ultimate Strength	3.3E+07	Pa		
15	Compressive Ultimate Strength	0	Pa		

Figure 4.9: Material properties for pipe structure.

In structural solver, pipe element was meshed accordingly. Mesh structure for pipe elements is shown in figure 4.10 and close up view shown in figure 4.11.

Table 4.4 presents pipe mesh statistics.

Table 4.4: Pipe mesh statistics.

Domain	Nodes	Elements
pipe	24136	3696

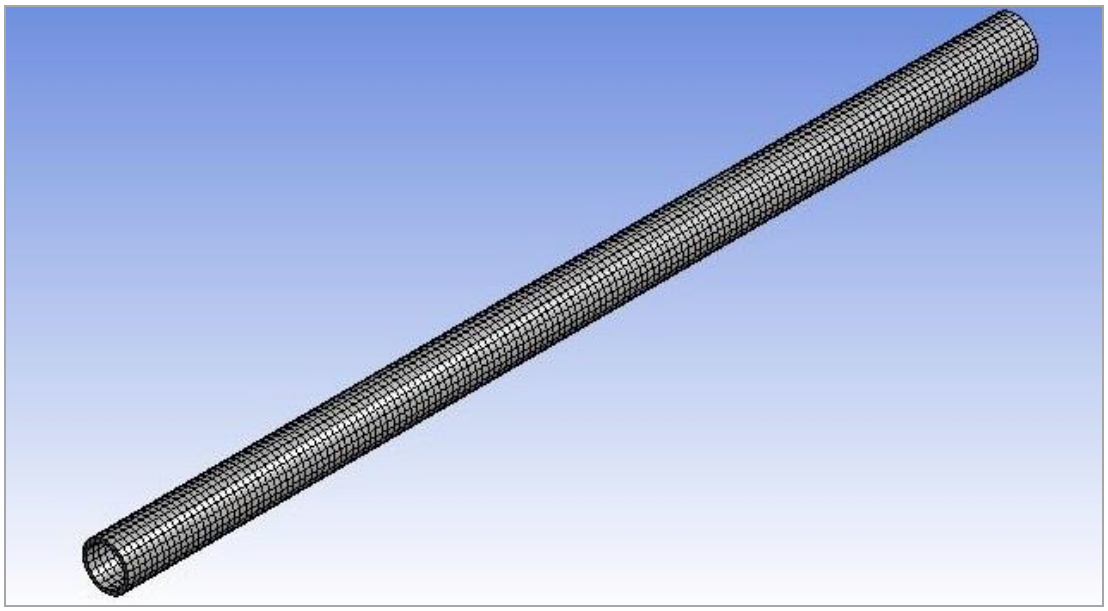

Figure 4.10: Mesh structure for pipe element.

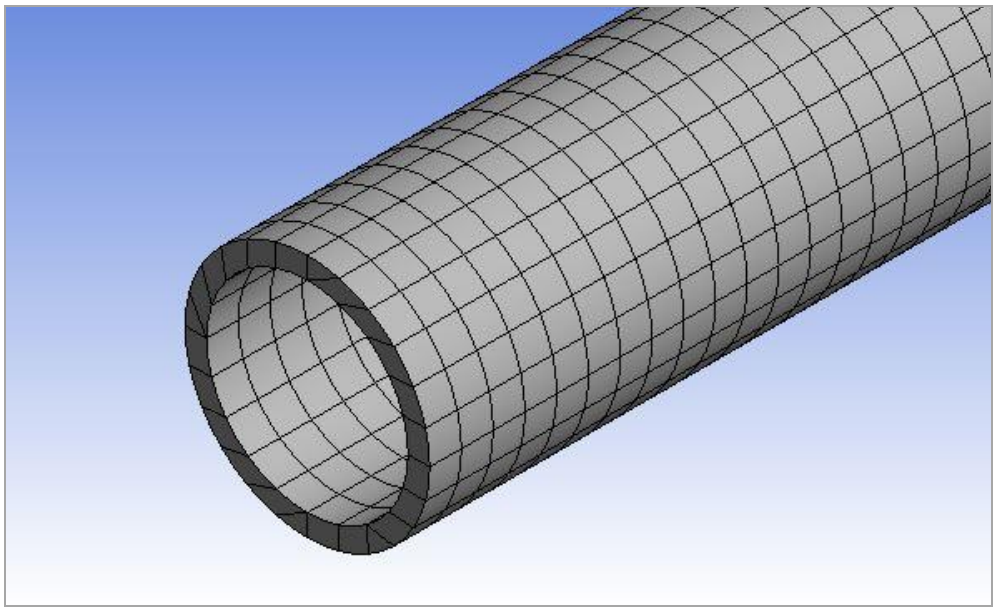

Figure 4.11: Close up view of mesh structure for pipe element.

In our study, we use Transient Structural solver for our coupled analyses.

4.1.3 Setup and input for system coupling

In the System Coupling modul, coupling mechanism and Fluid Structure Interface regions were defined and adjusted accordingly.

Figure 4.12 shows the System Coupling procedure for the entire problem domain.

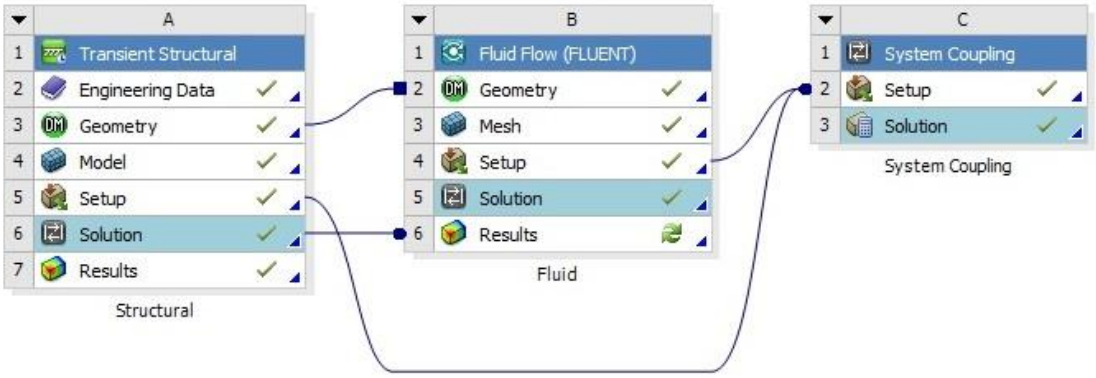

Figure 4.12: System Coupling Procedure.

Cylinder surface was defined as fluid-solid interface region. Figure 4.13 shows fluid-solid interface region.

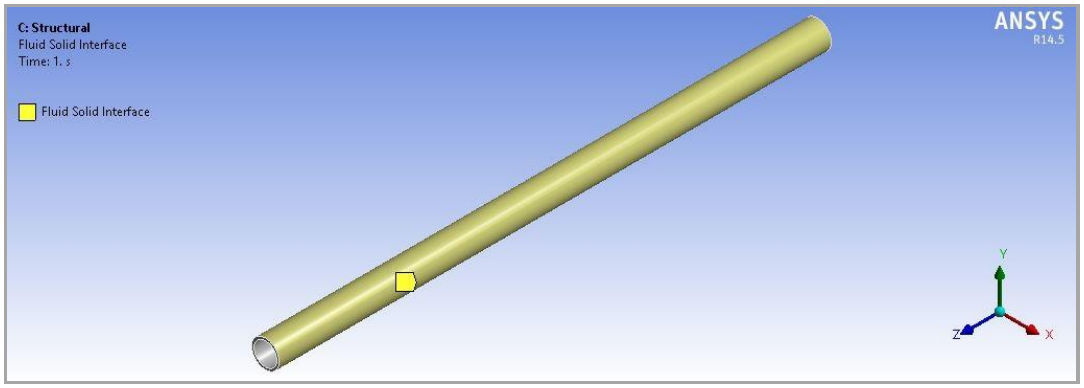

Figure 4.13 Fluid-Solid interface.

In fluid - structure interaction analyses, force components were transferred to mechanical module and calculated deformations were transferred back to CFD (Fluent) module and with dynamic mesh feature of the program, mesh structures were adjusted accordingly.

4.2 Analysis of Numerical Model Results

Numerical models were analyzed using aforementioned system setup. All models and each cases in numerical model matrix were run by using their predefined input parameters and calculation results were prepared for post-processing stage.

In these analyses for our computer models, Reynolds numbers values were ranging from ~5000 to ~31000.

For cases with wave loads, waves were assumed as sinusoidal waves and were input into the system as such, and loadings were applied accordingly.

Coupling system was defined with system coupling and for fluid domain Fluent, for pipe structural responses Mechanical modules were used.

Analyses of numerical model results were post-processed using Fluent's result analysis tools, mechanical results diagrams and ANSYS CFD-Post.

From the 3D computational domain, certain planes were defined and the contours, vectors and other results have been presented in these planes for fluid flow characteristics.

For pipe structure, resultant diagrams for deformation, minimum and maximum principle stresses and equivalent stress diagrams of a selected numerical model are presented in the section 7 and Appendix B.

Input parameters of the models and selected results are given in Appendix B.

Summary of the results from selected computer models and example cases are presented in Section 7.

5. PHYSICAL MODELLING

In order to determine the behaviour of the PE pipes under hydrodynamic loads, a physical laboratory models were prepared in Istanbul Technical University, Civil Engineering Faculty Hydraulic Lab.

This research is also a part of a Scientific Research Project.

In this phase of the research, pipe specimens were placed in the test system and long term hydrodynamic loadings have been applied to them.

In the physical model (laboratory model), test speciments (PE pipes) were subject to hydrodynamic forces (long term- approximately 1.5 months 7 hour every day, total of 300 hours) that were caused by current and wave effects. During these tests, 3 different conditions were applied. First one, only current was exist, in second one only wave effects was exist and in the last one current and wave effects were applied together. After these long term hydrodynamic loading, the pipes were sent to test in material laboratory to find out change in their material properties caused by these long term hydrodynamic loading.

PE80 and PE100 pipes (ϕ20, ϕ32, ϕ50, ϕ63, ϕ110 and ϕ125 mm in diameter) were tested against selected flow characteristics. After number of tests, these pipes were sent to materials lab to investigate the possible changes in their material properties.

5.1 Experimental Setup

In the ITU Hydraulics Laboratory, physical model for the long-term hydrodynamics test was prepared.

The experiments were carried out in the 22 m long, 1.45 m deep and 6 m wide channel at the Hydraulics lab of ITU. To observe the flow conditions, the channel width were narrowed down to 3 m. In addition to this, a glass wall and an observation room were placed.

Span lengths for test specimens were adjusted as 50 cm to 300 cm.

In the tests, wave period=1.2 s, wave height=30 cm and flow velocity=25 cm/s were selected.

Figure 5.1 and Figure 5.2 show the test channel plan and test channel longitudinal profiles respectively. Figure 5.3 shows system elements of the experimental setup. Figure 5.4 and Figure 5.5 show experimental set up after the test specimens fixed the channel. Setup plan sketch and sections are shown in Figure 5.6, 5.7 and 5.8. Other detailed photos, which show the experimental setup in more detail, are given in Appendix A.

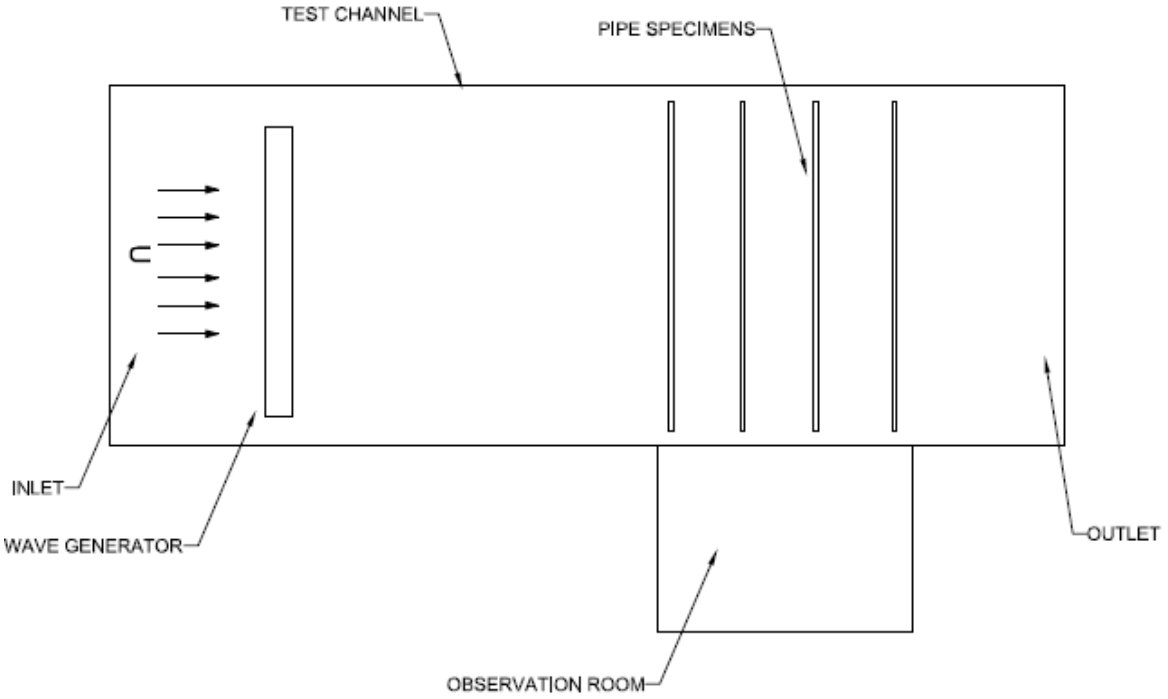

Figure 5.1: Test channel plan.

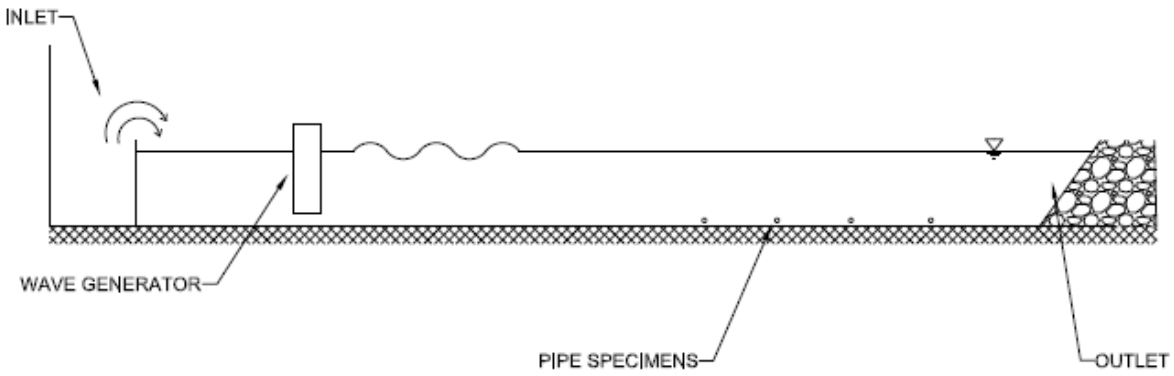

Figure 5.2: Test channel longitudinal profile.

System parts for experimental setup were:

- Water channel
- Wave and current generator
- Observation room
- Water outlet channel

Test specimen pipes were fixed the channel by using rectangular prism fixing claps.

Between these fixing points, pipe behaves as fixed at both ends cylindrical beam structure.

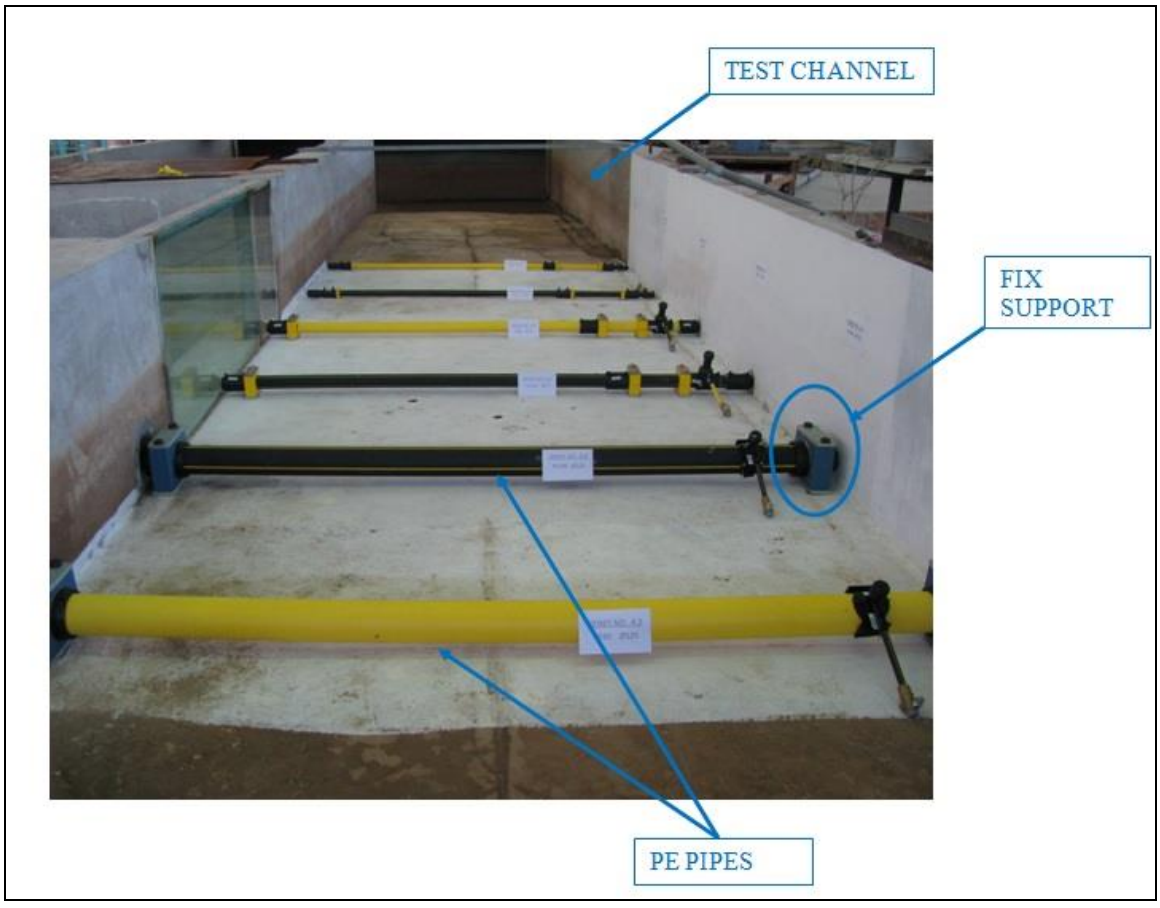

Figure 5.3: System elements of the experimental setup.

After installation of the pipes to the test channel, pipes were pressurized with 4 bar to simulate the real conditions in the prototype.

Moreover, in this model, there was no scaling factor. All elements in the system and all the conditions were same as the prototype so there were no scaling factors or corrections.

Figure 5.4: Experimental setup in the hydraulic lab.

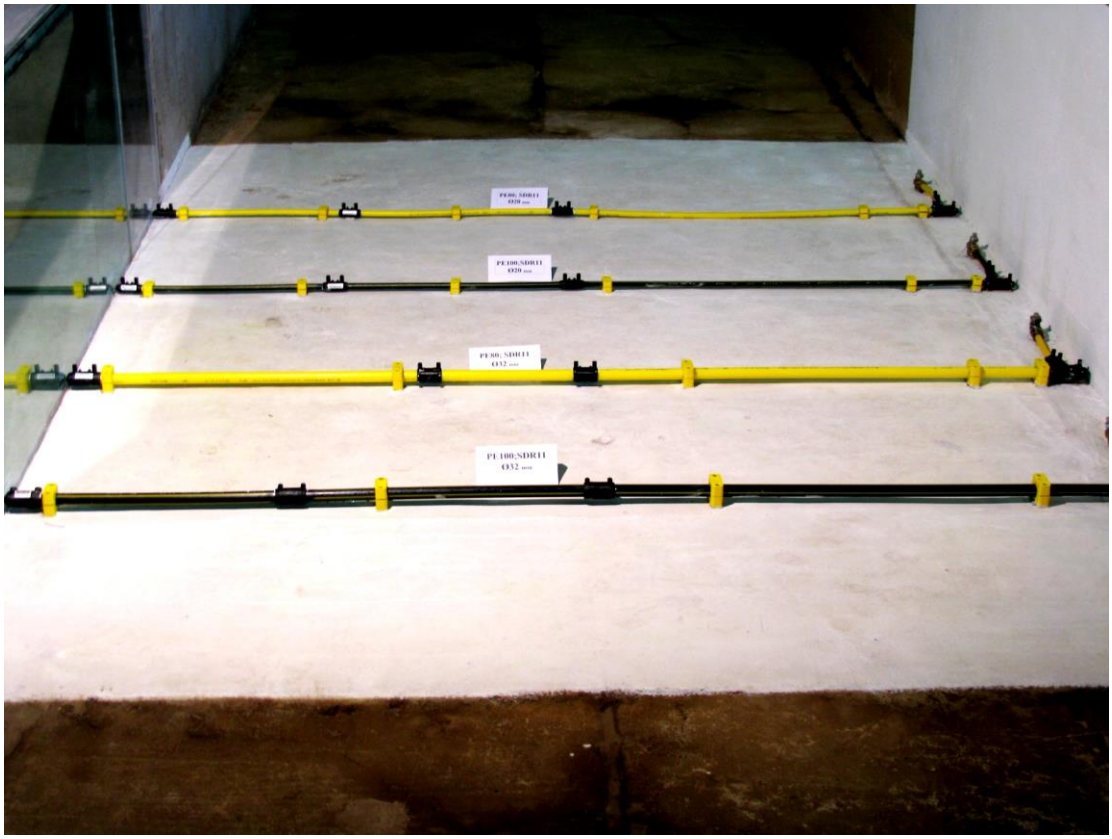

Figure 5.5: Experimental setup in the hydraulic lab.

Table 5.1 presents setup conditions that were used in the experimental laboratory setups for all three cases.

Table 5.1: Test setups.

Condition	Test Setup
Current	Flow velocity=25 cm/s
Wave	Wave height=30 cm and wave period = 1.2 s
Current+Wave	Flow velocity=25 cm/s + wave height=30 and wave period = 1.2 s

Work items during physical lab test and test setup conditions are explained in Table 5.2. Working plan for 2010 and 2011 is shown in Table 5.3 and revised working plan for 2012 is shown in Table 5.4.

Table 5.2: Work items and physical test setup conditions.

<table>
<tr><th>ITEM NO</th><th colspan="5">ITEM</th><th>TIME (week)</th></tr>
<tr><td>1</td><td colspan="5">Preparation of the test setup (İTÜ)</td><td></td></tr>
<tr><td>2</td><td colspan="5">Providing the required materials and equipments (Construction materials, software and measurement devices) (İTÜ, İGDAŞ, FIRAT)</td><td></td></tr>
<tr><td>3</td><td colspan="5">Preparation of the physical models (Model PE pipes, installation and adjustments)(İTÜ, İGDAŞ, FIRAT)</td><td></td></tr>
<tr><td rowspan="6">4</td><td rowspan="6">Physical Tests (İTÜ)</td><td rowspan="6">Pipe type, pipe diameter and test conditions</td><td rowspan="3">4.1</td><td rowspan="3">PE80: ϕ20 ve ϕ32
PE100: ϕ20 ve ϕ32</td><td>4.1.1 Current tests
(Water level, h=40 cm;
Flow velocity, U_C= 25 cm/s), (Re=U_cD/ν)</td><td>6</td></tr>
<tr><td>4.1.2 Dalga Deneyleri
(Water level, h= 40 cm
Wave period, T=1.2 s
Wave height, H_s=30 cm)(KC=UmT/D)</td><td>6</td></tr>
<tr><td>4.1.3 “Dalga + Akıntı” Deneyleri
(Water Level, h= 40 cm,
Flow velocity, U_T= 25 cm/s (U_c+U_m)
Wave Period, T= 1.2 sn
Wave height., H_s= 30 cm)</td><td>6</td></tr>
<tr><td rowspan="3">4.2</td><td rowspan="3">PE80:ϕ50, ϕ63, ϕ110, ϕ125
PE100:ϕ50, ϕ63, ϕ110, ϕ125</td><td>4.2.1 3 “Dalga + Akıntı” Deneyleri
(Water Level, h= 40 cm,
Flow velocity, U_T= 25 cm/s (U_c+U_m)
Wave Period, T= 1.2 sn
Wave height., H_s= 30 cm)</td><td>6</td></tr>
<tr><td>4.2.2 Dalga Deneyleri
(Water level, h= 40 cm
Wave period, T=1.2 s
Wave height, H_s=30 cm)(KC=UmT/D)</td><td>6</td></tr>
<tr><td>4.2.3 Current tests
(Water level, h=40 cm;
Flow velocity, U_C= 25 cm/s), (Re=U_cD/ν)</td><td>6</td></tr>
<tr><td>5</td><td colspan="6">Analyzing of the PE pipe specimens which are taken from ITU lab tests (UGETAM)</td></tr>
<tr><td>6</td><td colspan="6">Test, Measurements and analyze results evaluations (İTÜ İGDAŞ, UGETAM, FIRAT)</td></tr>
<tr><td>7</td><td colspan="6">Taking specimens from Kartal-Adalar Undersea PE Natural Gas Pipeline (Prototype) in every 2 years (İGDAŞ)</td></tr>
<tr><td>8</td><td colspan="6">Analyzing of the PE pipe specimens which are taken from the prototype (PE80, PE100 and Concrete Block) (UGETAM ve İTÜ):</td></tr>
<tr><td>9</td><td colspan="6">Test and measurement analyzes and their relations (İTÜ, İGDAŞ, UGETAM, FIRAT)</td></tr>
<tr><td>10</td><td colspan="6">Preparation of final reports</td></tr>
</table>

Table 5.3: Working plan for 2010 and 2011.

ITEM NO	2010												2011											
	MONTHS																							
	J	F	M	A	M	J	J	A	S	O	N	D	J	F	M	A	M	J	J	A	S	O	N	D
	1	2	3	4	5	6	7	8	9	10	11	12	13	14	15	16	17	18	19	20	21	22	23	24
1																								
2																								
3																								
4																								
5																								
6																								
7																								
8																								
9																								
10																								

Table 5.4: Revised working plan for 2012.

ITEM NO			2012											
			MONTHS											
			J	F	M	A	M	J	J	A	S	O	N	D
			1	2	3	4	5	6	7	8	9	10	11	12
1			DONE											
2			DONE											
3			DONE											
4	4.1	4.1.1	DONE											
		4.1.2	DONE											
		4.1.3	DONE											
	4.2	4.2.1	DONE											
		4.2.2	DONE											
		4.2.3	DONE											
5	5.4.1	5.4.1.1	DONE											
		5.4.1.2	DONE											
		5.4.1.3	DONE											
	5.4.2	5.4.2.1												
		5.4.2.2												
		5.4.2.3												
6	6.4.1	6.4.1.1	DONE											
		6.4.1.2	DONE											
		6.4.1.3	DONE											
	6.4.2	6.4.2.1												
		6.4.2.2												
		6.4.2.3												
7	7.1	First specimen was taken from seabed in june 2008and second one was taken in june 2010.												
	7.2	In june 2010, specimen was taken from land.												
	7.3	Collecting the 2. And 3. Specimens from land												
8	8.1	Material test for first specimens which are taken from seabed part of the prototype. DONE.												
	8.2	Material test for first specimens which are taken from land part of the prototype. DONE.												
	8.3	Material test for first specimens which are taken from seabed and land part of the prototype.(UGETAM)												
9	Test and measurement analyzes and their relations *(İTÜ, İGDAŞ, UGETAM, FIRAT)*													
10	Preparation of final reports													

In the lab, below pipes were installed to the test channel and loaded with long-term hydrodynamic loadings:

- Φ20 (PE80 and PE100)
- Φ32 (PE80 and PE100)
- Φ50 (PE80 and PE100)
- Φ63 (PE80 and PE100)
- Φ110 (PE80 and PE100)
- Φ125 (PE80 and PE100)

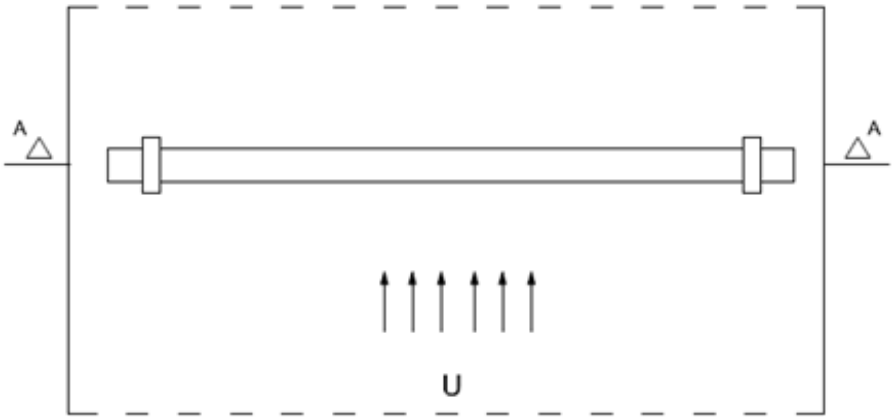

Figure 5.6: Experimental setup plan.

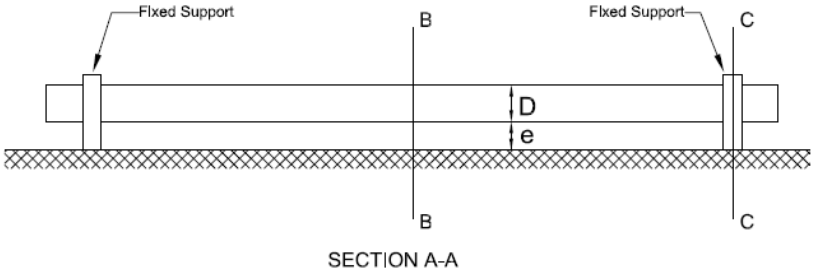

Figure 5.7: Experimental setup section A-A.

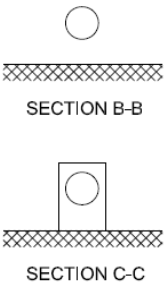

Figure 5.8: Experimental setup section B-B and section C-C.

All tests were carried out in natural conditions of the lab, and the temperatures during tests were between 15-20 ºC.

Figure 5.9 shows PE pipeline's deformed shape in static fluid conditions. (Pipeline deforms under buoyancy forces because both PE material and Natural gas are lighter than water.

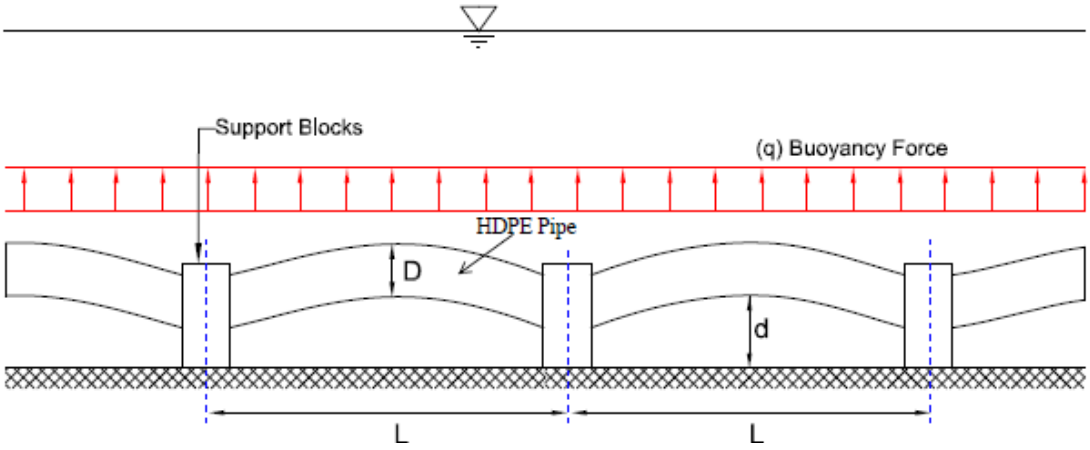

Figure 5.9: PE Pipeline's deformed shape in static fluid conditions.

Span lengths were chosen carefully based on pipe diameters and they vary between 50 cm to 300 cm respectively. (Span lengths were chosen based on pipe diameters, for larger diameters, longer span lengths were applied.)

5.2 Experimental Lab Test Methods

For the test specimens, "current", "wave" and "current + wave" conditions were applied to them. As test method, these installed pipe segments were loaded with these three different conditions in long time period.

Test system ran approximately 7 hours every day during 1.5 months (6 weeks) for every setup conditions and it is possible to conclude every test period equals to 300 hours hydrodynamic loading.

Hydrodynamic forces (Lift and Drag forces) were applied to pipes during lab experiments. In table 5.1 and table 5.2, physical laboratory test's setup conditions are briefly explained for each test case.

Figure 5.10 and Figure 5.11 show experimental setup during a test period. In this phase, current and wave were applied to the system in long time periods which explain in above.

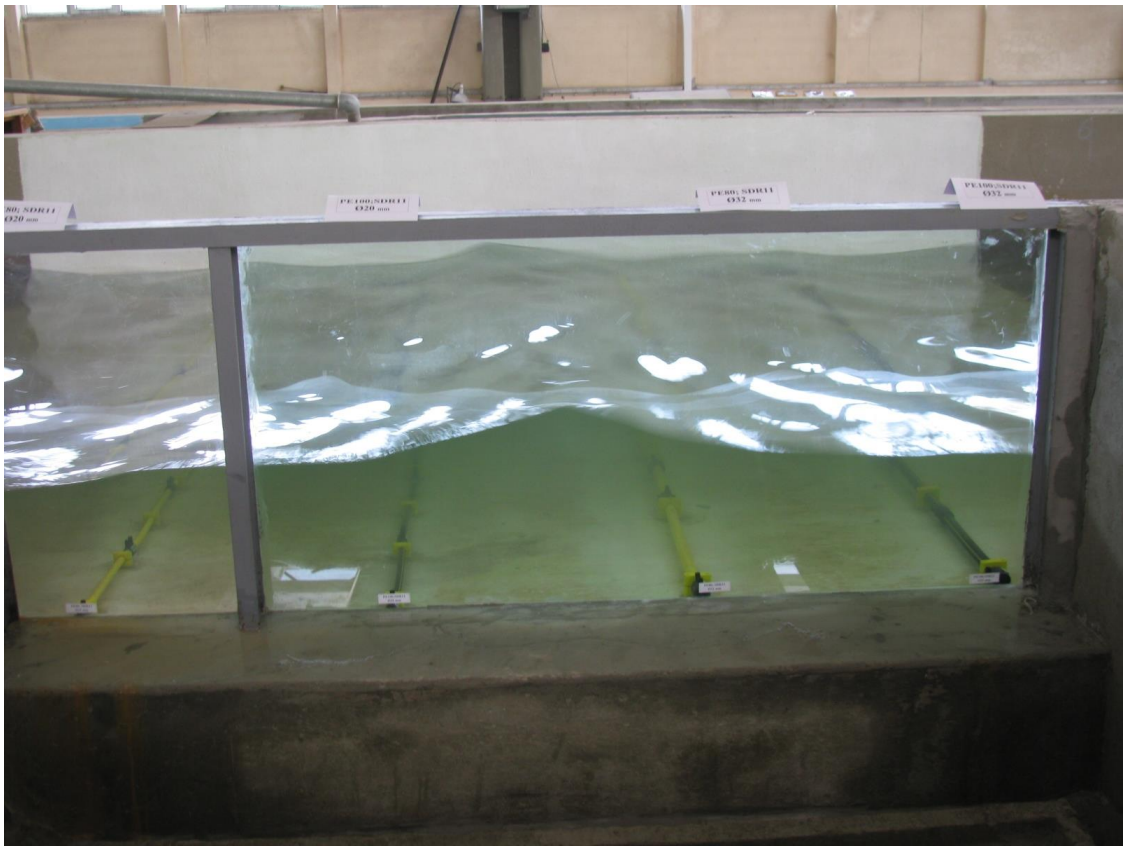

Figure 5.10: View of test setup during lab test.

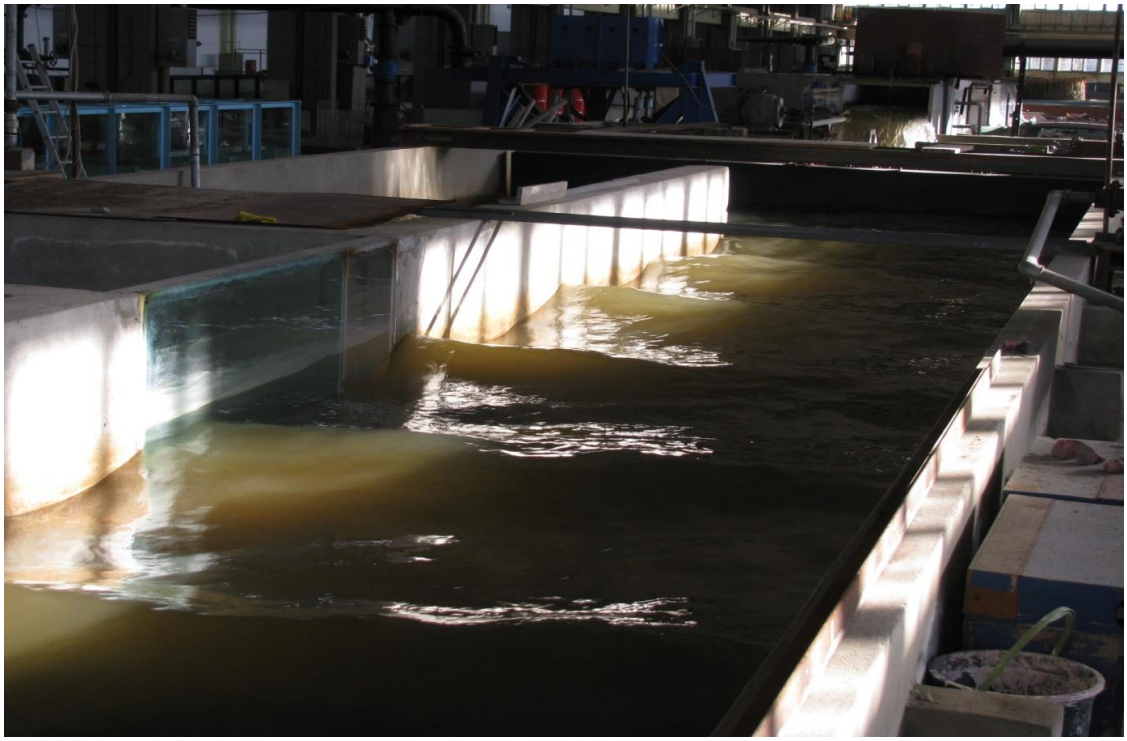

Figure 5.11: View of test channel during lab test.

For each group of test specimens, “current”, “wave” and “current+wave” loading cases were applied. For each case, approximately 300 hours of hydrodynamic loading were applied to pipes.

5.3 Test Specimens and Material Tests

After completing the required time period for every set of pipe specimens, these specimens were sent to material lab to measure their selected material properties.

For each specimens, material test (which are listed in table 5.5) were performed by UGETAM lab.

All material tests, which are explained in Table 5.5, were applied to each specimens and results were collected. These tests were carried out according to relevant specifications (which are listed in table 5.5 as well).

Table 5.5: Performed material tests

Material Test	Specification
Determination of the resistance to internal pressure	TS EN ISO 1167-1:2006
Determination of tensile properties	TS EN ISO 6259-1:2006
Slow crack growth on notched pipes (notch test)	TS EN ISO 13479
Determination of oxidation induction time	TS EN 728
Determination of the melt mass – Flow rate (MFR)	TS EN ISO 1133:2006
Longitudinal Reversion Test	TS EN ISO 2505:2006
Determining the density	TS EN ISO 1183

5.4 Results of Experiments

After completing the required test period for every set of pipe specimens and sending these specimens to material lab to measure their selected material properties, results of these tests were received.

Figure 5.12 shows one of the official material test’s result forms that were completed by UGETAM.

TÜRKAK
TÜRK AKREDİTASYON KURUMU
TURKISH ACCREDITATION AGENCY
tarafından akredite edilmiş

UGETAM

UGETAM TEST LABORATUVARI
Çamlık Mah. Yahya Kemal Beyatlı Cad. No:1
34906 Kurtköy-Pendik / İSTANBUL

AB-0094-T
T09-004
02-09

Deney Raporu
Testing Report

2.5 ÇEKME TESTİ

Test metodu: **TS EN ISO 6259 – 1: Çekme Özelliklerinin Tayini (Determination of tensile properties – Part 1 : General test method)**
ISO 6259 – 3 : **Thermoplastics pipes – Determination of tensile properties – Part 3 : Polyolefin pipes**
TS 1398-1 EN ISO 527-1 : **Plastikler - Çekme Özelliklerinin Tayini - Bölüm 1 : Genel Prensipler**
TS 1398-2 EN ISO 527-2 : **Plastikler - Çekme Özelliklerinin Tayini - Bölüm 2: Kalıplama ve Ekstrüzyon Plastikleri İçin Deney Şartları**
TS 1398-3 EN ISO 527-3 : **Plastikler - Çekme Özelliklerinin Tayini - Bölüm 3: Film ve Levhalar İçin Deney Şartları**

D63 PE100 PAKPLAST TURUNCU RENKLİ D.GAZ BORUSU-LOT : 164 – KASIM 08

Test numunesi tipi ve hazırlanma şekli		**: Tip 1 – Kaşık Numune / Makinede İşlenmiş**
Test Sıcaklığı	(^{0}C)	**: 23 ^{0}C ± 2^{0}C**
Test numunesi sayısı	(adet)	**: 5**
Çekme hızı	(mm/dakika)	**: 50**
Uzama ölçer ve boyut ölçer tipi		**: Elektronik uzama ölçer (S.N: 159948) ve Dijital kumpas**

Test numune No	Kalınlık (mm) a_s	Genişlik (mm) b_s	Kesit Alanı (mm^2) S_s	Baş. Ölçme Uzunluğu (mm) L_0	Akma gerilmesi (MPa) σ_Y	Akma Uzaması (%) ε_Y	Maksimum Çekme Gerilmesi (Mpa) σ_M	Kopma gerilmesi (MPa) σ_B	Kopma Uzaması (%) ε_B	Elastiklik Modülü (MPa) E_t
1	6,32	10,00	63,167	50	21,1	11,21	21,1	12,36	501,08	833,85
2	6,35	10,00	63,5	50	20,15	11,14	20,15	9,66	498,71	795,86
3	6,29	10,00	62,933	50	20,68	11,58	20,68	9,75	536,66	873,67
4	6,25	10,00	62,533	50	20,85	12,11	20,85	16,39	526,65	884,74
5	6,33	10,00	63,333	50	21,91	11,47	21,91	16,26	581,13	890,31
ORT	6,31	10,00	63,09	50,00	**20,94**	**11,50**	**20,94**	**12,88**	**529,65**	**855,69**
Std. Sapma	-	-	-	-	**0,65**	**0,39**	**0,65**	**3,32**	**33,56**	**40,07**
Belirsizlik	-	-	-	-	**0,49**	**0,13**	**0,49**	**0,30**	**6,15**	**44,40**

Ölçüm Belirsizliği ± (MPa) (k=2, %95 Güvenilirlik Seviyesinde)

* ***Kopma uzaması > % 529,65 (Cihazın boyunun en son noktasına kadar uzatılmıştır.)***

* ***Kopma uzaması, standartta istenen değere uygundur (Min. %350 kopma uzaması)***

Tel:0(216) 646 01 87 (3 hat) Faks: 0(216) 646 18 62
www.ugetam.com e-mail: ugetam@ugetam.com.tr

Form no: LTR-04-01
Yayın Tarihi: 28.11.2005 - Rev. No: 03/26.10.06

Figure 5.12: Official material test result form (UGETAM).

Below results were received from the UGETAM laboratory after completion of material tests;

- Determining the density
- Determination of tensile properties
- Determination of oxidation induction time
- Slow crack growth on notched pipes (notch test)
- Longitudinal Reversion Test
- Determination of the resistance to internal pressure

Summary of the physical test results are given in section 7 and details of the results are presented in Appendix A.

We also present one of the official test results in Appendix A and present other test results in summary tables in Appendix A.

6. KARTAL – ADALAR SEA CROSSING WITH PE PIPES

Using HDPE pipes for sea crossing has a few examples in real world applications. One of the examples for this type of projects is Kartal-Adalar sea crossing. Kartal-Adalar undersea crossing project was designed and constructed by IGDAS (Istanbul Gas Distribution Industry and Trade Incorporated Company). It was constructed in 2006 by using approximately 4000 m PE pipes. In this application, Φ125 mm PE 80 pipes were used. (In some part of the system, for research purposes, PE 80 type pipes were replaced with PE 100 during the research phase of the project.)

Figure 6.1: Project location.

During our study, we considered Kartal-Adalar Pipeline project as prototype system and we used results from this project accordingly.

6.1 Design Phase

In scope of Kartal-Adalar Sea crossing pipeline project, the main aim was to provide natural gas to Kinaliada, Burgazada, Heybeliada and Buyukada. To calculate required pipe diameter used in the pipeline system, total number of potential users were used as one of the design parameter. In the project, IGDAS used the maximum pipe diameter (Φ125 mm), because of the fact that this pipeline was also planned for research purposes. Theoretically, this pipeline can provide enough natural gas to

approximately 3675 user (based on per user demand as 1 m3/h and total theoretical value of 3675 m3/h). Moreover, this value is 50% of Buyukada's residents.

IGDAS preferred to use SDR 11 type of pipes in their applications, so in this specific application they used SDR 11 type pipes as well.

In this particular application, design team followed the below steps:

- Selecting of required pipe diameter (according to natural gas requirements in that region)
- Selecting of required pipe properties
- Designing of concrete blocks
- Selecting the site for preparing the pipeline and required equipment.
- Constructing the pipe line
- Connected to the main distribution line

In current situation these HDPE pipeline is not in service. This pipeline is kept and maintained for research purposes only, and an alternative steel pipeline serves as Natural Gas pipeline between mainlands to island.

It is important to note that, in the construction stage of this pipeline, only PE80 pipes were used but during this research project, some of the pipeline sections were replaced with PE100 type of pipes to investigate PE100 pipes behavior under real world conditions. Therefore, prototype system serves for both PE80 and PE100 pipe types. Table 6.1 shows the pipes used in the prototype pipeline system.

Table 6.1: Pipes that were used in the system.

Pipe Diameter (mm)	Pipe Material Type
Φ125	PE 80
Φ125	PE 100

Prototype system is subject to hydrodynamic effects but mainly current effects are significant in the systems installation depth. In the projects locations, sea waves do not have strong effects in 9 m and 15 m depths.

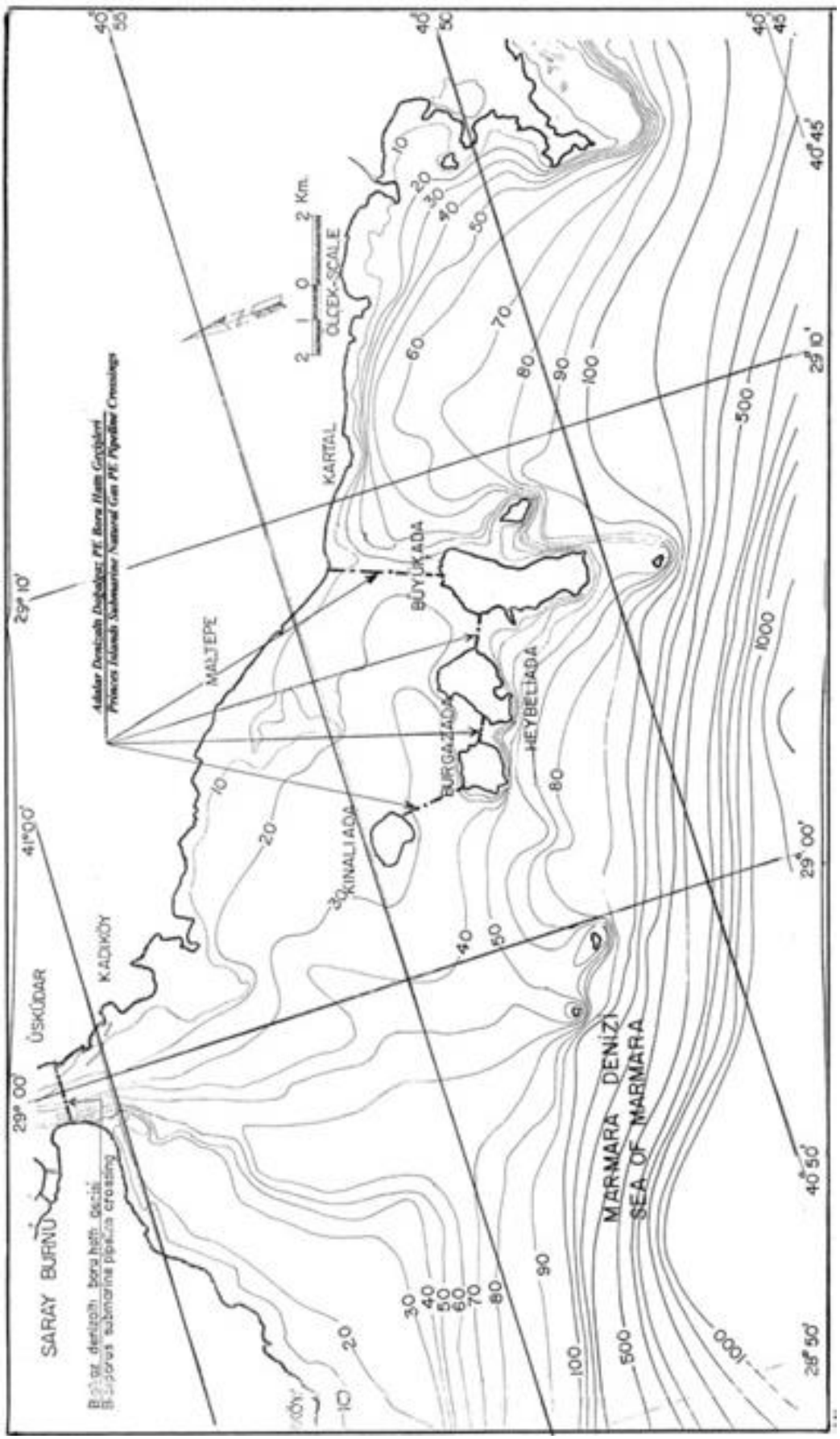

Figure 6.2: General location plan.

6.2 Installation of the Pipeline

Because of the small pipe diameter, IGDAS did not need to assemble the pipe in land. Therefore, pipes assembled in the boat and then concrete blocks were placed to the pipes with predefined intervals. Completed system was carefully placed in to the sea (Figure 6.3).

Precast concrete blocks were used with max 3 m intervals. 3 m interval selected after determining buoyancy forces versus self-weight of selected pipeline parts.

Figure 6.3: During construction and installation of the pipeline.

Figure 6.4: Installation of the concrete blocks.

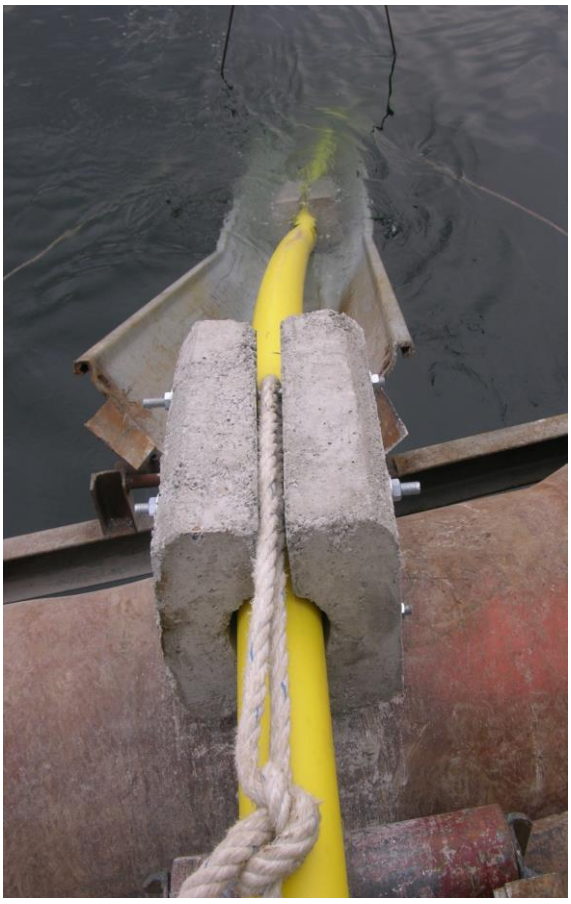

Figure 6.5: During installation of the pipeline to the seabed.

6.3 Test Specimens and Material Tests

To understand such a systems behavior in real world situation, test specimens were taken from Kartal-Buyukada pipeline. In several dates, test specimens were taken from the pipeline system to monitor its performance against hydrodynamic effects caused by current and waves.

Figure 6.6 shows the test specimen's collection process.

Figure 6.6: During test specimen collection.

Table 6.2 shows material tests that were performed in the project.

Table 6.2: Performed material tests.

Material Test	Specification
Determination of the resistance to internal pressure	TS EN ISO 1167-1:2006
Determination of tensile properties	TS EN ISO 6259-1:2006
Slow crack growth on notched pipes (notch test)	TS EN ISO 13479
Determination of oxidation induction time	TS EN 728
Determination of the melt mass – Flow rate (MFR)	TS EN ISO 1133:2006
Longitudinal Reversion Test	TS EN ISO 2505:2006
Determining the density	TS EN ISO 1183

After taking specimens, those specimens were sent to the material lab for material test. Table 6.3 briefly shows the specimens which were taken. Some specimens were taken from landside to investigate changes in their material properties during these long terms.

Table 6.3: Collected test specimens.

Pipe Diameter (mm)	PE Strength Class	Collection Date	Collection Depth
125	PE80	2008	9 m
125	PE80	2008	15 m
125	PE80	2008	From land
125	PE100	2008	9 m
125	PE100	2008	15 m
125	PE80	2010	9 m
125	PE80	2010	15 m
125	PE100	2010	9 m
125	PE100	2010	15 m

Below list briefly explains which material tests were performed:

- To measure resistance to internal pressure, "TS EN ISO 1167-1:2006, Determination of the resistance to internal pressure" test.
- For tensile properties, "TS EN ISO 6259-1:2006, Determination of tensile properties"
- To investigate crack growth characteristics, "TS EN ISO 13479, Slow crack growth on notched pipes (notch test)"
- To measure density, "TS EN ISO 1183, Determining the density

Material tests were carried out by UGETAM (accrediated material test lab). One set of official UGETAM test results are given in Appendix A for information purposes. Figure 6.7 and Figure 6.8 present two example of the official test result forms.

Summary of the test results are presented in Appendix A.

TÜRKAK
TÜRK AKREDİTASYON KURUMU
TURKISH ACCREDITATION AGENCY
tarafından akredite edilmiş

UGETAM

UGETAM TEST LABORATUVARI
Çamlık Mah. Yahya Kemal Beyatlı Cad. No:1
34906 Kurtköy-Pendik / İSTANBUL

AB-0094-T
T09-004
02-09

Deney Raporu
Testing Report

Sayfa: 15/21

4.5 ÇEKME TESTİ

Test metodu: **TS EN ISO 6259 – 1: Çekme Özelliklerinin Tayini (Determination of tensile properties – Part 1 : General test method)**
ISO 6259 – 3 : **Thermoplastics pipes – Determination of tensile properties – Part 3 : Polyolefin pipes**
TS 1398-1 EN ISO 527-1 : **Plastikler - Çekme Özelliklerinin Tayini - Bölüm 1 : Genel Prensipler**
TS 1398-2 EN ISO 527-2 : **Plastikler - Çekme Özelliklerinin Tayini - Bölüm 2: Kalıplama ve Ekstrüzyon Plastikleri İçin Deney Şartları**
TS 1398-3 EN ISO 527-3 : **Plastikler - Çekme Özelliklerinin Tayini - Bölüm 3: Film ve Levhalar İçin Deney Şartları**

D125 PE100 PAKPLAST TURUNCU RENKLİ D.GAZ BORUSU-LOT : 162 – KASIM 08

Test numunesi tipi ve hazırlanma şekli		: **Tip 1 – Kaşık Numune / Makinede İşlenmiş**
Test Sıcaklığı	(^{0}C)	: **23 ^{0}C ± 2^{0}C**
Test numunesi sayısı	(adet)	: **5**
Çekme hızı	(mm/dakika)	: **50**
Uzama ölçer ve boyut ölçer tipi		: **Elektronik uzama ölçer (S.N: 159948) ve Dijital kumpas**

Test numune No	Kalınlık (mm) a_0	Genişlik (mm) b_0	Kesit Alanı (mm^2) S_0	Baş. Ölçme Uzunluğu (mm) L_0	Akma gerilmesi (MPa) σ_y	Akma Uzaması (%) ε_y	Maksimum Çekme Gerilmesi (Mpa) σ_M	Kopma gerilmesi (MPa) σ_B	Kopma Uzaması (%) ε_B	Elastiklik Modülü (MPa) E_t
1.	11,61	10,00	116,1	50	22,51	11,27	22,51	15,73	559,02	834,15
2.	11,55	10,00	115,5	50	22,29	11,28	22,29	15,89	564,72	803,61
3.	11,56	10,00	115,57	50	21,25	12,56	21,25	15,46	563,05	787,25
4.	11,58	10,00	115,8	50	21,96	12,3	21,96	15,35	559,85	869,97
5.	11,56	10,00	115,83	50	21,4	12,99	21,4	10,65	546,38	801,03
ORT.	11,58	10,00	115,76	50,00	**21,88**	**12,08**	**21,88**	**14,62**	**558,60**	**819,20**
Std. Sapma	-	-	-	-	**0,55**	**0,78**	**0,55**	**2,23**	**7,22**	**33,15**
Belirsizlik	-	-	-	-	**0,41**	**0,14**	**0,41**	**0,27**	**6,48**	**35,83**

Ölçüm Belirsizliği ± (MPa) (k=2, %95 Güvenilirlik Seviyesinde)

* ***Kopma uzaması > % 558,60 (Cihazın boyunun en son noktasına kadar uzatılmıştır.)***
* ***Kopma uzaması, standartta istenen değere uygundur (Min. %350 kopma uzaması)***

Tel:0(216) 646 01 87 (3 hat) Faks: 0(216) 646 18 62 Form no: LTR-04-01
www.ugetam.com e-mail: ugetam@ugetam.com.tr Yayın Tarihi: 28.11.2005 - Rev. No: 03/26.10.06

Figure 6.7: Official material test result form (UGETAM).

TÜRKAK
TÜRK AKREDİTASYON KURUMU
TURKISH ACCREDITATION AGENCY
tarafından akredite edilmiş

UGETAM TEST LABORATUVARI

Çamlık Mah. Yahya Kemal Beyatlı Cad. No:1
34906 Kurtköy-Pendik / İSTANBUL

Deney Raporu
Testing Report

AB-0094-T
T10-217
10-10

3. **NUMUNE : T10 - 217 – 03:**

Marka	: **FIRAT PLASTIK**	Renk	: **SARI**
Örneklerin Tanımı (Lot, Seri No, Üretim Tarihi v.s.)	: **İ.T. EKİM 05 LOT:129**	Nominal Boyutları	: d_n = 125 e_n = 11,4
Malzeme Tipi (PE 80, PE 100 v.s.)	: **PE 80**	Markalama	: **FIRAT PE80 GAZ 4 SDR11 SINIF C DN125x11,4 SDR11 LOT:129 EKİM 05**
SDR / PN	: **SDR11**	İlave açıklama	: **15m Derinlik**

T10-217-03-01 HİDROSTATİK İÇ BASINCA MUKAVEMET

Test metodu : **TS EN ISO 1167-1-Sabit sıcaklık altında iç basınca dayanımın tayini. (Determination of resistance to internal pressure at constant temparature)**
Atıf Yapılan Standartlar : TS EN ISO 1167-2, TS EN ISO 3126

Nominal Boyutları : d_n = 125 e_n = 11,4
Test Sıcaklığı ve doğruluğu : 80 ^{0}C ± 1^{0}C
Test Cihazının Tanımı : **SCITEQ-HAMMEL-2000: Hidrostatik test ünitesi:9742-01571 – Termo Tank:15377, 17748**

Uygulanan Çevresel Gerilme – σ	**4,5**	±	**0,11**	**Mpa**
Rapor edilen ölçüm belirsizliği, genişletilmiş belirsizlik olup bileşik belirsizlikten kapsam faktörü k=2 kullanılarak elde edilmiştir. Güvenilirlik düzeyi %95'tir.				

Testin Süresi (saat) : **165**

Test Numunesinin Ölçülen Boyutları

Ortalama dış çap (mm) : d_e = 125
Minimum et kalınlığı (mm) : e_{min} = 11,4
Test numunesinin toplam boyu (mm) : L= 575
Test numunesinin serbest uzunluğu (mm) : L_0 = 375

Uygulanan test basıncı (bar) : **P = (20 x σ) / (SDR-1) = 9,0**

Test Ortamı : **Su içinde –Su ile**
Numunelerin şartlandırma sıcaklık ve süresi : **80^{0}C – 6 Saat**
Test başlıklarının tipi : **A tipi**
Test edilen numune sayısı : **1**
Test parçalarının termo tank içindeki vaziyeti : **Dikey**
Test basıncına gelme zamanı (30 sn – 1 dk.) : **60sn.**
Varsa hasarın tipi (yumuşak veya kırılgan) : **Hasar Yok**

Tel:0(216) 646 01 87 (3 hat) Faks: 0(216) 646 18 62
www.ugetam.com.tr e-mail: ugetam@ugetam.com.tr

Form no: LTR-42-01
Yayın Tarihi: 14.08.2008 - Rev. No: 01/29.06.09

Figure 6.8: Official material test result form (UGETAM).

Received test results were analyzed and summary tables of these results were prepared for further investigation

In the summary tables, test results for important items are presented. For important material properties, individual graphs were plotted.

Detailed results for these test are presented in section 7.

7. RESULTS OF NUMERICAL AND PHYSICAL MODELS

In this study, flow around elastic circular cylindrical pipes (which are made of PE material) and fluid structure interactions between water and PE pipe were investigated. As we explain in the earlier chapters, the pipe material is PE and the most characteristic property of this material is being highly elastic.

Working with pipes, which are made of elastic materials, requires us to model and analyzed over all system accordingly.

In lab models, physical models behave in a naturally elastic way. In computer models, we designed it to reflect elastic behavior of the pipe material. To achieve this, we used a commercially available software package as FSI system. We used ANSYS Fluent as fluid solver, ANSYS Mechanical as structural solver and ANSYS system coupling component as coupling algorithm.

Our computer model designed in 3D and because of the limited software license available to our disposal, our computer model's total mesh arrangement refined in medium level.

After the long-term tests in the ITU Hydraulics laboratory, we sent the test specimens to UGETAM material test laboratory for material tests. With these test results, we tried to conclude a general idea of possible effects in these pipes.

In the materials test laboratory, aforementioned material tests were conducted for each pipe specimen sets. Pipe sets in physical model (taken from ITU Hydraulics lab) and pipe sets that were taken from prototype system (Kartal-Adalar natural gas pipeline) were tested individually.

7.1 Summary of Numerical Model Results

Numerical model results were analyzed and relevant diagrams are presented in this section. (Detailed results are presented in Appendix B). We identified and analyzed flow around the pipe structure from computer model results. We investigated flow

characteristics in two sections, around fixed supports and in middle of span length. Differences in behaviors between these two plane sections were identified.

Figure 7.1 and Figure 7.2 show results from numerical system. We present additional results in Appendix B.

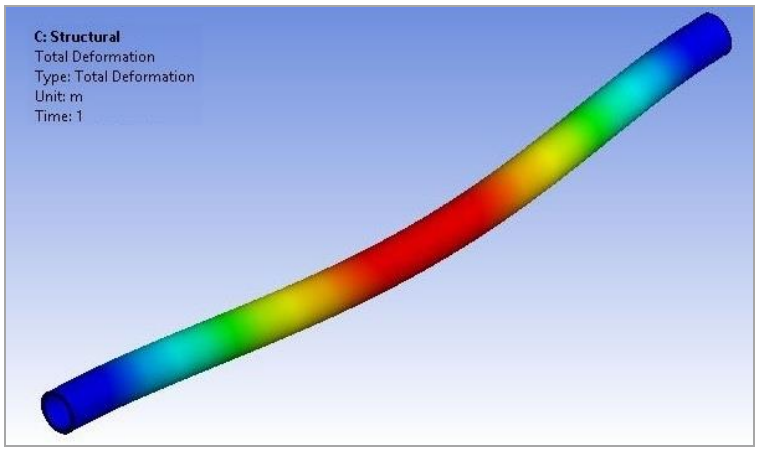

Figure 7.1: Deformation of pipe.

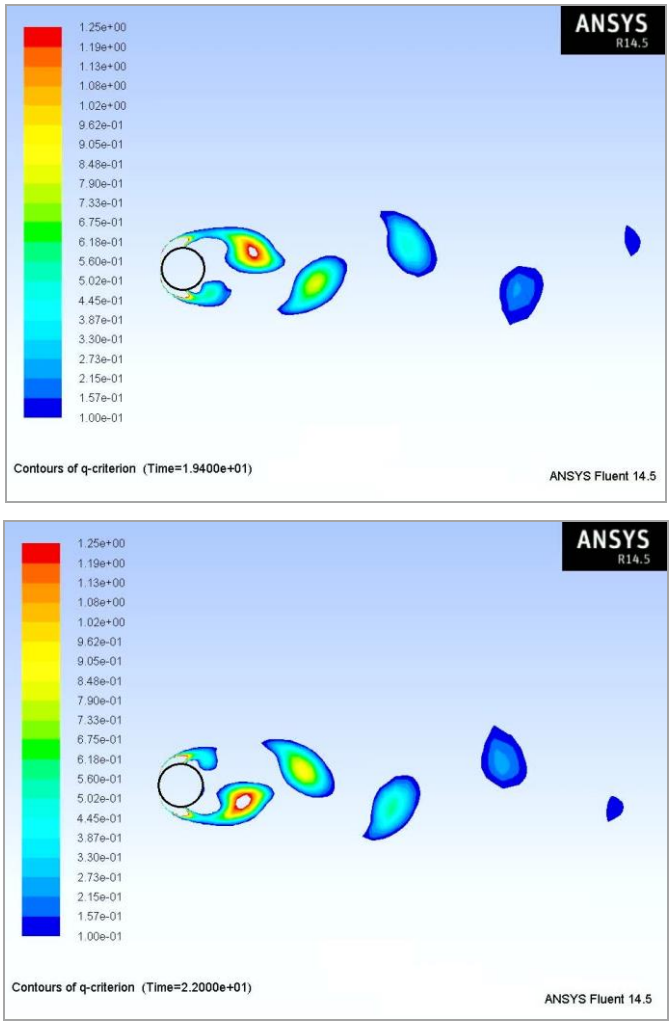

Figure 7.2: Vortices for the first plane section.

7.2 Summary of Physical Model Results

We analyzed material test results for both ITU Hydraulic Laboratory specimens and Kartal – Adalar Natural gas pipeline system (prototype). We present important points and some of the summary tables and graphs in this section. Detailed results are presented in Appendix A.

The most important properties were investigated. All results were compared with minimum required values defined in relevant specifications.

Table 7.1 summarizes test results from physical model (for specimens PE100 SDR 11, D20, D32 and D50). (Other summary tables are presented in Appendix A.)

Table 7.1: Summary table for specimens PE100 SDR 11, D20, D32 and D50.

TEST	D20	D32	D50
Determination of the melt-flow rate MFR (gr/10dak)	0.220	0.210	0.210
Determining the density (23 C)	0.952	0.952	0.953
Determination of oxidation induction time	>37	>37	>37
Determination of the resistance to internal pressure	5.4	5.4	5.4
Elongation at break (%)	456.360	569.430	617.280
Dimensional stability (%)	1.870	1.730	0.630
Slow crack growth on notched pipes (notch test) (NOTCH: e>5mm)	0.25	0.25	0.25

Figure 7.3 presents Elongation at Break graph for specimens taken from ITU tests (PE 100 SDR 11 D20, D32 and D50). Table 7.1 and Figure 7.3 clearly show that all three pipes specimens' selected material properties in the final stage are much higher than required min. acceptable value that are defined in relevant specifications.

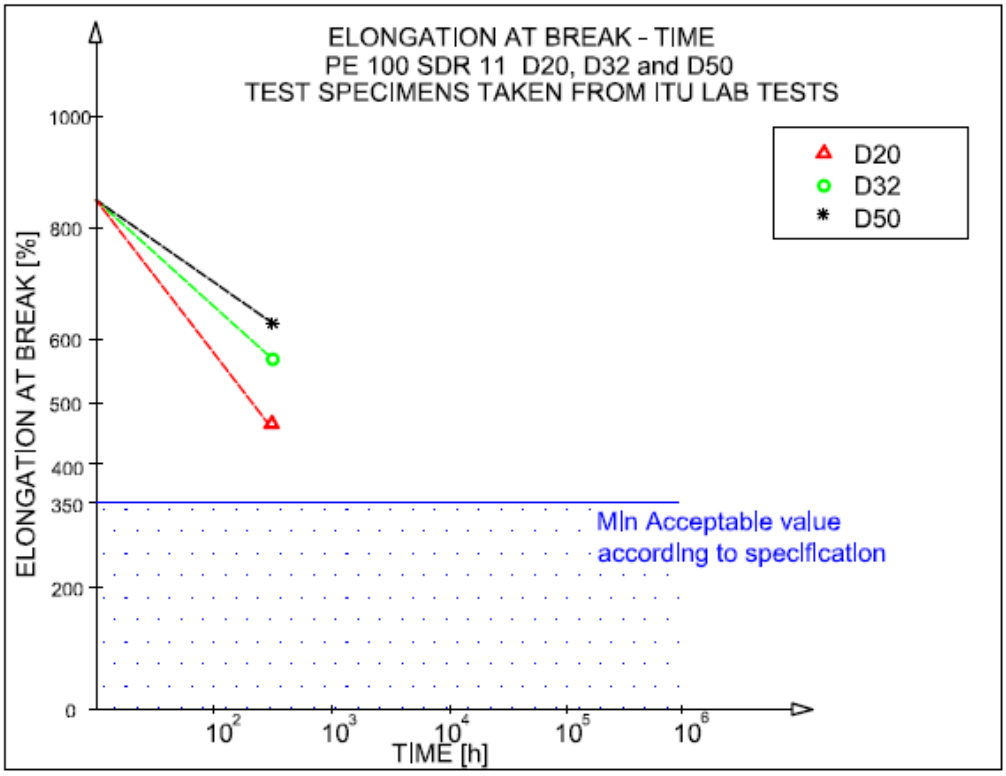

Figure 7.3: Elongation at break graph for specimens taken from ITU tests (PE 100 SDR 11 D20, D32 and D50).

Table 7.2 summarizes test results from prototype (for specimens taken from prototype (9 m deep seabed DN 125x11.4 PE 80 SDR). (Other summary tables are presented in Appendix A.)

Table 7.2: Summary table for specimens taken from prototype (9 m deep seabed DN 125x11.4 PE 80 SDR 11).

TEST	After Manufacturing (2008)	Test Speciments From Seabed (August-2008) For Lot no: 129/October 2005
Determination of the melt-flow rate MFR (gr/10dak)	0.930	0.930
Determining the density (23 C)	0.939	0.934
Determination of oxidation induction time		>37
Determination of the resistance to internal pressure	No Damage	No Damage
Elongation at break (%)	849.010	586.970
Dimensional stability (%)	0.870	1.410
Slow crack growth on notched pipes (notch test) (NOTCH: e>5mm)	No Damage	No Damage

Table 7.3: Summary table for specimens taken from prototype (15 m deep seabed DN 125x11.4 PE 80 SDR 11).

TEST	After Manufacturing 2008	Test Speciments From Seabed (August-2008) For Lot no: 129/October 2005
Determination of the melt-flow rate MFR (gr/10dak)	0.930	0.910
Determining the density (23 C)	0.939	0.933
Determination of oxidation induction time		>37
Determination of the resistance to internal pressure	No Damage	No Damage
Elongation at break (%)	849.010	580.390
Dimensional stability (%)	0.870	1.400
Slow crack growth on notched pipes (notch test) (NOTCH: e>5mm)	No Damage	No Damage

Figure 7.4 presents Elongation at Break graph for specimens taken from prototype (DN 125x11.4 PE 80 SDR) from 9 m deep seabed, and Figure 7.5 presents Elongation at Break graph for specimens taken from prototype (DN 125x11.4 PE 80 SDR) from 15 m deep seabed and decrease in their material properties. After investigation period, material properties are completely satisfactory.

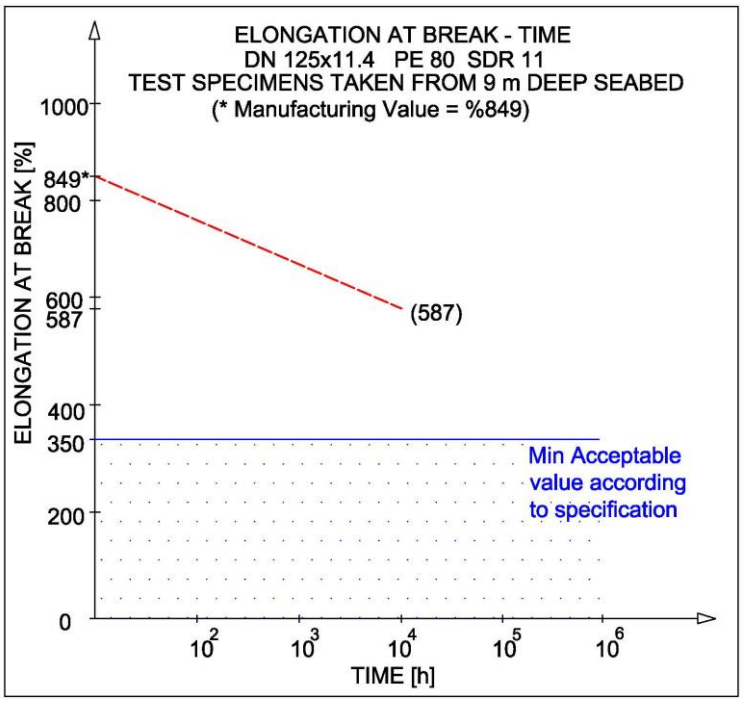

Figure 7.4: Elongation at Break graph for specimens taken from prototype (9 m deep seabed DN 125x11.4 PE 80 SDR 11).

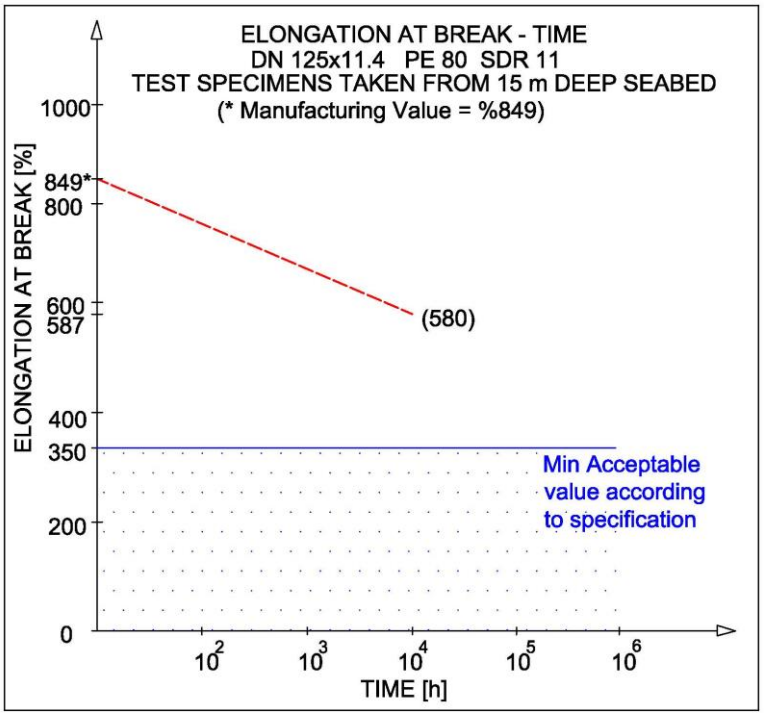

Figure 7.5: Elongation at Break graph for specimens taken from prototype (15 m deep seabed DN 125x11.4 PE 80 SDR 11).

Creep modulus is also a very important material property to investigate. Figure 7.6 presents the changes in creep modulus (E) during test period in a PE 80 specimen, which was taken from prototype. Figure 7.7 present changes in creep modulus (E) for PE 100 pipe specimens. (Appendix A presents results for other specimens)

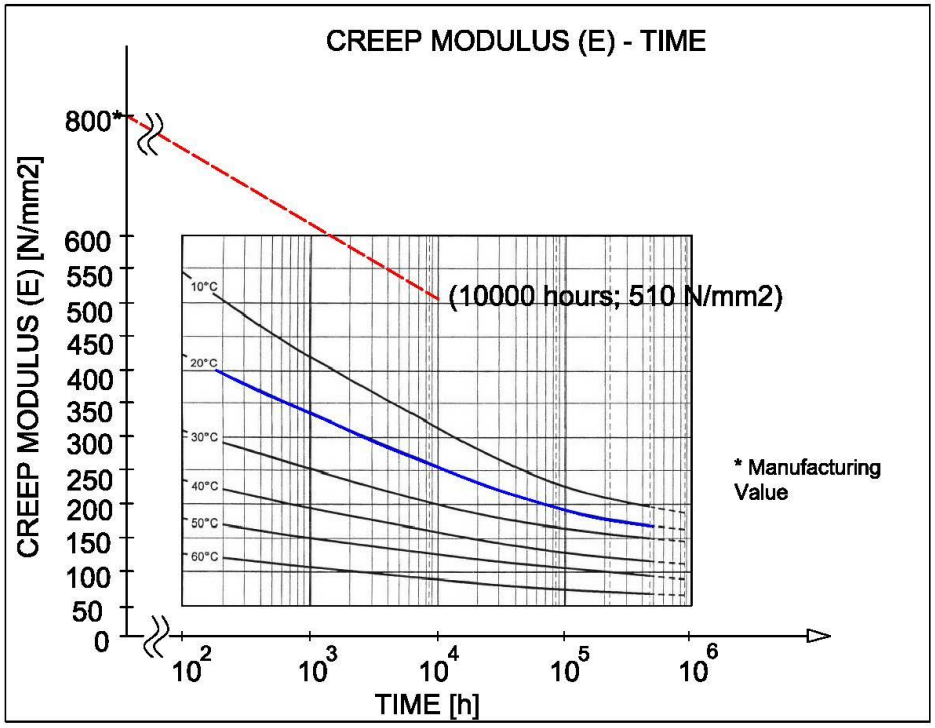

Figure 7.6: Creep modulus (E) – Time (for PE 80 pipe specimen).

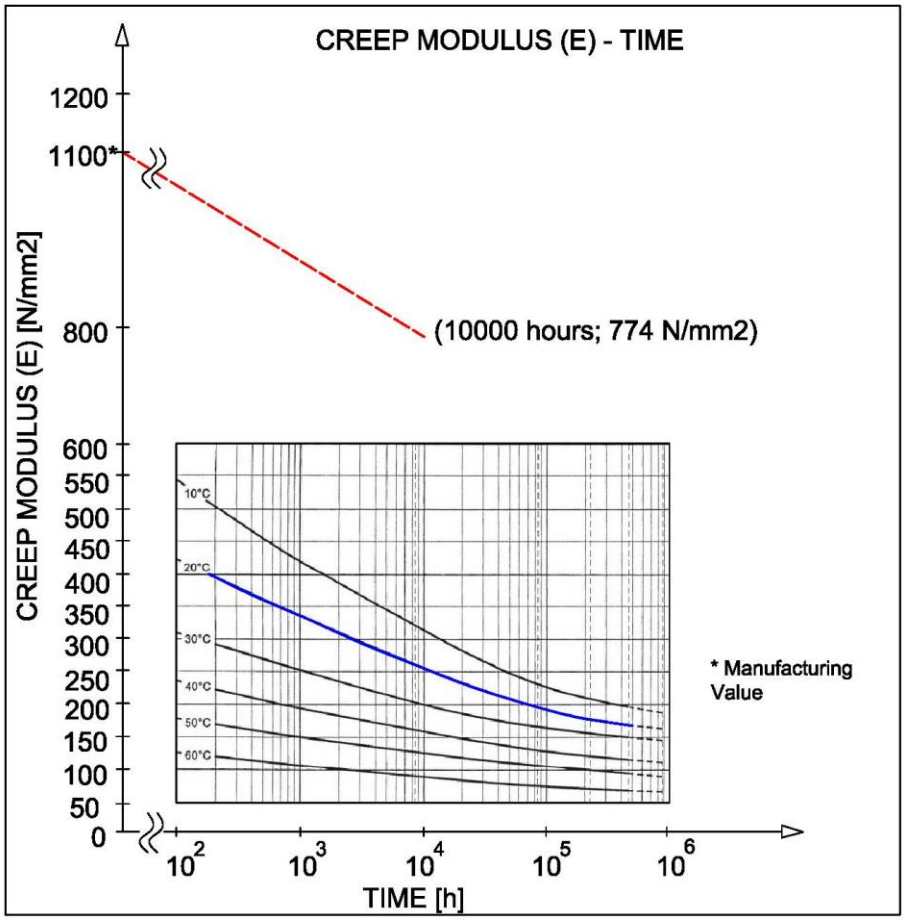

Figure 7.7: Creep modulus (E) – Time (for PE 100 pipe specimen).

7.3 Comparison of Results

Physical lab model (experimental lab model) results were compared with relevant specifications and all results are met the required specification conditions. For material properties perspective, conditions are satisfactory.

Figure 7.3 to Figure 7.7 clearly show that, final degrees of the material properties are higher than required specification values. In these graphs two important material properties, elongation at break and creep modulus were compared with the required values.

Figure 7.6 and Figure 7.7, creep modulus values were compared with SIMONA AG pipe manufacturer's catalog values. These creep modulus (E) – time graphs are nearly identical for same type of HDPE materials.

Material tests results are satisfies the relevant specifications and during the observation period (approximately 2 years and 4 years), both PE80 and PE100 pipes holds their material properties and material strenghts in specification limits.

Numerical results were analyzed. Rigid and elastic setups were compared and modelled systems elastical behaviors were captured in acceptable accuracy.

Figure 7.8 shows numerical model results for different plane sections in the system.

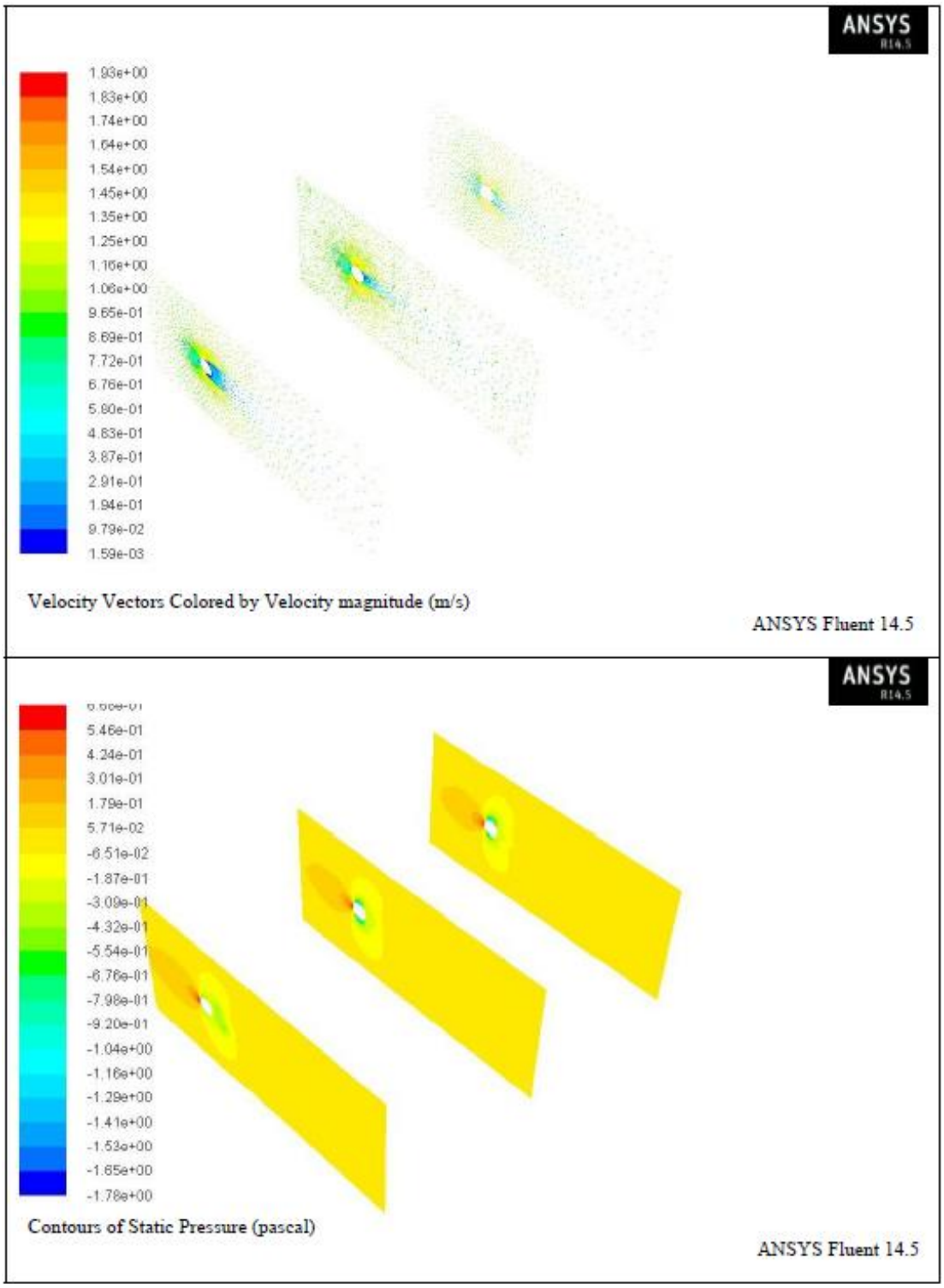

Figure 7.8: Numerical model comparison results. (Flow velocity and static pressure diagrams).

8. CONCLUSIONS

In this study, flow around elastic circular cylindrical pipes (which are made of HDPE material) were investigated physically and numerically. To investigate their performance under long-term hydrodynamic loading conditions, physical laboratory models were prepared and various test specimens were tested in these laboratory setups.

The prototype system (Kartal-Adalar Natural Gas pipeline system) was studied and material results from pipe specimens of prototype system were evaluated.

To understand behavior of such a complex system, numerical (computer) models were prepared and the system was investigated numerically. As we explained in the earlier chapters, the pipe material is PE and the most characteristic property of this material is being highly elastic.

Working with pipes, which are made of elastic materials, requires us to model and analyze the overall system accordingly. In lab models, physical models behave in a naturally elastic way. In computer models, we designed it to reflect elastic behavior of the pipe material. To achieve this we used a commercially available software package as FSI system. We used ANSYS Fluent as fluid solver, ANSYS Mechanical as structural solver and ANSYS System Coupling component as coupling algorithm.

We designed our computer models in 3D and because of the limited software license available to our disposal; we refined our computer model's total mesh arrangement in medium level.

After the long-term physical hydrodynamic loading test in the ITU Hydraulics laboratory, test specimens were sent to material test laboratory for aforementioned material tests. With these material test results, we tried to conclude a general idea of possible hydrodynamic effects acting to these pipes.

8.1 Practical Application of This Study

Undersea pipelines have many application areas in civil engineering, coastal and ocean engineering. In these applications, modern composite materials started to be considered as great alternatives to materials like steel.

One of the most important features of the PE material is its highly elastic deformation property. Because of this important feature, in engineering applications, it is possible to design solutions that are more efficient.

As a result, we can briefly list below possible application areas of our study:

- Undersea pipe lines
- Starting point for more complex layouts
- For laboratory examples, to create a methodology for long-term test under hydrodynamic forces.
- To examine the performance of the selected commercial software package for Fluid-Structure Interaction problems.
- To get introductory practical information about FSI modeling.
- The study can be an example for Coupling systems and their possible limitations.
- To understand the performance of HDPE pipes under similar conditions.
- To understand prototype system's (Kartal-Adalar natural gas pipelines) performance under long-term hydrodynamic effects.

In hydrodynamics and engineering applications, primitive shapes (like circular or rectangular cylinders) have great importance. They serve as a base point for more complex shapes and applications. Our study also serves as a base point for more complex shapes in future applications

8.2 Suggestions for Future Studies

With the technological improvements, our study can be advanced in different perspectives. Suggestions for future studies are briefly listed below.

- In physical models, more tests can be done to increase the physical data set.

1. Different Re and KC values can be used in the long-term lab test to simulated more situations.
2. Other pipe diameters can be used.
3. Longer test periods can be used in the laboratory tests.

- To create a more efficient comparison base, in the laboratory tests the pipe's deformations and stresses can be monitored with accurate devices.
- More detailed computer models can be designed to capture details.
    1. Mesh structures can be refined in finer stage.
    2. Shorter time intervals and larger iteration values can be used in the solutions.
- With the possible future technological improvements, less computational time can be possible for every run. So, under same computational expenses different designs can be checked.
- Prototype system's (Kartal-Adalar natural gas pipelines) performance can be monitored for determining its behavior in longer observation periods.

8.3 Results and Discussions

Our study mainly consists of three parts and these parts are numerical models, physical models and analysis of prototype system. We investigated our problem domain based on these three parts and analyzed the results. Results from the current study show the proposed method is successful in capturing numerical and physical behaviors such system.

We used different pipe diameters with different span lengths in our setups and our physical laboratory tests were showed us pipes behavior in different setup conditions are relatively similar and pipe system reactions have nearly identical trends. In addition, the experimental system successfully replicated real world application conditions.

For our problem domain, one of the most notable difficulties is capturing fluid structure interaction of the system. Our proposed computer model successfully managed to highlight important features of FSI system overall behavior. In principle,

fluid-structure interaction system and related coupling algorithm is able to take into account time-dependent FSI system and turbulent flow characteristics. It is important to note that, selected software package (ANSYS Fluent, ANSYS Mechanical and System Coupling module) was found to be capable in modelling such systems. The results obtained also indicates that this coupling method is acceptably accurate and logical, which can be used in similar engineering applications. Furthermore, this method is a general way that can also be employed to solve other kinds of fluid-structure interaction problems in various engineering fields.

By using the results and prepared diagrams, we concluded that our numerical system capable of capturing flow formation and structural behaviors of such system.

Analysis of the prototype pipeline (Kartal-Adalar Natural Gas pipeline) was successfully completed. Specimens for two different dates (for 2008 and 2010) provide us enough information about systems performance under hydrodynamic loading conditions. We were collected pipe specimens in two different locations from prototype system (from 9 m deep and 15 deep). We were compared set of results for both locations and we found that in both locations, pipes subjected to similar effects. Their material test results showed us that changes in their material properties follow similar trends.

Based on these material test results, it is seen that selected material properties in final stage are much higher than required min. acceptable values that are defined in relevant specifications. Elongation at break values for pipe specimens have similar trends and they decrease over time. In normal conditions, elongation at break values for PE material has a trend that decreased over time, and during our project, we successfully captured these trends and additional affects that were caused by hydrodynamic loadings. This trends can be explained as, in addition to known changes in material properties, hydrodynamic effects cause periodical loading and this periodical loadings lead to fatigue. These fatigue conditions effects material strengths directly. In long-term hydrodynamic loading conditions that we performed in our laboratory tests, resultant material strengths are in acceptable ranges.

In our study, these three parts (numerical model, physical model and prototype system) complete each other and they formed a complete analysis infrastructure. To understand overall system, we used these individual parts together. Every part in the

system served as planed in the beginning of our research and supported the other two parts in our system.

8.4 Conclusions

This study provides an effective and complete system for investigation of subsea pipeline system under different flow conditions numerically and experimentally.

In this study, flow around elastic circular cylindrical pipes (which are made of HDPE material) were investigated physically and numerically and in addition to them, a prototype system was evaluated. After our numerical and experimental study, the major conclusions can be summarized as follows.

a) Material results from ITU laboratory hydrodynamic loading tests were shown us; HDPE pipes performance for similar conditions is feasible. It is possible to conclude that HDPE pipes are usable in different flow conditions. For all three cases ("current", "wave" and "current + wave") these pipes performed similar to manufacturers claimed performance diagrams. Their final test results are larger than required values in specifications and it is possible to conclude that pipes made HDPE materials can be further analyzed for more detailed design investigations.

b) Prototype system's (Kartal-Adalar Natural Gas pipeline) performance during investigation period is promising. Material results from specimens taken from this pipeline are in acceptable limits according to relevant specifications. For further detailed investigation, this prototype system should be monitored continuously and new observations should be combined with our results and observations for overall conclusion.

c) Prepared numerical models highlighted systems important features and flow characteristics were observed correctly. Fluid-Structure interaction system behaved as planned and both solver successfully transfer deformation and force values each other. With these computer models, we presented an example setup and a solution technique.

d) This study will also serve as a starting point and road map for future researches to create numerical approximation methodology to estimate conditions of such pipe system without long-term physical laboratory experimental tests.

e) This study will also serve as a starting point and a guideline for future studies about a similar complex system in both numerical and physical modeling. In future researches, detailed design of similar systems may led to create numerical approximation methodology to estimate conditions of such pipe system without long-term physical laboratory experimental tests.

f) We can also conclude that, usability of HDPE pipes in sea crossing for natural gas pipelines is possible but similar research projects are necessary for detailed analysis.

REFERENCES

Abdullah, M. M., Walsh, K. K., Grady, S. and Wesson, G. D. (2005). Modelling flow around bluff bodies, *Journal of Computing in Civil Engineering*, 104-107.

Adli, R.N.F., Ibrahim, I. (2011). Modeling and Simulation of Vortex Induced Vibration on the Subsea Riser / Pipeline (GRP Pipe), *IEEE*, 978-1-4577-1884-7/11.

ANSYS Fluent (2012), Getting Started Guide, Release 14.5, ANSYS Inc., October 2012.

ANSYS Fluent (2012), Running ANSYS FLUENT Under LSF, Release 14.5, ANSYS Inc., October 2012.

ANSYS Fluent (2012), FLUENT V2F Turbulence Model Manual, Release 14.5, ANSYS Inc., October 2012

ANSYS (2012), Engineering Data User Guide , Release 14.5, ANSYS Inc., October 2012.

ANSYS (2012), ANSYS Workbench User's Guide, Release 14.5, ANSYS Inc., October 2012.

ANSYS (2012), ANSYS Meshing User's Guide, Release 14.5, ANSYS Inc., October 2012.

ANSYS (2012), System Coupling User's Guide, Release 14.5, ANSYS Inc., October 2012.

Avci, I., Bayazit, M., Cokgor, S., Sumer, BM (1996). Deniz Tabanına Oturan Bır Tünelin Yakınındaki Akım Alanı ve Tünele Etkiyen Kuvvetler, Proje No. INTAG 816, Sonuç Raporu, TÜBİTAK.

Bando, A., Otsuka, K., Ikeda, Y. (2001). Estimation of Hydrodynamic Forces on an Irregularly Oscillating Cylinder Using Symmetrical Vortices Model, *Proceedings of the Eleventh (2001) International Offshore and Polar Engineering Conference*, Stavanger, Norway, June 17-22, 2001.

Baranyi, L., Huynh, K., Mureithi, N. W. (2010). Dynamics of flow around a cylinder oscillating in-line for low Reynolds numbers, *Proceedings of the ASME 2010 3rd Joint US-European Fluids Engineering Summer Meeting and 8th International Conference on Nanochannels, Microchannels, and Minichannels*, FEDSM-ICNMM2010-31183, August 1-5, Montreal, Canada.

Bearman, P.W. and Zdravkovich, M.M. (1978). Flow around a circular cylinder near a plane boundary, *Journal of Fluid Mechanics*, 89(1), 33-48.

Bearman, P.W. (2011). Circular cylinder wakes and vortex-induced vibrations, *Journal of Fluids and Structures*, 27, 648-658.

Belver, A.V., Iban, A. L., Martin, C.E.L. (2012). Coupling between structural and fluid dynamic problems applied to vortex shedding in a 90 m steel chimney, *Journal of Wind Engineering and Industiral Aerodynamics*, 100, 30-37.

Blackburn, H. M. and Henderson, R. D. (1999). A study of two-dimensional flow past an oscillating cylinder, *Journal of Fluid Mechanics*, 385, 255-286.

Blevins, R. D. (2009). Models for Vortex-induced vibration of cylinders based on measured forces, *Journal of Fluids Engineering*, 131, 101203-1 – 101203-9.

Bollo, B., Baranyi, L. (2011), Flow around an oscillating or orbiting cylinder - comparative numerical investigation, *11th Hungarian Conference on Theoretical and Applied Mechanics HCTAM*, 2011 August 29-31, 2011 Miskole, Hungary.

Bourdier, S., Chaplin, J.R. (2012). Vortex-induced vibrations of an rigid cylinder on elastic supports with end-stops, Part 1: Experimental results, *Journal of Fluids and Structures*, 29, 62-78.

Carberry, J., Sheridan, J. and Rockwell, D. (2001). Stationary and oscillating cylinders in the presence of a free-surface, *14th Australian Fluid Mechanics Conference*, 10-14 December, Adelaide University, Adelaide, Australia.

Chen, X. Y. and Zha, G. C. (2005). Fully coupled fluid-structural interaction using an efficient high resolution upwind scheme, *Journal of Fluids and Structures*, 20, 1105-1125.

Cheng, L., Zhou, Y., Zhang, M.M. (2006). Controlled vortex-induced vibration on a fix-supported flexible cylinder in cross-flow, *Journal of Sound and Vibration*, 292, 279-299.

Choi, H.S. (2001). Free spanning analysis of offshore pipelines, *Ocean Engineering*, 28, 1325-1338.

Cokgor, S. (1997). Akıntılı deniz ortamında tabana otura silindirlere etkiyen kuvvetler, *Phd Thesis*, ITU, Graduate School of Science Engineering and Technology.

Cokgor, S. and Avcı, I. (2002). Hydrodynamic forces on partly buried cylinder exposed to combined waves and current, *Ocean Engineering*, 29, 7, 753-768.

Dipankar, A., Sengupta, T.K. (2005). Flow past a circular cylinder in the vicinity of a plane wall, *Journal of Fluids and Structures*, 20, 403-423.

Dong, S., Karniadakis, G.E. (2005). DNS of flow past a stationary and osciallating cylinder at Re=10000, *Journal of Fluids and Structures*, 20, 519-531.

Evangelinos, C., Lucor, D. and Karniadakis, G.E. (2000). DNS-Derived Force Distribution on Flexible Cylinders Subject to Vortex-Induced Vibration, *Journal of Fluids and Structures*, 14, 429-440

Gabbai, R. D. and Benaroya, H. (2005). An overview of modeling and experiments of vortex-induced vibration of circular cylinders, *Journal of Sound and Vibration*, 282, 575-616.

Galvao, R., Lee, E., Farrell, D., Hover, F., Triantafyllou, M., Kitney, N., Beynet, P. (2008). Flow control in flow-structure interaction, Journal of Fluids and Structures, 24, 1216-1226.

Glück, M., Breuer, M., Durst, F., Halfman, A. and Rank, E. (2001). Computation of fluid-structure interaction on lightweight structures, *Journal of Wind Engineering and Industrial Aerodynamics*, 89, 1351-1368.

Hatipoglu, F. (2000). Kararli bir akım ortamında tabana oturan yatay silindir(ler) etrafindaki akım alanının nümerik ve deneysel modellemesi, *Phd Thesis*, ITU, Graduate School of Science Engineering and Technology.

Hatipoglu, F., Avci, I. (2003). Flow Around a Partly Buried Cylinder in a Steady Current. *Ocean Engineering*, 30, 239-249.

Hemon, P., Santi, F. (2002). On the Aeroelastic Behaviour of Rectangular Cylinders in Cross-Flow, *Journal of Fluids and Structures*, 16(7), 855-889.

Huera-Huarte, F.J., Bearman, P.W., Chaplin, J.R. (2006). On the force distribution along the axis of a flexible circular cylinder undergoing multi-mode vortex-induced vibrations, *Journal of Fluids and Structures*, 22, 897-903

Huera-Huarte, F.J., Bearman, P.W. (2009). Wake structures and vortex-induced vibrations of a long flexible cylinder - Part 1:Dynamic response, *Journal of Fluids and Structures*, 25, 969-990.

Huera-Huarte, F.J., Bearman, P.W. (2009). Wake structures and vortex-induced vibrations of a long flexible cylinder - Part 2:Drag coefficients and vortex modes, Journal of Fluids and Structures, 25, 991-1006.

Kang, Z., Jia, L. (2013). An experiment study of a cylinder's two degree of freedom VIV trajectories, *Ocean Engineering*, 70, 129-140.

Khalak, A., Williamson, H.K. (1999). Motions, Forces, and Mode Transitions in Vortex-Induced Vibrations at Low Mass-Damping, *Journal of Fluids and Structures*, 13, 813-851.

Lam, K., Li, J.Y., So, R.M.C. (2003). Force coefficients and Strouhal numbers of four cylinder in cross flow, *Journal of Fluids and Structures*, 18, 305-324.

Lam, K. and Zou, L. (2010). Three-dimensional numerical simulations of cross-flow around four cylinders in an in-line square configuration, *Journal of Fluids and Structures*, 26, 482-502.

Lau, Y. L., So, R. M. C. and Leung, R. C. K. (2004). Flow-induced vibration of elastic slender structures in a cylinder wake, *Journal of Fluids and Structures*, 19, 1061-1083.

Lazarkov, M., Revstedt, J. (2008). Flow-Induced motion of a short circular cylinder spanning a rectangular channel, *Journal of Fluids and Structures*, 24, 449-466.

Li, T., Zhang, J. Y., Zhang, W. H. and Zhu, M. H. (2009). Vortex-induced vibration characteristics of an elastic circular cylinder, *World Academy of Science, Engineering and Technology,* 60, 56-65.

Liu, Y., **So, R. M. C., Lau, Y. L. and Zhou, Y.** (2001). Numerical studies of two side-by-side elastic cylinders in a cross-flow, *Journal of Fluids and Structures,* 15, 1009-1030.

Liu, Z.G., Liu, Y., Lu, J. (2012). Fluid-Structure interaction of single flexible cylinder in axial flow, *Computers & Fluids*, 56, 143-151.

Mazzilli, C.E.N., Andre, J.C., Soares, M.E.S., Ramos, I.B. (2000). A simple numerical model for the aeroelastic analysis of cable-stayed bridges, *Journal of Wind Engineering and Industrial Aerodynamics*, 84, 263-271.

Mittal, S. and Kumar, V. (2001). Flow-induced vibrations of a light circular cylinder at Reynolds number 10^3 to 10^4, *Journal of Sound and Vibration*, 245, 923-946.

Nishihara, T., Kaneko, S., Watanabe, T. (2005). Characteristics of fluid dynamic forces acting on a circular cylinder oscillated in the streamwise direction and its wake patterns, *Journal of Fluids and Structures*, 20, 505-518

Okajima, A., **Yasui, S., Kiwata, T. and Kimura, S.** (2007). Flow-induced streamwise oscillation of two circular cylinders in tandem arrangement, *International Journal of Heat and Fluid Flow*, 28, 552-560.

Pasto, S. (2008). Vortex-induced vibration of a circular cylinder in laminar and turbulent flows, *Journal of Fluids and Structures*, 24, 977-993.

Pham, A. -H., Lee, C. -Y., Seo, J. -H., Chun, H. -H., Kim, H. -J., Yoon, H. -S., ... Park, I. -R. (2010). Laminar flow past an oscillating circular cylinder in cross flow, *Journal of Marine Science and Technology*, 18, 361-368.

Pipelife Norge AS. (2002). PE Catalogue-Submarine Applications, December 2002.

PPI (Plastic Pipe Institute). (2005). Handbook of Polyethylene Pipe (Second Edition).

Sarpkaya, T. (1986a). Force on a circular cylinder in viscous oscillatory flow at low Keulegan-Carpenter numbers, *Journal of Fluid Mechnaics*, 165: 61-71.

Sha, Y. (2008). Vortex induced vibrations of finned cylinders, *Journal of Hydrodynamics*, 20(2): 195-201.

Shah, S. B. H. and Lu, X. -Y. (2008). Numerical simulation of an oscillating flow past a circular cylinder in the vicinity of a plane wall, *Journal of Hydrodynamics*, 20(5), 547-552.

Srinil, N., Zanganeh, H. and Day, A. (2013). Two degree of freedom VIV of circular cylinder with variable natural frequency ratio: Experimental and numerical investigations, *Ocean Engineering*, 73, 179-194.

So, R. M. C., Zhou, Y. and Liu, M. H. (2000). Free vibrations of an elastic cylinder in a cross flow and their effects on the near wake, *Experiments in fluids,* 29, 130-144.

So, R. M. C., Liu, Y. and Lai, Y. G. (2003). Mesh shape preservation for flow-induced vibration problems, *Journal of Fluids and Structures,* 18, 287-304.

So, R.M.C. and Wang, X. Q. (2003). Vortex-Induced vibrations of two side-by-side Euler-Bernoulli beams, *Journal of Sound and Vibration*, 259(3), 677-700.

So, R. M. C, Wang, X. Q., Xie, W. C. and Zhu, J. (2008). Free-stream turbulence effects on vortex-induced vibration and flow-induced force of an elastic cylinder, *Journal of Fluids and Structures,* 24, 481-495.

Someya, S., **Kuwabara, J., Li, Y. and Okamoto, K.** (2010). Experimental investigation of a flow-induced oscillating cylinder with two degrees-of-freedom, *Nuclear Engineering and Design*, 240, 4001-4007.

Sumer, M.B and Fredsoe, J. (2006). Hydrodynamics around Cylindrical Structures, World Scientific Publishing Co. Pte. Ltd.

Sumner, D. (2010). Two circular cylinders in cross-flow: A review, *Journal of Fluids and Structures*, 26, 849-899.

Szabo, G., Gyorgyi, J. (2009). Three-dimensional Fluid-Structure Interaction analysis for Bridge Aeroelasticity, *Proceedings of the World Congress on Engineering and Computer Science 2009 Vol II WCECS 2009*, October 20-22, 2009, San Francisco, USA.

Tsun-kuo Lin, Ming-huei Yu (2005), An experimental study on the cross-flow vibration of a flexible cylinder in cylinder arrays, *Experimental Thermal and Fluid Science*, 29, 523-536.

Xiaodong Wu, Fei Ge, Youshi Hong (2012), A review of recent studies on vortex-induced vibrations of long slender cylinders, *Journal of Fluids and Structures*, 28, 292-308.

Xie, F., Deng, J., Zheng, Y. (2011). Multi-Mode of vortex-induced vibration of flexible circular cylinder, *Journal of Hydrodynamics*, 23(4):483-490

Yamamoto, C.T., Meneghini, J.R., Saltara, F., Fregonesi, R.A., Ferrari, J.A. (2004). Numerical simulations of vortex-induced vibration on flexible cylinders, *Journal of Fluid and Structures*, 19, 467-489.

Yang, J., Preidikman, S., Balaras, E. (2008). A strongly coupled, embedded-boundary method for fluid-structure interactions of elastically mounted rigid bodies, *Journal of Fluids and Structures,* 24, 167-182.

Wanderley, J.B.V., Souza, G.H.B., Sphaier, S.H., Levi, C. (2008). Vortex-induced vibration of an elastically mounted circular cylinder using an upwind TVD two-dimensional numerical scheme, *Ocean Engineering,* 35, 1533-1544.

Wang, X. Q., So, R. M. C. and Liu, Y. (2001). Flow-induced vibration of an Euler-Bernoulli beam, *Journal of Sound and Vibration*, 243(2), 241-268.

Wang Yi-wei (2008). Combination of CFD and CSD packages for Fluid-Structure Interaction, *Journal of Hydrodynamics*, 20(6): 756-761.

Wang, Z. J., Zhou, Y. and So. R.M.C. (2003). Vortex-induced vibration characteristics of two fixed-supported elastic cylinders, *Journal of Fluids Engineering*, 125, 551-560.

Wang, Z. J. and Zhou, Y. (2005). Vortex-induced vibration characteristics of an elastic square cylinder on fixed supports, *Journal of Fluids Engineering*, 127, 241-249.

Williamson, C.H.K., Govardhan, R. (2008). A brief review of recent results in vortex-induced vibrations, *Journal of Wind Engineering and Industrial Aerodynamics*, 96, 713-735.

Zhang, H.J., Zhou, Y, So, R.M.C, Mignolet, M.P., Wang, Z.J. (2003). A note on the fluid damping of an elastic cylinder in a cross-flow, *Journal of Fluids and Structures*, 17, 479-483.

Zhao, M., Cheng, L. and An, H. -W. (2010). Three-dimensional numerical simulation of flow around a circular cylinder under combined steady and oscillatory flow, *9th International Conference on Hydrodynamics*, October 11-15, Shanghai, China.

Zhao, M., Cheng, L., An, H. (2012). Numerical investigation of vortex-induced vibration of a circular cylinder in transverse direction in oscillatory flow, *Ocean Engineering*, 41, 39-52.

Zhao, M., Cheng, L. (2011). Numerical simulation of two-degree of freedom vortex-induced vibration of circular cylinder close to a plane boundary, *Journal of Fluids and Structures*, 27, 1097-1110.

Zhao, M., Cheng L., Teng, B., Dong, G. (2007). Hydrodynamic forces on dual cylinders of different diameters in steady currents, *Journal of Fluids and Structures*, 23, 59-83.

Zhao, M., Kaja, K., Xiang, Y., Yan, G. (2013). Vortex-induced vibration (VIV) o a circular cylinder in combined steady and oscillaroty flow, *Ocean Engineering*, 73, 83-95.

Zhou, C.Y., So, R.M.C., Lam, K. (1999). Vortex-Induced Vibrations of an elastic circular cylinder, *Journal of Fluids and Structures*, 13, 165-189.

Zhou, C.Y., So, R.M.C. (2000). Fluid damping of an elastic cylinder in a cross-flow, *Journal of Fluids and Structures*, 14, 303-322

Zhu, S., **Cai, Y. and Chen, S. S.** (1995). Experimental fluid-force coefficients for wake-induced cylinder vibration, *Journal of Engineering Mechanics*, 1003-1015.

APPENDICES

APPENDIX A: Setup of Physical (Laboratory) Models
APPENDIX B: Results of Material Tests
APPENDIX C: Setup of Numerical Models
APPENDIX D: Numerical Model Results and Diagrams

APPENDIX A: Setup of Physical (Laboratory) Models

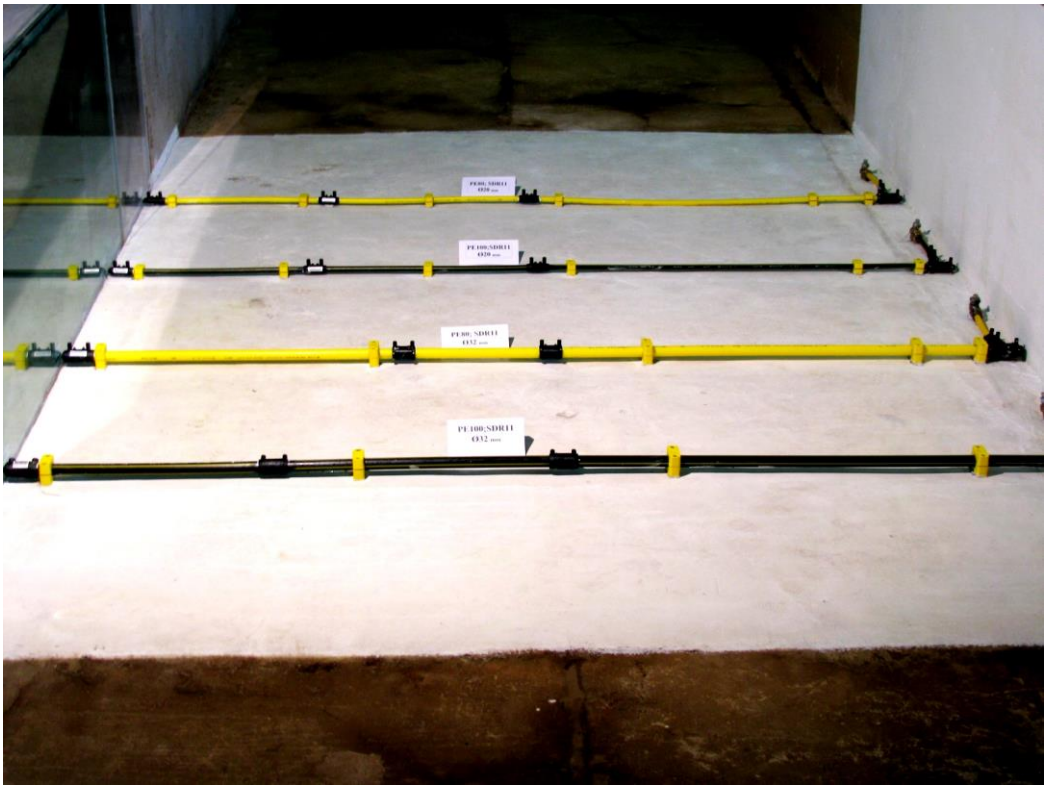

Figure A.1: Experimental setup for [PE80; SDR11; Φ20 and Φ32] and [PE100; SDR11; Φ20 and Φ32].

Figure A.2: Experimental Setup for [PE80; SDR11; Φ20 and Φ32] and [PE100; SDR11; Φ20 and Φ32].

Figure A.3: Experimental Setup for [PE80; Φ50, Φ75 and Φ125] and [PE100; Φ50, Φ75 and Φ125].

Figure A.4: Experimental Setup for [PE80; Φ50, Φ75 and Φ125] and [PE100; Φ50, Φ75 and Φ125].

Figure A.5: Experimental Setup for [PE80; Φ50, Φ75 and Φ125] and [PE100; Φ50, Φ75 and Φ125].

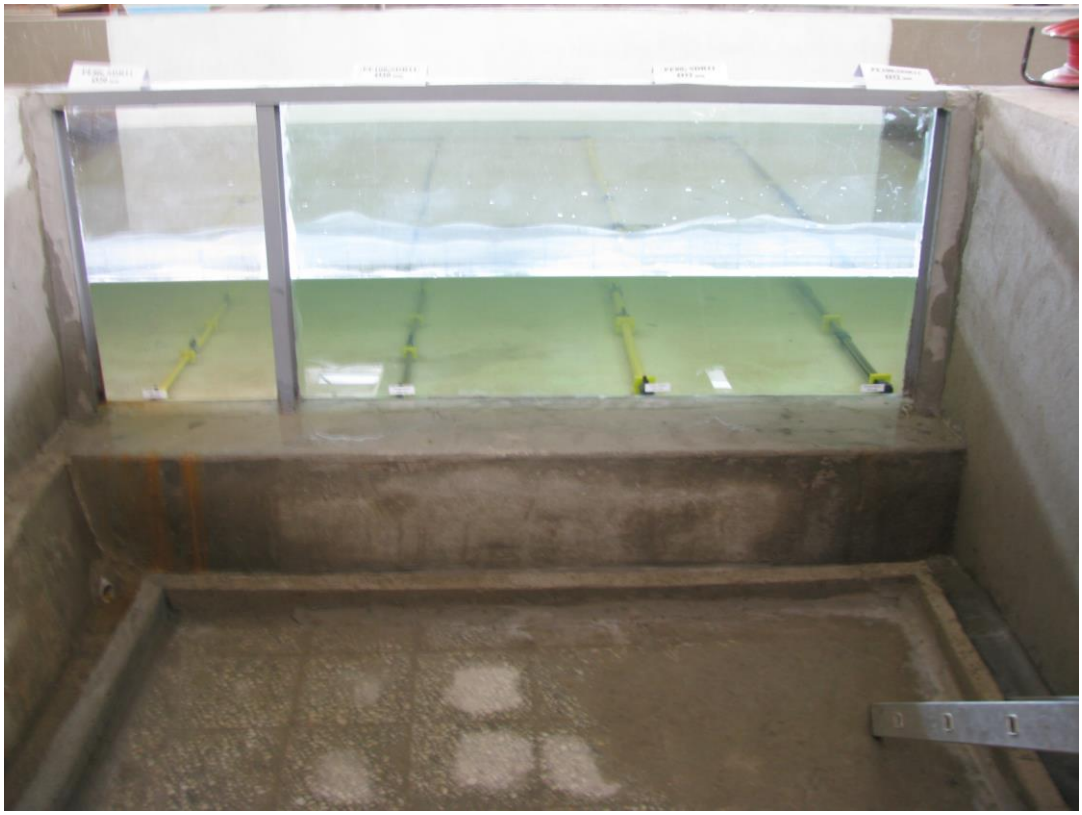

Figure A.6: During experiment [PE80; SDR11; Φ20 and Φ32] and [PE100; SDR11; Φ20 and Φ32].

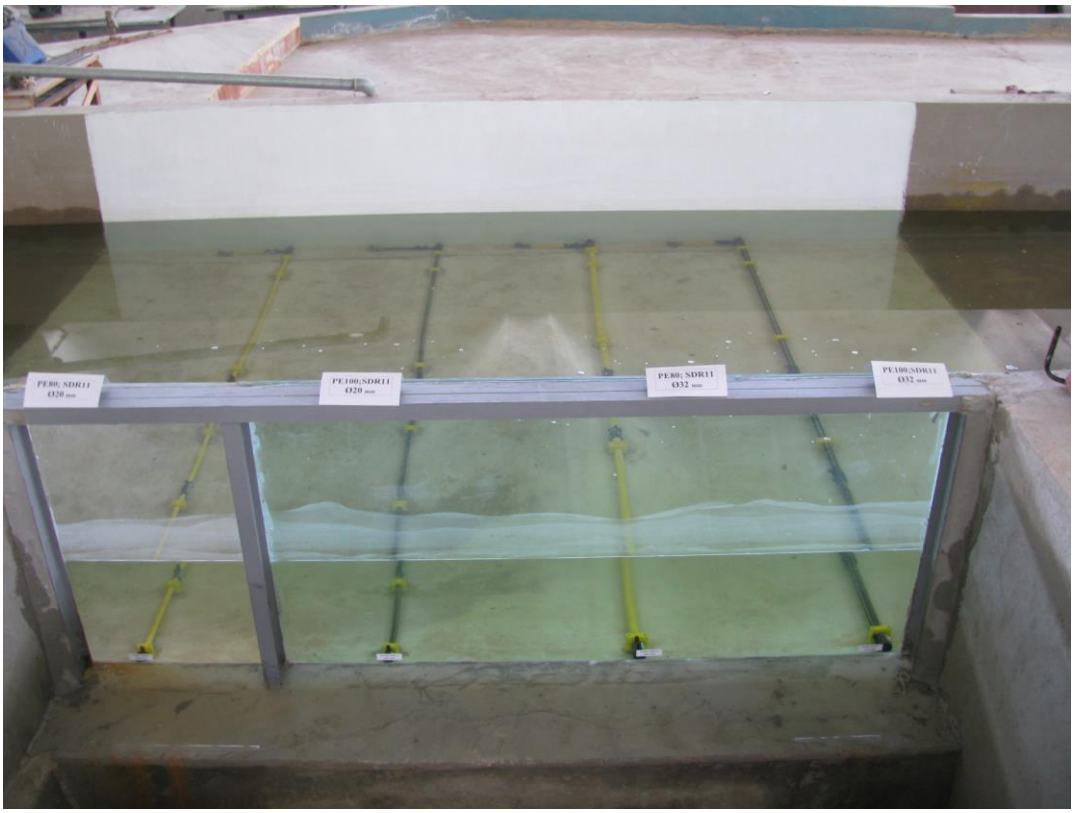

Figure A.7: During experiment [PE80; SDR11; Φ20 and Φ32] and [PE100; SDR11; Φ20 and Φ32].

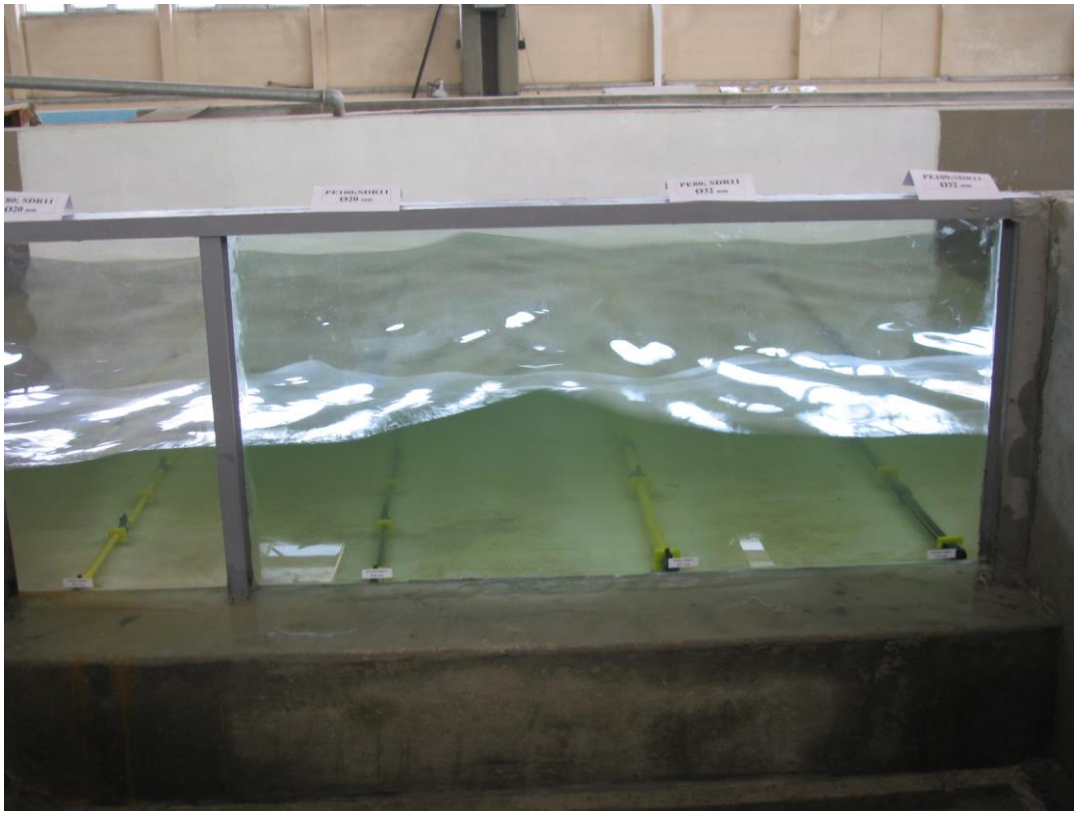

Figure A.8: Wave loading [PE80; SDR11; Φ20 and Φ32] and [PE100; SDR11; Φ20 and Φ32].

Figure A.9: Wave + Current loading [PE80; SDR11; Φ20 and Φ32] and [PE100; SDR11; Φ20 and Φ32].

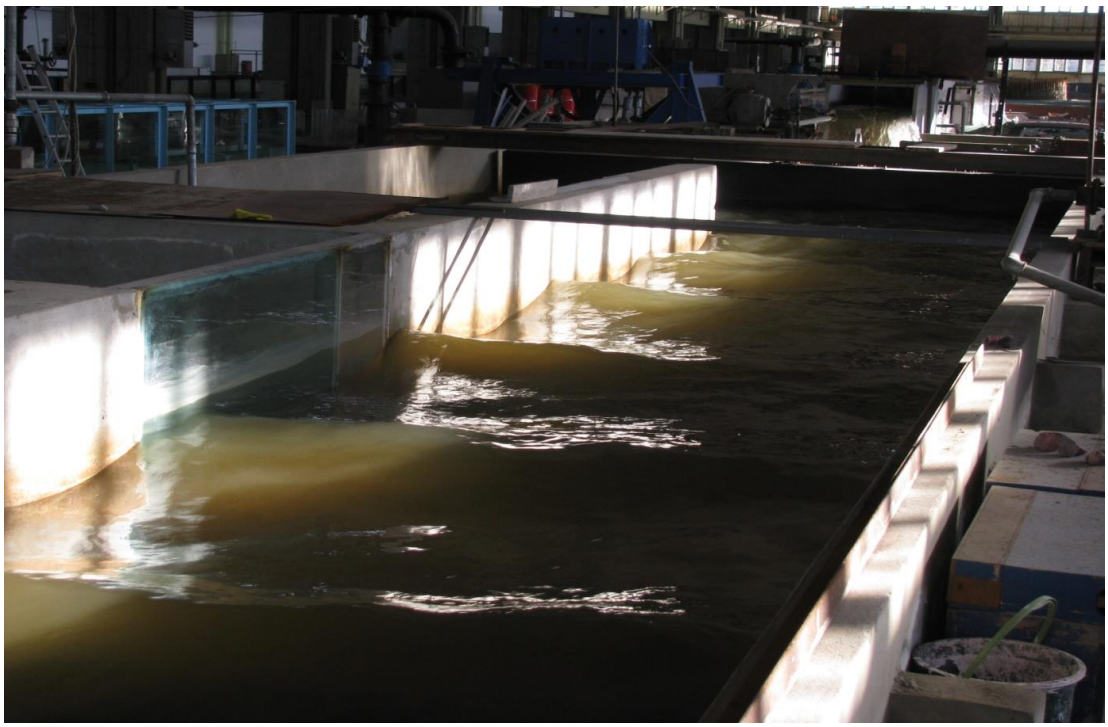

Figure A.10: Wave loading [PE80; Φ50, Φ75 and Φ125] and [PE100; Φ50, Φ75 and Φ125].

APPENDIX B: Results of Material Tests

Below test results are some of the official material test results for selected specimens. Only one set of results have been provided within this thesis. Other results are given in the summary tables.

Table B.1: Test result ID's descriptions.

Test Result ID	Description
PR_101_1	Specimens taken from 9 m deep seabed
PR_101_2	Specimens taken from 15 m deep seabed
PR_102_1	Specimens taken from 9 m deep seabed, DN 125 11.4 PE 80 SDR 11
PR_102_2	Specimens taken from 15 m deep seabed, DN 125 11.4 PE 80 SDR 11
PR_102_3	Specimens taken from land, DN 125 11.4 PE 80 SDR 11
PR_102_4	Specimens taken from seabed, DN 125 11.4 PE 100 SDR 11
PR_102_5	Specimens taken from ITU lab tests, D20, D32 and D50 PE80 SDR 11
PR_102_6	Specimens taken from ITU lab tests, D20, D32 and D50 PE100 SDR 11
PR_105	Specimens taken from seabed
PR_106	Specimens taken from seabed

SUMMARY TABLES FOR TEST RESULTS

Table B.2: Summary table for test results PR_101_1.

TEST	After Manufacturing (2008)	Test Speciments From Seabed (2008) For Lot no: 129/October 2005	Test Speciments From Seabed (2010) For Lot no: 129/October 2005	Test Speciments From Land (2008) For Lot no: 100/August 2005
Determination of the melt-flow rate MFR (gr/10dak)	0.930	0.930	0.920	0.760
Determining the density (23 C)	0.939	0.934	0.939	0.946
Determination of oxidation induction time		>37	>25	>37
Determination of the resistance to internal pressure	No Damage	No Damage	No Damage	No Damage
Elongation at break (%)	849.010	586.970	508.110	595.500
Dimensional stability (%)	0.870	1.410	1.450	0.780
Slow crack growth on notched pipes (notch test) (NOTCH: e>5mm)	No Damage	No Damage	No Damage	No Damage

Table B.3: Summary table for test results PR_101_2.

TEST	After Manufacturing (2008)	Test Speciments From Seabed (2008) For Lot no: 129/October 2005	Test Speciments From Seabed (2010) For Lot no: 129/October 2005	Test Speciments From Land (2008) For Lot no: 100/August 2005
Determination of the melt-flow rate MFR (gr/10dak)	0.930	0.910	0.900	0.760
Determining the density (23 C)	0.939	0.933	0.940	0.946
Determination of oxidation induction time		>37	>25	>37
Determination of the resistance to internal pressure	No Damage	No Damage	No Damage	No Damage
Elongation at break (%)	849.010	580.390	582.750	595.500
Dimensional stability (%)	0.870	1.400	1.440	0.780
Slow crack growth on notched pipes (notch test) (NOTCH: e>5mm)	No Damage	No Damage	No Damage	No Damage

Table B.4: Summary table for test results PR_102_1.

TEST	After Manufacturing (2008)	Test Speciments From Seabed (August-2008) For Lot no: 129/October 2005
Determination of the melt-flow rate MFR (gr/10dak)	0.930	0.930
Determining the density (23 C)	0.939	0.934
Determination of oxidation induction time		>37
Determination of the resistance to internal pressure	No Damage	No Damage
Elongation at break (%)	849.010	586.970
Dimensional stability (%)	0.870	1.410
Slow crack growth on notched pipes (notch test) (NOTCH: e>5mm)	No Damage	No Damage

Table B.5: Summary table for test results PR_102_2.

TEST	After Manufacturing 2008	Test Speciments From Seabed (August-2008) For Lot no: 129/October 2005
Determination of the melt-flow rate MFR (gr/10dak)	0.930	0.910
Determining the density (23 C)	0.939	0.933
Determination of oxidation induction time		>37
Determination of the resistance to internal pressure	No Damage	No Damage
Elongation at break (%)	849.010	580.390
Dimensional stability (%)	0.870	1.400
Slow crack growth on notched pipes (notch test) (NOTCH: e>5mm)	No Damage	No Damage

Table B.6: Summary table for test results PR_102_3.

TEST	After Manufacturing 2008	Test Speciments From Seabed (July-2008) For Lot no: 100/August 2005
Determination of the melt-flow rate MFR (gr/10dak)	0.780	0.760
Determining the density (23 C)	0.945	0.946
Determination of oxidation induction time		>37
Determination of the resistance to internal pressure	No Damage	No Damage
Elongation at break (%)	708.770	595.500
Dimensional stability (%)	0.840	0.780
Slow crack growth on notched pipes (notch test) (NOTCH: e>5mm)	No Damage	No Damage

Table B.7: Summary table for test results PR_102_4.

TEST	After Manufacturing 2008	Test Speciments From Seabed (July-2008)
Determination of the melt-flow rate MFR (gr/10dak)	0.230	0.230
Determining the density (23 C)	0.959	0.955
Determination of oxidation induction time	>40	>37
Determination of the resistance to internal pressure	No Damage	No Damage
Elongation at break (%)	650.230	624.040
Dimensional stability (%)	0.970	0.960
Slow crack growth on notched pipes (notch test) (NOTCH: e>5mm)	No Damage	No Damage

Table B.8: Summary table for test results PR_102_5.

TEST	D20	D32	D50
Determination of the melt-flow rate MFR (gr/10dak)	0.830	0.810	0.810
Determining the density (23 C)	0.938	0.938	0.940
Determination of oxidation induction time	>37	>37	>37
Determination of the resistance to internal pressure	4.5	4.5	4.5
Elongation at break (%)	504.640	664.040	659.020
Dimensional stability (%)	2.980	2.610	2.460
Slow crack growth on notched pipes (notch test) (NOTCH: e>5mm)	0.13	0.13	0.13

Table B.9: Summary table for test results PR_102_6.

TEST	D20	D32	D50
Determination of the melt-flow rate MFR (gr/10dak)	0.220	0.210	0.210
Determining the density (23 C)	0.952	0.952	0.953
Determination of oxidation induction time	>37	>37	>37
Determination of the resistance to internal pressure	5.4	5.4	5.4
Elongation at break (%)	456.360	569.430	617.280
Dimensional stability (%)	1.870	1.730	0.630
Slow crack growth on notched pipes (notch test) (NOTCH: e>5mm)	0.25	0.25	0.25

Table B.10: Summary table for test results PR_105 and PR_106.

Diameter	Type	Source	Temperature	Date	Depth	Specimen no	Thickness	Width	Section Area	Beginning length	Yield Stress	Yield strain	Maximum Tensile Stress	Breaking Stress	Elongation At Break	Modulus of Elasticity
mm	PE	Test ID	C		m		mm	mm	mm2	mm	MPa	%	MPa	MPa	%	MPa
20	100	PR_105_11	23	11.2008		1	3.35	5.80	19.419	25	21.01	12.22	21.26	20.39	578.34	818.45
						2	3.29	5.93	19.499	25	12.76	1.96	20.29	13.24	525.32	774.41
						3	3.20	5.84	18.718	25	20.12	10.64	24.07	22.60	551.26	722.08
63	100	PR_105_12	23	11.2008		1	6.32	10	63.167	50	21.10	11.21	21.10	12.36	501.08	833.85
						2	6.35	10	63.500	50	20.15	11.14	20.15	9.66	498.71	795.86
						3	6.29	10	62.933	50	20.68	11.58	20.68	9.75	538.66	873.67
						4	6.25	10	62.533	50	20.85	12.11	20.85	16.39	528.65	884.74
						5	6.33	10	63.333	50	21.91	11.47	21.91	16.26	581.13	890.31
110	100	PR_105_13	23	11.2008		1	10.84	10	108.370	50	22.13	11.92	22.13	15.75	561.64	768.98
						2	10.69	10	106.930	50	22.05	11.39	22.05	10.31	419.65	916.90
						3	10.57	10	105.670	50	22.77	11.09	22.77	16.24	557.03	854.71
						4	10.93	10	109.300	50	21.72	12.18	21.72	10.78	557.40	867.94
						5	10.81	10	108.100	50	22.67	11.21	22.67	10.87	550.03	894.05
125	100	PR_105_14	23	11.2008		1	11.61	10	116.100	50	22.51	11.27	22.51	15.73	559.02	834.15
						2	11.55	10	115.500	50	22.29	11.28	22.29	15.89	564.72	803.61
						3	11.56	10	115.570	50	21.25	12.56	21.25	15.46	563.05	787.25
						4	11.58	10	115.800	50	21.96	12.30	21.96	15.35	559.85	869.97
						5	11.58	10	115.830	50	21.40	12.99	21.40	10.65	546.38	801.03
125	80	PR_106_5	23	01.10.2010	9	1	12.05	9.81	118.210	50	16.49	13.01	16.49	3.45	429.77	561.99
						2	12.03	9.74	117.240	50	15.90	13.54	15.90	14.54	534.72	498.47
						3	12.03	9.74	117.140	50	16.02	13.37	16.02	14.46	539.34	526.22
						4	12.12	9.76	118.320	50	16.20	13.22	16.20	3.55	497.39	510.06
						5	12.06	9.82	118.500	50	16.00	14.35	16.00	14.23	539.35	459.23
125	100	PR_106_10	23	01.10.2010	9	1	11.51	9.77	112.370	50	21.44	10.44	21.44	17.42	567.06	929.47
						2	11.58	9.75	112.830	50	21.99	10.71	21.99	17.93	580.69	800.14
						3	11.92	9.75	116.290	50	20.25	10.35	20.25	16.47	577.93	849.84
						4	11.42	9.78	111.690	50	21.77	10.75	21.77	16.98	591.15	904.79
						5	11.48	9.81	112.620	50	17.13	13.21	17.13	15.85	529.89	591.10
125	80	PR_106_15	23	01.10.2010	15	1	11.73	9.74	114.250	50	2.46	0.13	16.47	10.68	536.19	467.65
						2	12.01	9.78	117.390	50	16.77	13.11	16.77	10.92	590.47	472.56
						3	11.86	9.81	116.270	50	16.78	13.66	16.78	11.55	602.57	486.56
						4	11.87	9.82	116.490	50	16.94	13.96	16.94	10.44	592.63	521.59
						5	11.94	9.79	116.930	50	17.27	12.53	17.27	11.23	591.91	528.38
125	100	PR_106_21	23	01.10.2010	15	1	12.15	9.80	119.080	50	20.74	11.26	20.74	9.26	583.27	1007.77
						2	11.55	9.71	112.190	50	20.87	12.34	20.87	16.20	597.33	852.15
						3	11.51	9.69	111.600	50	21.78	9.70	21.78	16.81	586.15	928.29
						4	11.71	9.71	113.700	50	5.37	0.39	21.08	16.59	588.79	882.96
						5	11.66	9.86	114.930	50	20.65	11.17	20.65	16.19	592.70	959.19

SUMMARY GRAPHS FOR TEST RESULTS

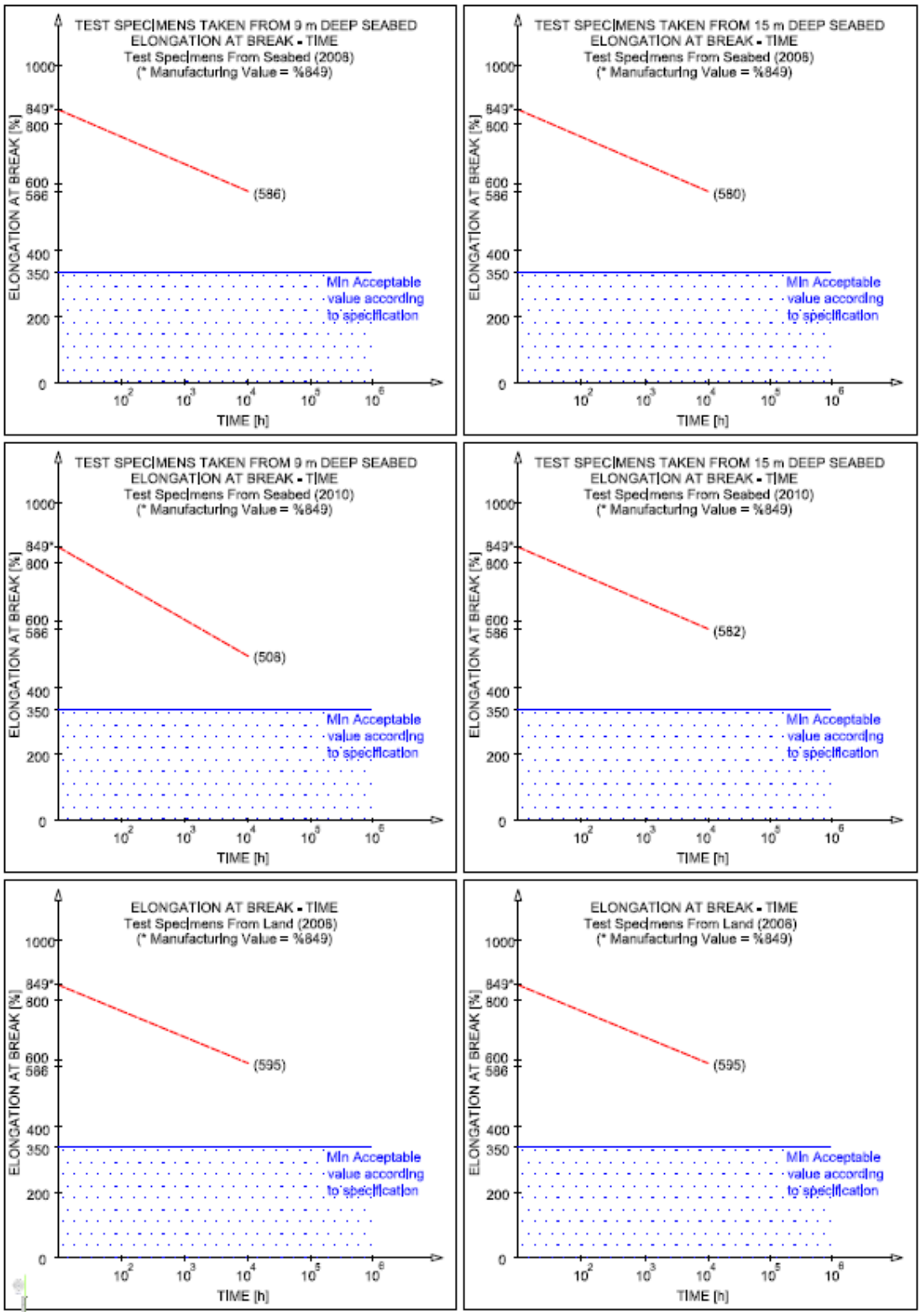

Figure B.1: Elongation at Break graph for specimens taken from 9 m, 15 m deep and landside.

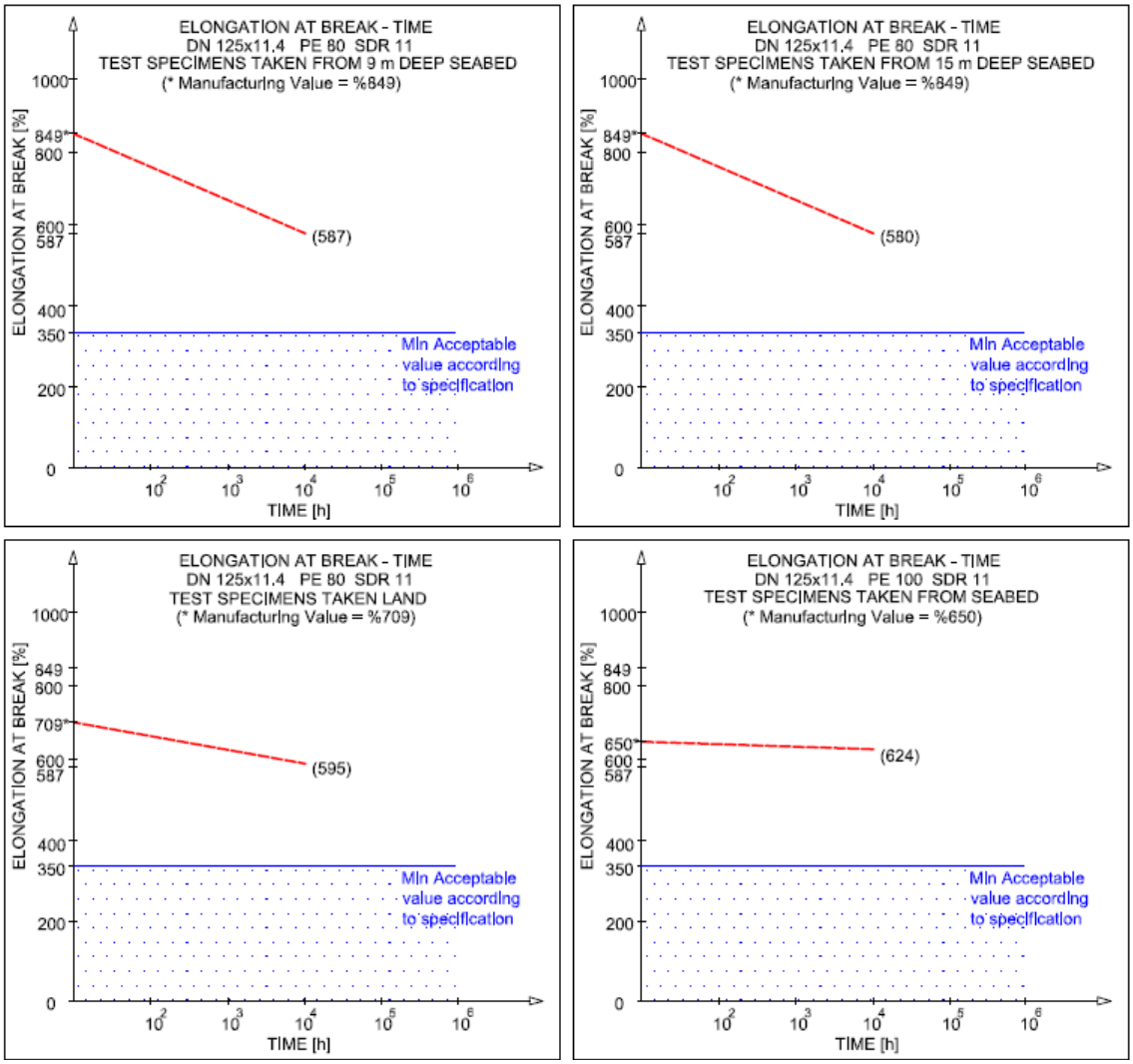

Figure B.2: Elongation at Break graph for DN 125x11.4 PE 80 SDR 11 and DN 125 PE 100 SDR 11.

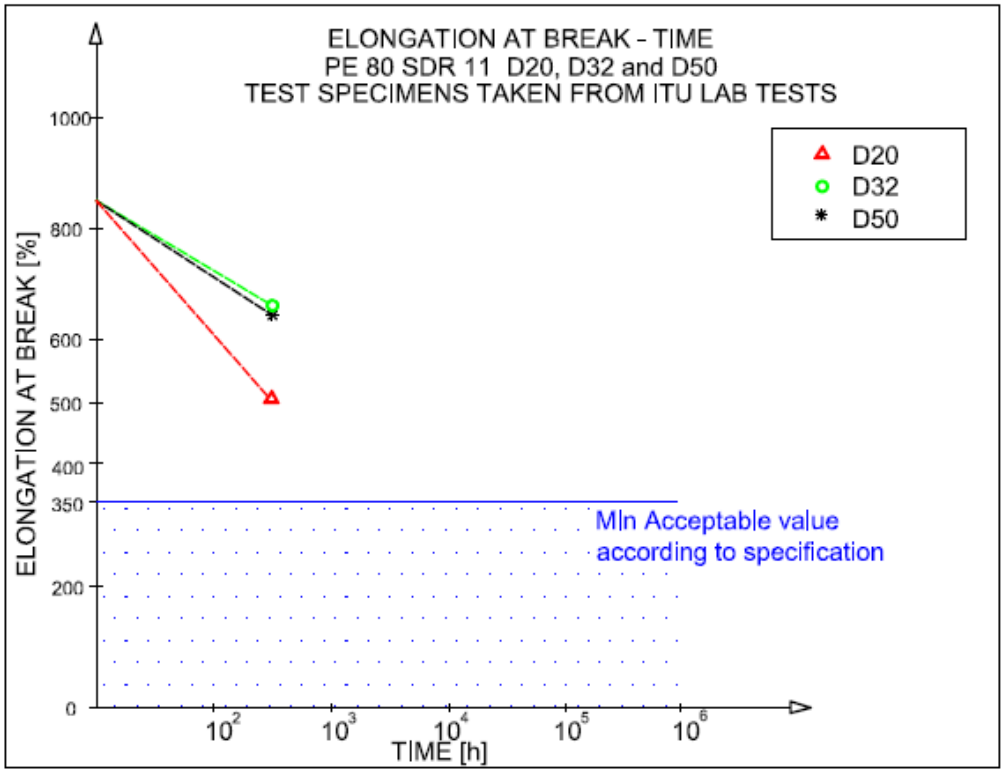

Figure B.3: Elongation at Break graph for specimens taken from ITU tests (PE 80 SDR 11 D20, D32 and D50).

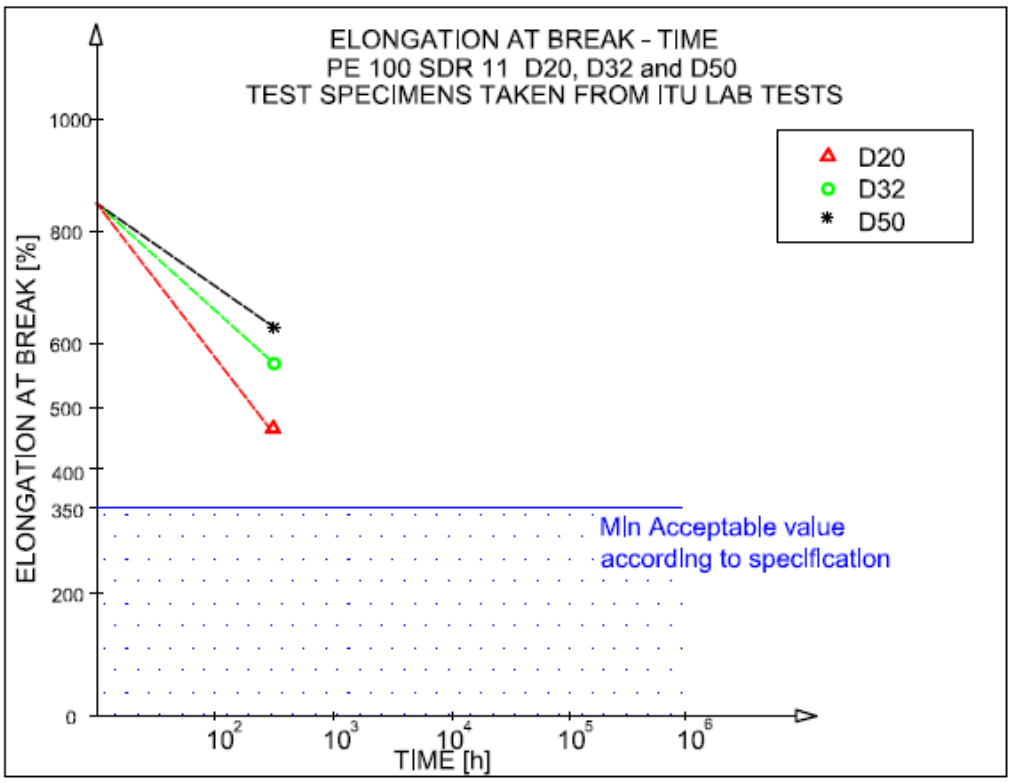

Figure B.4: Elongation at Break graph for specimens taken from ITU tests (PE 100 SDR 11 D20, D32 and D50).

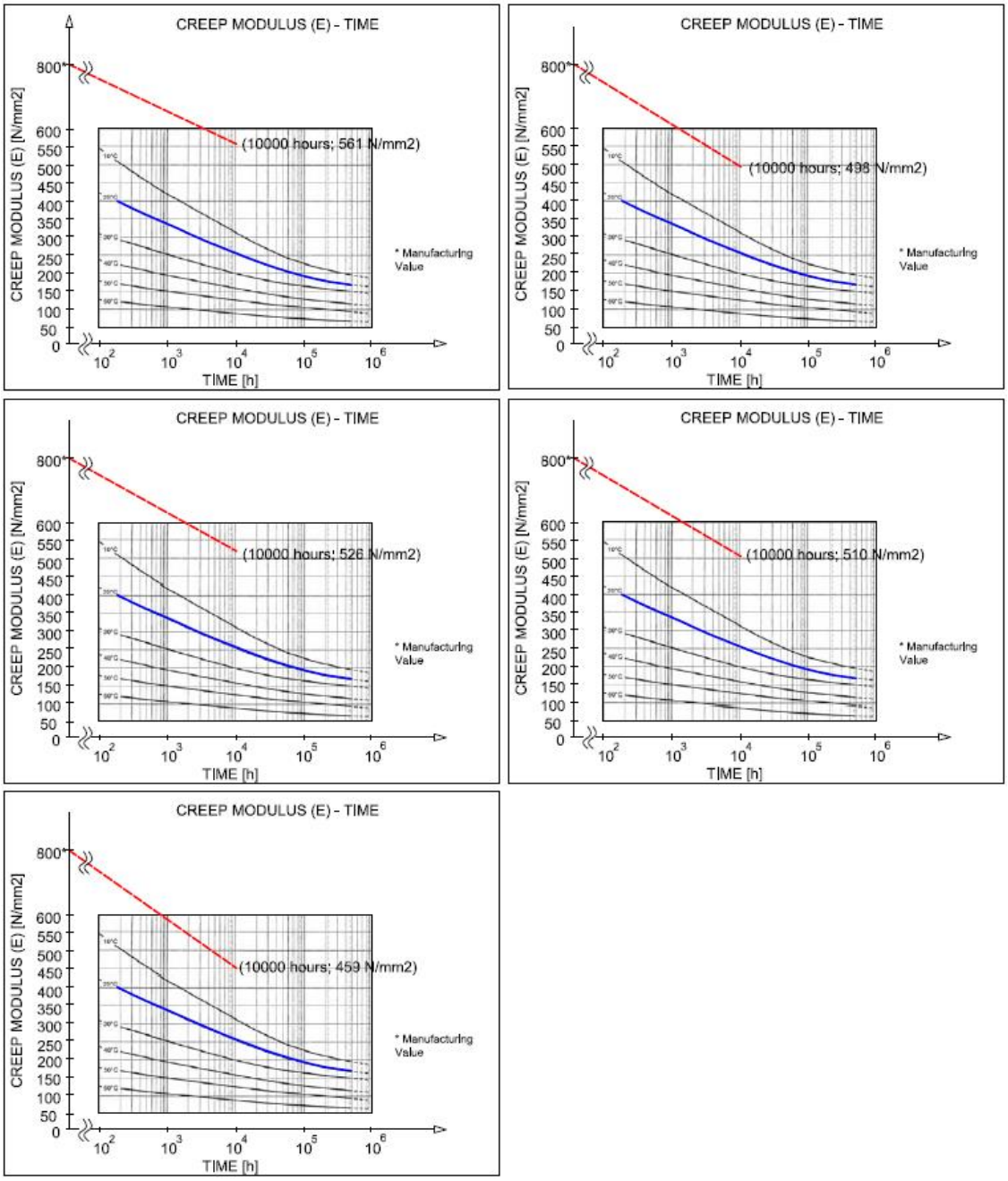

Figure B.5: Creep Modulus (E) – Time graph for PE 80 Pipe specimens.

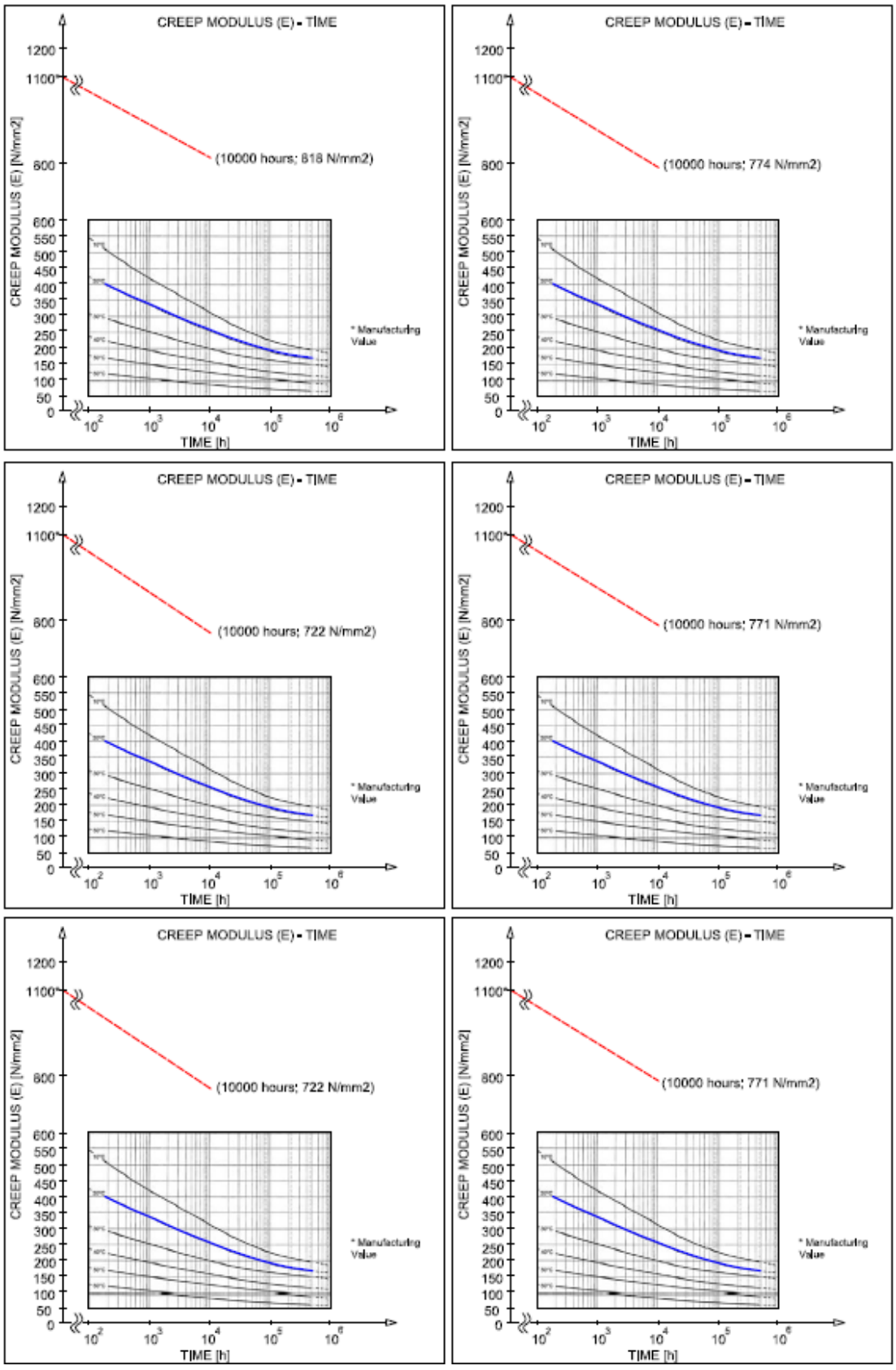

Figure B.6: Creep Modulus (E) – Time graph for PE 100 Pipe specimens.

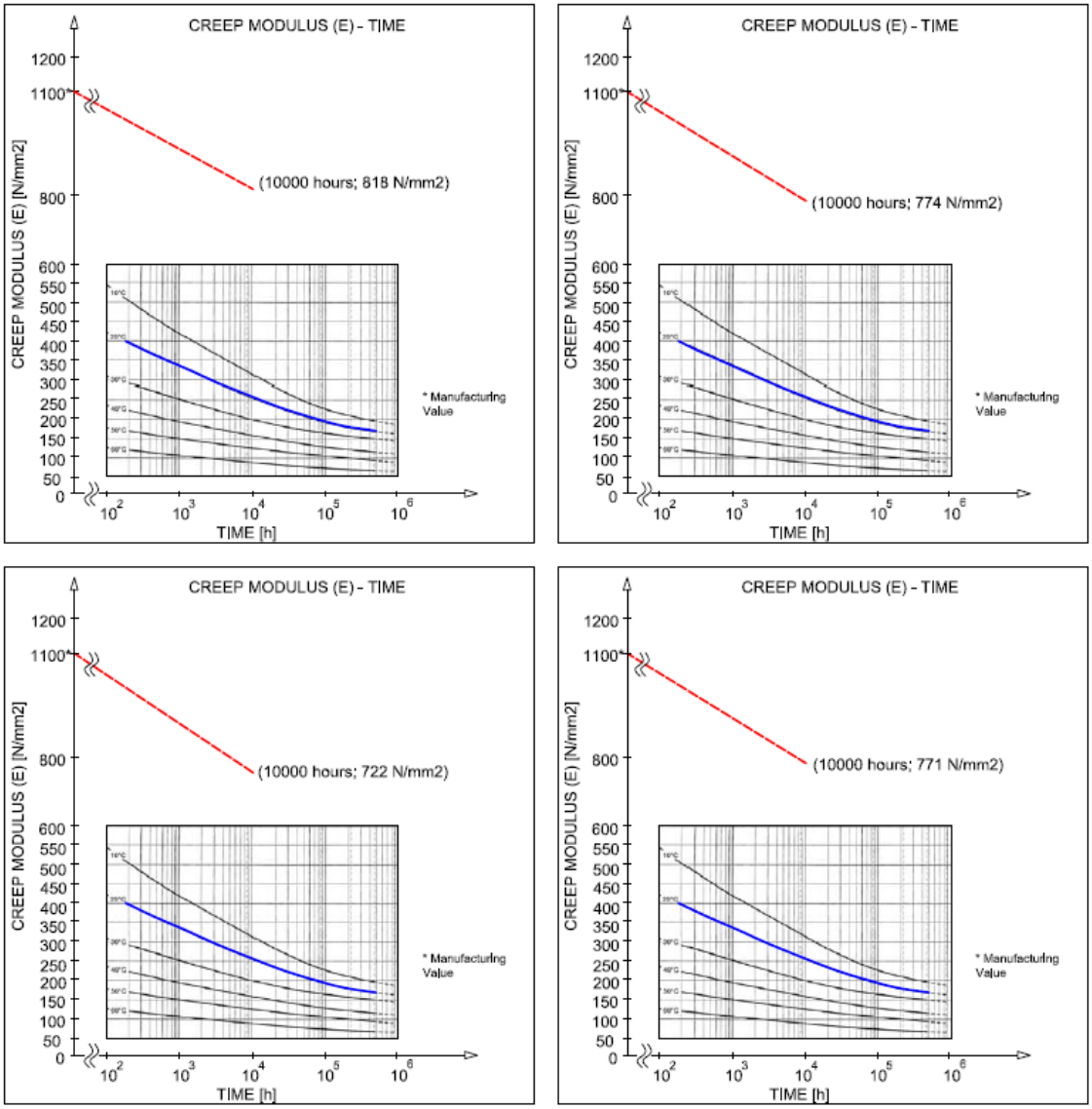

Figure B.7: Creep Modulus (E) – Time graph for PE 100 Pipe specimens.

OFFICIAL TEST RESULTS FOR SELECTED SPECIMENS
(These results are official material lab results. Material tests were performed by UGETAM Test Lab. Only one set of result is presented in this section.)

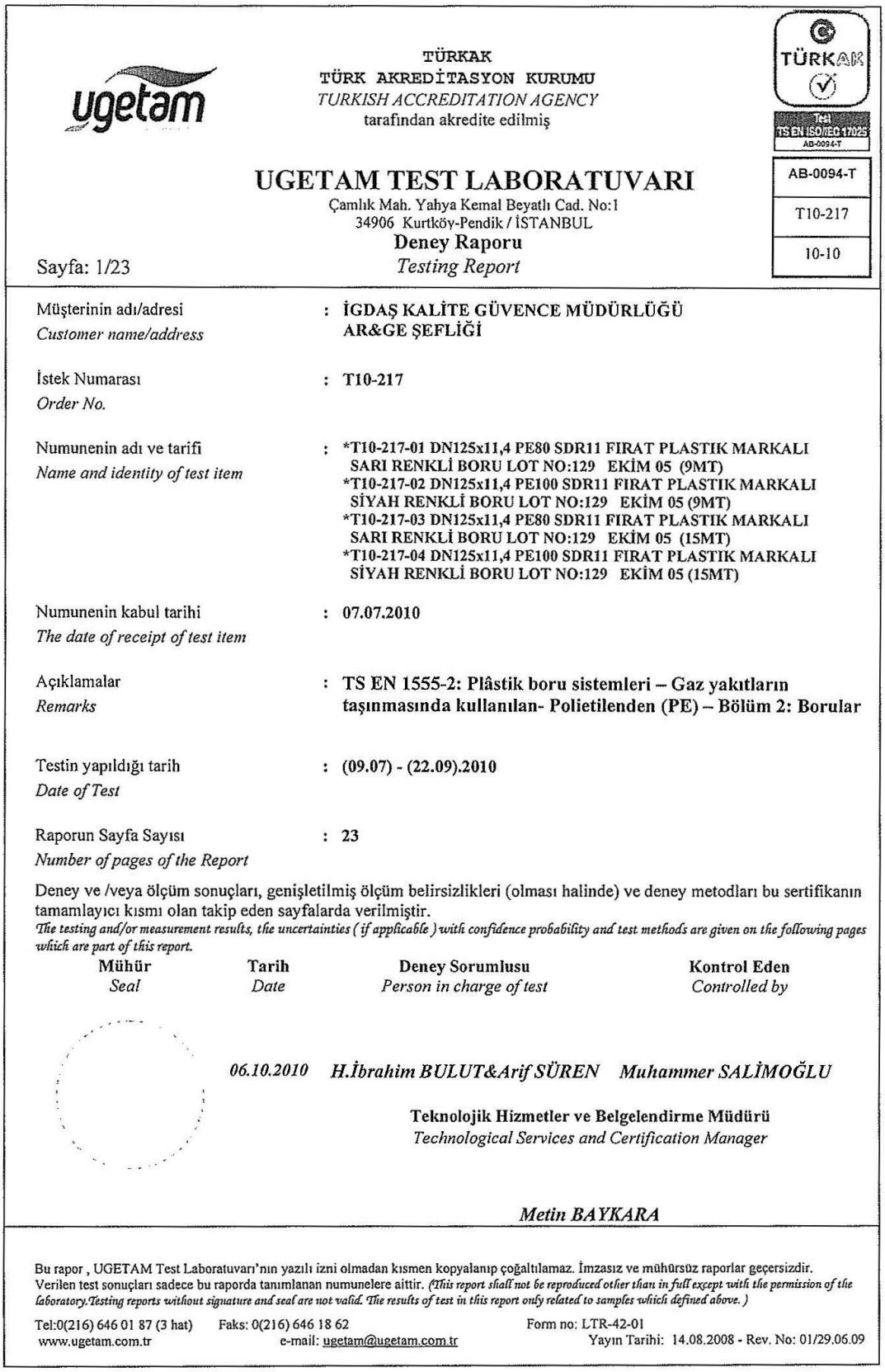

TÜRKAK
TÜRK AKREDİTASYON KURUMU
TURKISH ACCREDITATION AGENCY
tarafından akredite edilmiş

TÜRKAK
TS EN ISO/IEC 17025
AB-0094-T

UGETAM TEST LABORATUVARI
Çamlık Mah. Yahya Kemal Beyatlı Cad. No:1
34906 Kurtköy-Pendik / İSTANBUL
Deney Raporu
Testing Report

AB-0094-T
T10-217
10-10

Sayfa: 1/23

Müşterinin adı/adresi *Customer name/address*	:	**İGDAŞ KALİTE GÜVENCE MÜDÜRLÜĞÜ AR&GE ŞEFLİĞİ**
İstek Numarası *Order No.*	:	**T10-217**
Numunenin adı ve tarifi *Name and identity of test item*	:	***T10-217-01 DN125x11,4 PE80 SDR11 FIRAT PLASTIK MARKALI SARI RENKLİ BORU LOT NO:129 EKİM 05 (9MT)** ***T10-217-02 DN125x11,4 PE100 SDR11 FIRAT PLASTIK MARKALI SİYAH RENKLİ BORU LOT NO:129 EKİM 05 (9MT)** ***T10-217-03 DN125x11,4 PE80 SDR11 FIRAT PLASTIK MARKALI SARI RENKLİ BORU LOT NO:129 EKİM 05 (15MT)** ***T10-217-04 DN125x11,4 PE100 SDR11 FIRAT PLASTIK MARKALI SİYAH RENKLİ BORU LOT NO:129 EKİM 05 (15MT)**
Numunenin kabul tarihi *The date of receipt of test item*	:	**07.07.2010**
Açıklamalar *Remarks*	:	**TS EN 1555-2: Plâstik boru sistemleri – Gaz yakıtların taşınmasında kullanılan- Polietilenden (PE) – Bölüm 2: Borular**
Testin yapıldığı tarih *Date of Test*	:	**(09.07) - (22.09).2010**
Raporun Sayfa Sayısı *Number of pages of the Report*	:	**23**

Deney ve /veya ölçüm sonuçları, genişletilmiş ölçüm belirsizlikleri (olması halinde) ve deney metodları bu sertifikanın tamamlayıcı kısmı olan takip eden sayfalarda verilmiştir.
The testing and/or measurement results, the uncertainties (if applicable) with confidence probability and test methods are given on the following pages which are part of this report.

Mühür *Seal*	**Tarih** *Date*	**Deney Sorumlusu** *Person in charge of test*	**Kontrol Eden** *Controlled by*
	06.10.2010	*H.İbrahim BULUT&Arif SÜREN*	*Muhammer SALİMOĞLU*

Teknolojik Hizmetler ve Belgelendirme Müdürü
Technological Services and Certification Manager

Metin BAYKARA

Tel:0(216) 646 01 87 (3 hat) Faks: 0(216) 646 18 62
www.ugetam.com.tr e-mail: ugetam@ugetam.com.tr
Form no: LTR-42-01
Yayın Tarihi: 14.08.2008 - Rev. No: 01/29.06.09

Figure B.8: Official material test result, test: T10-217, page: 1/23.

TÜRKAK
TÜRK AKREDİTASYON KURUMU
TURKISH ACCREDITATION AGENCY
tarafından akredite edilmiş

UGETAM TEST LABORATUVARI

Çamlık Mah. Yahya Kemal Beyatlı Cad. No:1
34906 Kurtköy-Pendik / İSTANBUL

Deney Raporu
Testing Report

AB-0094-T
T10-217
10-10

ÖZET DENEY SONUÇLARI:

NUMUNE NO	NUMUNE TANIMI	TEST STANDARDI	DENEY ADI	İSTENEN ÖZELLİKLER	BİRİM	SONUÇ
T10-217-01	DN125x11,4 PE80 SDR11 FIRAT PLASTİK MARKALI SARI RENKLİ BORU(9MT)	TS EN ISO 1167-1	Hidrostatik Mukavemet (80°C – 165h)	4,5 MPa >165	h (saat)	Hasar Yok
		TS EN ISO 6259-1	Kopma Uzaması	Min. 350	%	508,11
		TS EN ISO 1133:2006	Kütle Erime Akış Hızı (190°C – 5 Kg)	Hammadde ± %20	g/10 dakika	0,92
		TS EN ISO 1183-1	Yoğunluk	> 0,930	g/cm3	0,939
		TS EN 728	Yükseltgeme İndüksiyon Süresi (OIT)	>20	dakika	>25
		TS EN ISO 13479	Yükseltgeme İndüksiyon Süresi (OIT) (200°C)	8 Bar > 165	h (saat)	Hasar Yok
		TS EN ISO 2505	Boyutsal Kararlılık	≤3	%	1,45
T10-217-02	DN125x11,4 PE100 SDR11 FIRAT PLASTİK MARKALI SİYAH RENKLİ BORU(9MT)	TS EN ISO 1167-1	Hidrostatik Mukavemet (80°C – 165h)	5,4 MPa >165	h (saat)	Hasar Yok
		TS EN ISO 6259-1	Kopma Uzaması	Min. 350	%	569,34
		TS EN ISO 1133:2006	Kütle Erime Akış Hızı (190°C – 5 Kg)	Hammadde ± %20	g/10 dakika	0,23
		TS EN ISO 1183-1	Yoğunluk	> 0,930	g/cm3	0,960
		TS EN 728	Yükseltgeme İndüksiyon Süresi (OIT) (200°C)	>20	dakika	>25
		TS EN ISO 13479	Yavaş Çatlak İlerlemesi (Çentik) Deneyi	9,2 Bar > 165	h (saat)	Hasar Yok
		TS EN ISO 2505	Boyutsal Kararlılık	≤3	%	0,99

Tel:0(216) 646 01 87 (3 hat) Faks: 0(216) 646 18 62
www.ugetam.com.tr e-mail: ugetam@ugetam.com.tr

Form no: LTR-42-01
Yayın Tarihi: 14.08.2008 - Rev. No: 01/29.06.09

Figure B.9: Official material test result, test: T10-217, page: 2/23.

TÜRKAK
TÜRK AKREDİTASYON KURUMU
TURKISH ACCREDITATION AGENCY
tarafından akredite edilmiş

UGETAM TEST LABORATUVARI

Çamlık Mah. Yahya Kemal Beyatlı Cad. No:1
34906 Kurtköy-Pendik / İSTANBUL

Deney Raporu
Testing Report

AB-0094-T
T10-217
10-10

NUMUNE NO	NUMUNE TANIMI	TEST STANDARDI	DENEY ADI	İSTENEN ÖZELLİKLER	BİRİM	SONUÇ
T10-217-03	DN125x11,4 PE80 SDR11 FIRAT PLASTİK MARKALI SARI RENKLİ BORU (15MT)	TS EN ISO 1167-1	Hidrostatik Mukavemet (80°C – 165h)	4,5 MPa >165	h (saat)	Hasar Yok
		TS EN ISO 6259-1	Kopma Uzaması	Min. 350	%	582,75
		TS EN ISO 1133:2006	Kütle Erime Akış Hızı (190°C – 5 Kg)	Hammadde ± %20	g/10 dakika	0,90
		TS EN ISO 1183-1	Yoğunluk	> 0,930	g/cm3	0,940
		TS EN 728	Yükseltgeme İndüksiyon Süresi (OIT) (200°C)	>20	dakika	>25
		TS EN ISO 13479	Yavaş Çatlak İlerlemesi (Çentik) Deneyi	8 Bar > 165	h (saat)	Hasar Yok
		TS EN ISO 2505	Boyutsal Kararlılık	≤3	%	1,44
T10-217-04	DN125x11,4 PE100 SDR11 FIRAT PLASTİK MARKALI SİYAH RENKLİ BORU(15MT)	TS EN ISO 1167-1	Hidrostatik Mukavemet (80°C – 165h)	5,4 MPa >165	h (saat)	Hasar Yok
		TS EN ISO 6259-1	Kopma Uzaması	Min. 350	%	589,65
		TS EN ISO 1133:2006	Kütle Erime Akış Hızı (190°C – 5 Kg)	Hammadde ± %20	g/10 dakika	0,23
		TS EN ISO 1183-1	Yoğunluk	> 0,930	g/cm3	0,961
		TS EN 728	Yükseltgeme İndüksiyon Süresi (OIT) (200°C)	>20	dakika	>25
		TS EN ISO 13479	Yavaş Çatlak İlerlemesi (Çentik) Deneyi	9,2 Bar > 165	h (saat)	Hasar Yok
		TS EN ISO 2505	Boyutsal Kararlılık	≤3	%	0,97

Tel:0(216) 646 01 87 (3 hat) Faks: 0(216) 646 18 62
www.ugetam.com.tr e-mail: ugetam@ugetam.com.tr

Form no: LTR-42-01
Yayın Tarihi: 14.08.2008 - Rev. No: 01/29.06.09

Figure B.10: Official material test result, test: T10-217, page: 3/23.

TÜRKAK
TÜRK AKREDİTASYON KURUMU
TURKISH ACCREDITATION AGENCY
tarafından akredite edilmiş

UGETAM TEST LABORATUVARI

Çamlık Mah. Yahya Kemal Beyatlı Cad. No:1
34906 Kurtköy-Pendik / İSTANBUL

Deney Raporu
Testing Report

AB-0094-T
T10-217
10-10

DETAY DENEY SONUÇLARI:

1. NUMUNE : T10 - 217 – 01:

Marka	: **FIRAT PLASTIK**	Renk	: **SARI**
Örneklerin Tanımı (Lot, Seri No, Üretim Tarihi v.s.)	: **İ.T. EKİM 05 LOT:129**	Nominal Boyutları	: d_n = 125 e_n = 11,4
Malzeme Tipi (PE 80, PE 100 v.s.)	: **PE 80**	Markalama	: **FIRAT PE80 GAZ 4 SDR11 SINIF C DN125x11,4 SDR11 LOT:129 EKİM 05**
SDR / PN	: **SDR11**	İlave açıklama	: **9m Derinlik**

T10-217-01-01 HİDROSTATİK İÇ BASINCA MUKAVEMET

Test metodu : **TS EN ISO 1167-1-Sabit sıcaklık altında iç basınca dayanımın tayini. (Determination of resistance to internal pressure at constant temparature)**
Atıf Yapılan Standartlar : TS EN ISO 1167-2, TS EN ISO 3126

Nominal Boyutları : d_n = 125 e_n = 11,4
Test Sıcaklığı ve doğruluğu : 80 ^{0}C ± 1^{0}C
Test Cihazının Tanımı : **SCITEQ-HAMMEL-2000: Hidrostatik test ünitesi:9742-01571 – Termo Tank:15377, 17748**

Uygulanan Çevresel Gerilme – σ	4,5	±	0,11	Mpa
Rapor edilen ölçüm belirsizliği, genişletilmiş belirsizlik olup bileşik belirsizlikten kapsam faktörü k=2 kullanılarak elde edilmiştir. Güvenilirlik düzeyi %95'tir.				

Testin Süresi (saat) : **165**

Test Numunesinin Ölçülen Boyutları

Ortalama dış çap (mm) : d_e = 125
Minimum et kalınlığı (mm) : e_{min} = 11,4
Test numunesinin toplam boyu (mm) : L= 575
Test numunesinin serbest uzunluğu (mm) : L_0 = 375
Uygulanan test basıncı (bar) : **P = (20 x σ) / (SDR-1) = 9,0**
Test Ortamı : **Su içinde –Su ile**
Numunelerin şartlandırma sıcaklık ve süresi : **80^{0}C – 6 Saat**
Test başlıklarının tipi : **A tipi**
Test edilen numune sayısı : **1**
Test parçalarının termo tank içindeki vaziyeti : **Dikey**
Test basıncına gelme zamanı (30 sn – 1 dk.) : **60sn.**
Varsa hasarın tipi (yumuşak veya kırılgan) : **Hasar Yok**

Tel:0(216) 646 01 87 (3 hat) Faks: 0(216) 646 18 62
www.ugetam.com.tr e-mail: ugetam@ugetam.com.tr
Form no: LTR-42-01
Yayın Tarihi: 14.08.2008 - Rev. No: 01/29.06.09

Figure B.11: Official material test result, test: T10-217, page: 4/23.

TÜRKAK
TÜRK AKREDİTASYON KURUMU
TURKISH ACCREDITATION AGENCY
tarafından akredite edilmiş

UGETAM TEST LABORATUVARI

Çamlık Mah. Yahya Kemal Beyatlı Cad. No:1
34906 Kurtköy-Pendik / İSTANBUL

Deney Raporu
Testing Report

AB-0094-T
T10-217
10-10

T10-217-01-02 KOPMA UZAMASI (ÇEKME ÖZELLİKLERİNİN TAYİNİ)

Test metodu: **TS EN ISO 6259 – 1: Çekme Özelliklerinin Tayini (Determination of tensile properties – Part 1 : General test method)**
ISO 6259 – 3 : Thermoplastics pipes – Determination of tensile properties – Part 3 : Polyolefin pipes

Test numunesi tipi ve hazırlanma şekli : **Tip1 – Kaşık Numune / Makinede İşlenmiş**
Test Sıcaklığı (^{0}C) : **23 ^{0}C ± 2^{0}C**
Test numunesi sayısı (adet) : **5**
Çekme hızı (mm/dakika) : **100**
Uzama ölçer ve boyut ölçer tipi : **Elektronik uzama ölçer (S.N: 159948) ve Dijital kumpas**

Test numune No	Kalınlık (mm) a_0	Genişlik (mm) b_0	Kesit Alanı (mm^2) S_0	Baş. Ölçme Uzunluğu (mm) L_0	Akma gerilmesi (MPa) σ_Y	Akma Uzaması (%) ε_Y	Maksimm Çekme Gerilmesi (Mpa) σ_M	Kopma gerilmesi (MPa) σ_B	Kopma Uzaması (%) ε_B	Elastiklik Modülü (MPa) E_t
1.	12,05	9,81	118,21	50,00	16,49	13,01	16,49	3,45	429,77	561,99
2.	12,03	9,74	117,24	50,00	15,90	13,54	15,90	14,54	534,72	498,47
3.	12,03	9,74	117,14	50,00	16,02	13,37	16,02	14,46	539,34	526,22
4.	12,12	9,76	118,32	50,00	16,20	13,22	16,20	3,55	497,39	510,06
5.	12,06	9,82	118,50	50,00	16,00	14,35	16,00	14,23	539,35	459,23
ORT.	12,06	9,78	117,88	50,00	**16,12**	**13,50**	**16,12**	**10,05**	**508,11**	**511,19**
Std. Sapma	-	-	-	-	**0,23**	**0,51**	**0,23**	**5,98**	**47,20**	**37,65**
Belirsizlik	-	-	-	-	**0,30**	**0,16**	**0,30**	**0,19**	**5,90**	**22,30**

Ölçüm Belirsizliği ± (MPa) (k=2, %95 Güvenilirlik Seviyesinde)

T10-217-01-03 KÜTLESEL ERİME AKIŞ HIZI (MFR)

Test metot standardı adı : **TS EN ISO 1133- Metot A -Plastikler – Termoplastiklerin erime kütle –akış oranı (MFR) nın tayini *(Plastics – Determination of the melt mass-flow rate (MFR) of thermoplastics)***
Şartlandırma Ortamı : **23^{0}C ± 2^{0}C**
Test Sıcaklığı : **190^{0}C**
Uygulanan Test Yükü (kg) : **5**
Kesme Zaman Aralığı (sn) : **120**
Kesilen Parçaların Kütleleri (gr)

1. Parça = 0,1844
2. Parça = 0,1852
3. Parça = 0,1865
4. Parça = 0,1870
5. Parça= 0,1848
6. Parça= 0,1780
7. parça= 0,1823

Kütlesel Erime Akış Oranı – MFR	0,92	±	0,03	gr/10 dak
Rapor edilen ölçüm belirsizliği, genişletilmiş belirsizlik olup bileşik belirsizlikten kapsam faktörü k=2 kullanılarak elde edilmiştir. Güvenilirlik düzeyi %95'tir.				

Tel:0(216) 646 01 87 (3 hat) Faks: 0(216) 646 18 62 Form no: LTR-42-01
www.ugetam.com.tr e-mail: ugetam@ugetam.com.tr Yayın Tarihi: 14.08.2008 - Rev. No: 01/29.06.09

Figure B.12: Official material test result, test: T10-217, page: 5/23.

TÜRKAK
TÜRK AKREDİTASYON KURUMU
TURKISH ACCREDITATION AGENCY
tarafından akredite edilmiş

UGETAM TEST LABORATUVARI

Çamlık Mah. Yahya Kemal Beyatlı Cad. No:1
34906 Kurtköy-Pendik / İSTANBUL

Deney Raporu
Testing Report

AB-0094-T
T10-217
10-10

T10-217-01-04 YOĞUNLUK TAYİNİ

Test metot standardı adı : **TS EN ISO 1183-1-Plastikler-Yoğunluk ve Bağıl Yoğunluk** ***Tayini (Plastics – Methods for Determining the density and relative density of non-cellular plastics)***

Numune Formu (şekli) : **1 – 2gr. Kübik Şekil**
Şartlandırma Ortamı : **Hava, Min.2 saat 23^{0}C ± 2^{0}C , %50 ± %10 Bağıl Nem**
Test Sıcaklığı ve doğruluğu : **23^{0}C ± 2^{0}C (Daldırma sıvısının sıcaklığı)**

Ölçülen numune yoğunlukları (g/cm3) :

Parça = 0,9399
Parça = 0,9388
Parça = 0,9390

Ortalama Yoğunluk ($\rho_{s,23^0C}$):	**0,939**	±	**0,0005**	g/cm^3
Rapor edilen ölçüm belirsizliği, genişletilmiş belirsizlik olup bileşik belirsizlikten kapsam faktörü k=2 kullanılarak elde edilmiştir. Güvenilirlik düzeyi %95'tir.				

T10-217-01-05 OKSİDASYON İNDÜKSİYON SÜRESİ (OIT)

Test metodu : **TS EN 728-Oksidasyon İndüksiyon Süresinin Tayini** ***(Determination of the oxidation induction time)***
Atıf Yapılan Standartlar : TS 1148 ISO 293, TS EN ISO 1133:2006

Numunelerin boru veya ekleme parçasının çeperlerinden alındığı yerler : **DIŞ –ORTA – İÇ YÜZEYLER**
Deney parçasının kütlesi (mg) : **16,0 – 13,1 –15,9**
Deney Sıcaklığı (^{0}C) : **200**
Kullanılan DSC cihazının markası, türü, modeli, imalat yeri, seri numarası : **Perkin Elmer JADE, İntercooler, USA, SN: 520A6092505**

Her bir numunenin OIT değeri (dak)

Oksidasyon İndüksiyon Süresi – OIT (dak)			**Belirsizlik (dak)**	
Dış Yüzey	OIT >	**25**	±	**2,5**
Orta Yüzey	OIT >	**25**	±	**2,5**
İç Yüzey	OIT >	**25**	±	**2,5**

Rapor edilen ölçüm belirsizliği, genişletilmiş belirsizlik olup bileşik belirsizlikten kapsam faktörü k=2 kullanılarak elde edilmiştir. Güvenilirlik düzeyi %95'tir.

Tel:0(216) 646 01 87 (3 hat) Faks: 0(216) 646 18 62
www.ugetam.com.tr e-mail: ugetam@ugetam.com.tr
Form no: LTR-42-01
Yayın Tarihi: 14.08.2008 - Rev. No: 01/29.06.09

Figure B.13: Official material test result, test: T10-217, page: 6/23.

TÜRKAK
TÜRK AKREDİTASYON KURUMU
TURKISH ACCREDITATION AGENCY
tarafından akredite edilmiş

UGETAM TEST LABORATUVARI

Çamlık Mah. Yahya Kemal Beyatlı Cad. No:1
34906 Kurtköy-Pendik / İSTANBUL

Deney Raporu
Testing Report

AB-0094-T
T10-217
10-10

T10-217-01-06 -YAVAŞ ÇATLAK İLERLEMESİNE MUKAVEMET (NOTCH: e> 5 mm)

Test metodu : **TS EN ISO 13479-Çentikli borular üzerinde çatlak ilerlemesi deneyi** ***(Test method for slow crack growth on notched pipes -notch test)***
Atıf Yapılan Standartlar : TS EN 1167-1:2006

Örneklerin Tanımı : **FIRAT PE80 SDR11 DN125x11,4 SDR11 LOT:129 EKİM 05**

Çakı çapı, diş sayısı, çakı açısı	**: D=168,8 mm, 20 diş, 60^0**
Çakı Dönme hızı (devir/dakika)	**: 700 dev/dakika**
Çakı İlerleme (travers) Hızı (mm/dakika)	**: 150 mm/dakika**
Basınç altındaki deney süresi (veya hasarlanma süresi) (saat)	**: 165**
Deney Basıncı (bar)	**: 8**

Test Numunesindeki çentik ölçüleri

Çentik tabanındaki et kalınlığı (mm)	**9,3**
Çentik Derinliği	**2,10**
% Çentik Derinliği	**18**

Hasarlanmış çentiğin konumu	**: Hasar Yok**
Uç kapakları arasındaki en küçük serbest uzunluk (Lo=3xdn±5mm)	**: Lo= 375**
Test Ortamı	**: Su içinde –Su ile**
Test başlıklarının tipi	**: A tipi**
Test edilen numune sayısı	**: 1**
Test parçalarının termo tank içindeki vaziyeti	**: Dikey**

Uygulanan Deney Basıncı – P (bar)	**8**	±	**0,38**	**bar**

Rapor edilen ölçüm belirsizliği, genişletilmiş belirsizlik olup bileşik belirsizlikten kapsam faktörü k=2 kullanılarak elde edilmiştir. Güvenilirlik düzeyi %95'tir.

Tel:0(216) 646 01 87 (3 hat) Faks: 0(216) 646 18 62
www.ugetam.com.tr e-mail: ugetam@ugetam.com.tr

Form no: LTR-42-01
Yayın Tarihi: 14.08.2008 - Rev. No: 01/29.06.09

Figure B.14: Official material test result, test: T10-217, page: 7/23.

TÜRKAK
TÜRK AKREDİTASYON KURUMU
TURKISH ACCREDITATION AGENCY
tarafından akredite edilmiş

UGETAM TEST LABORATUVARI

Çamlık Mah. Yahya Kemal Beyatlı Cad. No:1
34906 Kurtköy-Pendik / İSTANBUL

Deney Raporu
Testing Report

AB-0094-T
T10-217
10-10

T10-217-01-07 BOYUTSAL KARARLILIK

Test metodu : **TS EN ISO 2505-Termoplastik Borular – Boyca Eski Halini Alabilme Özelliğinin Tayini**
(Thermoplastics pipes - Longitudinal reversion - Test method and parameters (ISO 2505:2005)

Nominal Boyutları	: d_n=125 e_n=11,4
Şartlandırma Ortamı, süresi	: **Hava, 23°C ± 2°C, min. 6 saat**
Test Sıcaklığı ve doğruluğu	: **110°C ± 2°C**
Testin Süresi (saat)	: **120 dak**
Test Ortamı	: **Etüv (Hava)**
Test edilen numune sayısı	: **3**
Test parçalarının etüv içindeki vaziyeti	: **Yatay-Askı**

Her parçanın boyca değişikliği (%):

$$R_L = \frac{(L_0 - L)}{L_0} \times 100$$

1.Parça:	L_0=	100,00	L=	98,50	ΔL=	1,50	R_L=	1,50
2.Parça:	L_0=	100,00	L=	98,60	ΔL=	1,40	R_L=	1,40
3.Parça:	L_0=	100,00	L=	98,54	ΔL=	1,46	R_L=	1,46

L_0 : Test numunesinin etüve konmadan önceki boyu (mm), L : Test numunesinin etüvden alındıktan sonraki boyu (mm)

Ortalama boyca değişim – $R_{L,m}$ (%)	**1,45**	±	**0,12**	%
Rapor edilen ölçüm belirsizliği, genişletilmiş belirsizlik olup bileşik belirsizlikten kapsam faktörü k=2 kullanılarak elde edilmiştir. Güvenilirlik düzeyi %95'tir.				

Figure B.15: Official material test result, test: T10-217, page: 8/23.

TÜRKAK
TÜRK AKREDİTASYON KURUMU
TURKISH ACCREDITATION AGENCY
tarafından akredite edilmiş

UGETAM TEST LABORATUVARI

Çamlık Mah. Yahya Kemal Beyatlı Cad. No:1
34906 Kurtköy-Pendik / İSTANBUL

Deney Raporu
Testing Report

AB-0094-T
T10-217
10-10

2. NUMUNE : T10 - 217 – 02:

Marka	: FIRAT PLASTIK	Renk	: SARI
Örneklerin Tanımı (Lot, Seri No, Üretim Tarihi v.s.)	: İ.T. EKİM 05 LOT:129	Nominal Boyutları	: d_n= 125 e_n= 11,4
Malzeme Tipi (PE 80, PE 100 v.s.)	: PE 100	Markalama	: FIRAT PE100 GAZ 4 SDR11 SINIF C DN125x11,4 SDR11 LOT:129 EKİM 05
SDR / PN	: SDR11	İlave açıklama	: 9m Derinlik

T10-217-02-01 HİDROSTATİK İÇ BASINCA MUKAVEMET

Test metodu : **TS EN ISO 1167-1-Sabit sıcaklık altında iç basınca dayanımın tayini. (Determination of resistance to internal pressure at constant temparature)**
Atıf Yapılan Standartlar : TS EN ISO 1167-2, TS EN ISO 3126

Nominal Boyutları : d_n= 125 e_n= 11,4
Test Sıcaklığı ve doğruluğu : 80 ^{0}C ± 1^{0}C
Test Cihazının Tanımı : SCITEQ-HAMMEL-2000: Hidrostatik test ünitesi:9742-01571 – Termo Tank:15377, 17748

Uygulanan Çevresel Gerilme – σ	5,4	±	0,13	Mpa
Rapor edilen ölçüm belirsizliği, genişletilmiş belirsizlik olup bileşik belirsizlikten kapsam faktörü k=2 kullanılarak elde edilmiştir. Güvenilirlik düzeyi %95'tir.				

Testin Süresi (saat)	: 165
Test Numunesinin Ölçülen Boyutları	
Ortalama dış çap (mm)	: d_e = 125
Minimum et kalınlığı (mm)	: e_{min}= 11,4
Test numunesinin toplam boyu (mm)	: L= 575
Test numunesinin serbest uzunluğu (mm)	: L_0 = 375
Uygulanan test basıncı (bar)	**: P = (20 x σ) / (SDR-1) = 10,80**
Test Ortamı	: Su içinde –Su ile
Numunelerin şartlandırma sıcaklık ve süresi	: 80^{0}C – 6 Saat
Test başlıklarının tipi	: A tipi
Test edilen numune sayısı	: 1
Test parçalarının termo tank içindeki vaziyeti	: Dikey
Test basıncına gelme zamanı (30 sn – 1 dk.)	: 60sn.
Varsa hasarın tipi (yumuşak veya kırılgan)	: Hasar Yok

Tel:0(216) 646 01 87 (3 hat) Faks: 0(216) 646 18 62
www.ugetam.com.tr e-mail: ugetam@ugetam.com.tr

Form no: LTR-42-01
Yayın Tarihi: 14.08.2008 - Rev. No: 01/29.06.09

Figure B.16: Official material test result, test: T10-217, page: 9/23.

TÜRKAK
TÜRK AKREDİTASYON KURUMU
TURKISH ACCREDITATION AGENCY
tarafından akredite edilmiş

UGETAM TEST LABORATUVARI

Çamlık Mah. Yahya Kemal Beyatlı Cad. No:1
34906 Kurtköy-Pendik / İSTANBUL

Deney Raporu
Testing Report

AB-0094-T
T10-217
10-10

T10-217-02-02 KOPMA UZAMASI (ÇEKME ÖZELLİKLERİNİN TAYİNİ)

Test metodu: **TS EN ISO 6259 – 1: Çekme Özelliklerinin Tayini (Determination of tensile properties – Part 1 : General test method)**
ISO 6259 – 3 : **Thermoplastics pipes – Determination of tensile properties – Part 3 : Polyolefin pipes**

Test numunesi tipi ve hazırlanma şekli : **Tip1 – Kaşık Numune / Makinede İşlenmiş**
Test Sıcaklığı (^{0}C) : **23 ^{0}C ± 2^{0}C**
Test numunesi sayısı (adet) : **5**
Çekme hızı (mm/dakika) : **50**
Uzama ölçer ve boyut ölçer tipi : **Elektronik uzama ölçer (S.N: 159948) ve Dijital kumpas**

Test numune No	Kalınlık (mm) a_0	Genişlik (mm) b_0	Kesit Alanı (mm^2) S_0	Baş. Ölçme Uzunluğu (mm) L_0	Akma gerilmesi (MPa) σ_Y	Akma Uzaması (%) ε_Y	Maksimm Çekme Gerilmesi (Mpa) σ_M	Kopma gerilmesi (MPa) σ_B	Kopma Uzaması (%) ε_B	Elastiklik Modülü (MPa) E_t
1.	11,51	9,77	112,37	50,00	21,44	10,44	21,44	17,42	567,06	927,47
2.	11,58	9,75	112,83	50,00	21,99	10,71	21,99	17,93	580,69	800,14
3.	11,92	9,75	116,29	50,00	20,25	10,35	20,25	16,47	577,93	849,84
4.	11,42	9,78	111,69	50,00	21,77	10,75	21,77	16,98	591,15	904,79
5.	11,48	9,81	112,62	50,00	17,13	13,21	17,13	15,85	529,89	591,10
ORT.	11,58	9,77	113,16	50,00	**20,52**	**11,09**	**20,52**	**16,93**	**569,34**	**814,67**
Std. Sapma	-	-	-	-	**2,01**	**1,20**	**2,01**	**0,81**	**23,66**	**134,42**
Belirsizlik	-	-	-	-	**0,38**	**0,13**	**0,38**	**0,32**	**6,61**	**35,82**

Ölçüm Belirsizliği ± (MPa) (k=2, %95 Güvenilirlik Seviyesinde)

T10-217-02-03 KÜTLESEL ERİME AKIŞ HIZI (MFR)

Test metot standardı adı : **TS EN ISO 1133- Metot A -Plastikler – Termoplastiklerin erime kütle –akış oranı (MFR) nın tayini** ***(Plastics – Determination of the melt mass-flow rate (MFR) of thermoplastics)***
Şartlandırma Ortamı : **23^{0}C ± 2^{0}C**
Test Sıcaklığı : **190^{0}C**
Uygulanan Test Yükü (kg) : **5**
Kesme Zaman Aralığı (sn) : **240**
Kesilen Parçaların Kütleleri (gr)

1.Parça = 0,0909
2.Parça = 0,0909
3.Parça = 0,0909
4.Parça = 0,0917

Kütlesel Erime Akış Oranı – MFR	**0,23**	±	**0,01**	**gr/10 dak**

Rapor edilen ölçüm belirsizliği, genişletilmiş belirsizlik olup bileşik belirsizlikten kapsam faktörü k=2 kullanılarak elde edilmiştir. Güvenilirlik düzeyi %95'tir.

Tel:0(216) 646 01 87 (3 hat) Faks: 0(216) 646 18 62
www.ugetam.com.tr e-mail: ugetam@ugetam.com.tr

Form no: LTR-42-01
Yayın Tarihi: 14.08.2008 - Rev. No: 01/29.06.09

Figure B.17: Official material test result, test: T10-217, page: 10/23.

TÜRKAK
TÜRK AKREDİTASYON KURUMU
TURKISH ACCREDITATION AGENCY
tarafından akredite edilmiş

UGETAM TEST LABORATUVARI

Çamlık Mah. Yahya Kemal Beyatlı Cad. No:1
34906 Kurtköy-Pendik / İSTANBUL

Deney Raporu
Testing Report

AB-0094-T
T10-217
10-10

Sayfa: 11/23

T10-217-02-04 YOĞUNLUK TAYİNİ

Test metot standardı adı : **TS EN ISO 1183-1-Plastikler-Yoğunluk ve Bağıl Yoğunluk** ***Tayini*** ***(Plastics – Methods for Determining the density and relative density of non-cellular plastics)***

Numune Formu (şekli) : **1 – 2gr. Kübik Şekil**
Şartlandırma Ortamı : **Hava, Min.2 saat 23^{0}C ± 2^{0}C , %50 ± %10 Bağıl Nem**
Test Sıcaklığı ve doğruluğu : **23^{0}C ± 2^{0}C (Daldırma sıvısının sıcaklığı)**

Ölçülen numune yoğunlukları (g/cm3) :

Parça = 0,9596
Parça = 0,9598
Parça = 0,9596

Ortalama Yoğunluk ($\rho_{s,23^0C}$):	**0,960**	±	**0,0005**	g/cm^3

T10-217-02-05 OKSİDASYON İNDÜKSİYON SÜRESİ (OIT)

Test metodu : **TS EN 728-Oksidasyon İndüksiyon Süresinin Tayini** ***(Determination of the oxidation induction time)***
Atıf Yapılan Standartlar : TS 1148 ISO 293, TS EN ISO 1133:2006

Numunelerin boru veya ekleme parçasının çeperlerinden alındığı yerler : **DIŞ –ORTA – İÇ YÜZEYLER**
Deney parçasının kütlesi (mg) : **15,3 – 15,3 –15,5**
Deney Sıcaklığı (^{0}C) : **200**
Kullanılan DSC cihazının markası, türü, modeli, imalat yeri, seri numarası : **Perkin Elmer JADE, İntercooler, USA, SN: 520A6092505**

Her bir numunenin OIT değeri (dak)

Oksidasyon İndüksiyon Süresi – OIT (dak)			**Belirsizlik (dak)**	
Dış Yüzey	OIT >	**25**	±	**2,5**
Orta Yüzey	OIT >	**25**	±	**2,5**
İç Yüzey	OIT >	**25**	±	**2,5**

Rapor edilen ölçüm belirsizliği, genişletilmiş belirsizlik olup bileşik belirsizlikten kapsam faktörü k=2 kullanılarak elde edilmiştir. Güvenilirlik düzeyi %95'tir.

Tel:0(216) 646 01 87 (3 hat) Faks: 0(216) 646 18 62
www.ugetam.com.tr e-mail: ugetam@ugetam.com.tr

Form no: LTR-42-01
Yayın Tarihi: 14.08.2008 - Rev. No: 01/29.06.09

Figure B.18: Official material test result, test: T10-217, page: 11/23.

TÜRKAK
TÜRK AKREDİTASYON KURUMU
TURKISH ACCREDITATION AGENCY
tarafından akredite edilmiş

UGETAM TEST LABORATUVARI

Çamlık Mah. Yahya Kemal Beyatlı Cad. No:1
34906 Kurtköy-Pendik / İSTANBUL

Deney Raporu
Testing Report

AB-0094-T
T10-217
10-10

T10-217-02-06-YAVAŞ ÇATLAK İLERLEMESİNE MUKAVEMET (NOTCH: e> 5 mm)

Test metodu : **TS EN ISO 13479-Çentikli borular üzerinde çatlak ilerlemesi deneyi** ***(Test method for slow crack growth on notched pipes -notch test)***
Atıf Yapılan Standartlar : TS EN 1167-1:2006

Örneklerin Tanımı : **FIRAT PE100 SDR11 DN125x11,4 SDR11 LOT:129 EKİM 05**

Çakı çapı, diş sayısı, çakı açısı : **D=168,8 mm, 20 diş, 60^0**
Çakı Dönme hızı (devir/dakika) : **700 dev/dakika**
Çakı İlerleme (travers) Hızı (mm/dakika) : **150 mm/dakika**
Basınç altındaki deney süresi (veya hasarlanma süresi) (saat) : **165**
Deney Basıncı (bar) : **8**

Test Numunesindeki çentik ölçüleri

Çentik tabanındaki et kalınlığı (mm)	**9,3**
Çentik Derinliği	**2,10**
% Çentik Derinliği	**18**

Hasarlanmış çentiğin konumu : **Hasar Yok**
Uç kapakları arasındaki en küçük serbest uzunluk (Lo=3xdn±5mm) : **Lo= 375**
Test Ortamı : **Su içinde –Su ile**
Test başlıklarının tipi : **A tipi**
Test edilen numune sayısı : **1**
Test parçalarının termo tank içindeki vaziyeti : **Dikey**

Uygulanan Deney Basıncı – P (bar)	**9,20**	±	**0,44**	**bar**

Rapor edilen ölçüm belirsizliği, genişletilmiş belirsizlik olup bileşik belirsizlikten kapsam faktörü k=2 kullanılarak elde edilmiştir. Güvenilirlik düzeyi %95'tir.

Tel:0(216) 646 01 87 (3 hat) Faks: 0(216) 646 18 62
www.ugetam.com.tr e-mail: ugetam@ugetam.com.tr
Form no: LTR-42-01
Yayın Tarihi: 14.08.2008 - Rev. No: 01/29.06.09

Figure B.19: Official material test result, test: T10-217, page: 12/23.

TÜRKAK
TÜRK AKREDİTASYON KURUMU
TURKISH ACCREDITATION AGENCY
tarafından akredite edilmiş

UGETAM TEST LABORATUVARI

Çamlık Mah. Yahya Kemal Beyatlı Cad. No:1
34906 Kurtköy-Pendik / İSTANBUL

Deney Raporu
Testing Report

AB-0094-T
T10-217
10-10

Sayfa: 13/23

T10-217-02-07 BOYUTSAL KARARLILIK

Test metodu : **TS EN ISO 2505-Termoplastik Borular – Boyca Eski Halini Alabilme Özelliğinin Tayini**
(Thermoplastics pipes - Longitudinal reversion - Test method and parameters (ISO 2505:2005)

Nominal Boyutları	: d_n=125 e_n=11,4
Şartlandırma Ortamı, süresi	: **Hava, 23°C ± 2°C, min. 6 saat**
Test Sıcaklığı ve doğruluğu	: **110°C ± 2°C**
Testin Süresi (saat)	: **120 dak**
Test Ortamı	: **Etüv (Hava)**
Test edilen numune sayısı	: **3**
Test parçalarının etüv içindeki vaziyeti	: **Yatay-Askı**

Her parçanın boyca değişikliği (%):

$$R_L = \frac{(L_0 - L)}{L_0} \times 100$$

1.Parça:	L_0=	**100,00**	L=	**99,08**	ΔL=	**0,92**	R_L=	**0,92**
2.Parça:	L_0=	**100,00**	L=	**99,03**	ΔL=	**0,97**	R_L=	**0,97**
3.Parça:	L_0=	**100,00**	L=	**98,91**	ΔL=	**1,09**	R_L=	**1,09**

L_0 : Test numunesinin etüve konmadan önceki boyu (mm), L : Test numunesinin etüvden alındıktan sonraki boyu (mm)

Ortalama boyca değişim – $R_{L,m}$ (%)	**0,99**	±	**0,08**	%
Rapor edilen ölçüm belirsizliği, genişletilmiş belirsizlik olup bileşik belirsizlikten kapsam faktörü k=2 kullanılarak elde edilmiştir. Güvenilirlik düzeyi %95'tir.				

Tel:0(216) 646 01 87 (3 hat) Faks: 0(216) 646 18 62
www.ugetam.com.tr e-mail: ugetam@ugetam.com.tr

Form no: LTR-42-01
Yayın Tarihi: 14.08.2008 - Rev. No: 01/29.06.09

Figure B.20: Official material test result, test: T10-217, page: 13/23.

TÜRKAK
TÜRK AKREDİTASYON KURUMU
TURKISH ACCREDITATION AGENCY
tarafından akredite edilmiş

UGETAM TEST LABORATUVARI

Çamlık Mah. Yahya Kemal Beyatlı Cad. No:1
34906 Kurtköy-Pendik / İSTANBUL

Deney Raporu
Testing Report

AB-0094-T
T10-217
10-10

3. NUMUNE : T10 - 217 – 03:

Marka	: **FIRAT PLASTIK**	Renk	: **SARI**
Örneklerin Tanımı (Lot, Seri No, Üretim Tarihi v.s.)	: **İ.T. EKİM 05 LOT:129**	Nominal Boyutları	: **d_n= 125** **e_n= 11,4**
Malzeme Tipi (PE 80, PE 100 v.s.)	: **PE 80**	Markalama	: **FIRAT PE80 GAZ 4 SDR11 SINIF C DN125x11,4 SDR11 LOT:129 EKİM 05**
SDR / PN	: **SDR11**	İlave açıklama	: **15m Derinlik**

T10-217-03-01 HİDROSTATİK İÇ BASINCA MUKAVEMET

Test metodu : **TS EN ISO 1167-1-Sabit sıcaklık altında iç basınca dayanımın tayini. (Determination of resistance to internal pressure at constant temparature)**
Atıf Yapılan Standartlar : TS EN ISO 1167-2, TS EN ISO 3126

Nominal Boyutları : **d_n= 125** **e_n= 11,4**
Test Sıcaklığı ve doğruluğu : **80 ^{0}C ± 1^{0}C**
Test Cihazının Tanımı : **SCITEQ-HAMMEL-2000: Hidrostatik test ünitesi:9742-01571 – Termo Tank:15377, 17748**

Uygulanan Çevresel Gerilme – σ	4,5	±	0,11	Mpa
Rapor edilen ölçüm belirsizliği, genişletilmiş belirsizlik olup bileşik belirsizlikten kapsam faktörü k=2 kullanılarak elde edilmiştir. Güvenilirlik düzeyi %95'tir.				

Testin Süresi (saat) : **165**

Test Numunesinin Ölçülen Boyutları

Ortalama dış çap (mm)	: **d_e = 125**
Minimum et kalınlığı (mm)	: **e_{min}= 11,4**
Test numunesinin toplam boyu (mm)	: **L= 575**
Test numunesinin serbest uzunluğu (mm)	: **L_0 = 375**
Uygulanan test basıncı (bar)	: **P = (20 x σ) / (SDR-1) = 9,0**
Test Ortamı	: **Su içinde –Su ile**
Numunelerin şartlandırma sıcaklık ve süresi	: **80^{0}C – 6 Saat**
Test başlıklarının tipi	: **A tipi**
Test edilen numune sayısı	: **1**
Test parçalarının termo tank içindeki vaziyeti	: **Dikey**
Test basıncına gelme zamanı (30 sn – 1 dk.)	: **60sn.**
Varsa hasarın tipi (yumuşak veya kırılgan)	: **Hasar Yok**

Tel:0(216) 646 01 87 (3 hat) Faks: 0(216) 646 18 62
www.ugetam.com.tr e-mail: ugetam@ugetam.com.tr

Form no: LTR-42-01
Yayın Tarihi: 14.08.2008 - Rev. No: 01/29.06.09

Figure B.21: Official material test result, test: T10-217, page: 14/23.

TÜRKAK
TÜRK AKREDİTASYON KURUMU
TURKISH ACCREDITATION AGENCY
tarafından akredite edilmiş

UGETAM TEST LABORATUVARI

Çamlık Mah. Yahya Kemal Beyatlı Cad. No:1
34906 Kurtköy-Pendik / İSTANBUL

Deney Raporu
Testing Report

AB-0094-T
T10-217
10-10

T10-217-03-02 KOPMA UZAMASI (ÇEKME ÖZELLİKLERİNİN TAYİNİ)

Test metodu: **TS EN ISO 6259 – 1: Çekme Özelliklerinin Tayini (Determination of tensile properties – Part 1 : General test method)**
ISO 6259 – 3 : Thermoplastics pipes – Determination of tensile properties – Part 3 : Polyolefin pipes

Test numunesi tipi ve hazırlanma şekli : **Tip1 – Kaşık Numune / Makinede İşlenmiş**
Test Sıcaklığı (^{0}C) : **23 ^{0}C ± 2^{0}C**
Test numunesi sayısı (adet) : **5**
Çekme hızı (mm/dakika) : **100**
Uzama ölçer ve boyut ölçer tipi : **Elektronik uzama ölçer (S.N: 159948) ve Dijital kumpas**

Test numune No	Kalınlık (mm) a_0	Genişlik (mm) b_0	Kesit Alanı (mm^2) S_0	Baş. Ölçme Uzunluğu (mm) L_0	Akma gerilmesi (MPa) σ_Y	Akma Uzaması (%) ε_Y	Maksimm Çekme Gerilmesi (Mpa) σ_M	Kopma gerilmesi (MPa) σ_B	Kopma Uzaması (%) ε_B	Elastiklik Modülü (MPa) E_t
1.	11,73	9,74	114,25	50,00	2,46	0,13	16,47	10,68	536,19	467,65
2.	12,01	9,78	117,39	50,00	16,77	13,11	16,77	10,92	590,47	472,56
3.	11,86	9,81	116,27	50,00	16,78	13,66	16,78	11,55	602,57	486,56
4.	11,87	9,82	116,49	50,00	16,94	13,96	16,94	10,44	592,63	521,59
5.	11,94	9,79	116,93	50,00	17,27	12,53	17,27	11,23	591,91	528,38
ORT.	11,88	9,79	116,27	50,00	**14,04**	**10,68**	**16,85**	**10,96**	**582,75**	**495,35**
Std. Sapma	-	-	-	-	**6,48**	**5,92**	**0,29**	**0,44**	**26,47**	**28,03**
Belirsizlik	-	-	-	-	**0,26**	**0,12**	**0,31**	**0,20**	**6,74**	**21,64**

Ölçüm Belirsizliği ± (MPa) (k=2, %95 Güvenilirlik Seviyesinde)

T10-217-03-03 KÜTLESEL ERİME AKIŞ HIZI (MFR)

Test metot standardı adı : **TS EN ISO 1133- Metot A -Plastikler – Termoplastiklerin erime kütle –akış oranı (MFR) nın tayini *(Plastics – Determination of the melt mass-flow rate (MFR) of thermoplastics)***
Şartlandırma Ortamı : **23^{0}C ± 2^{0}C**
Test Sıcaklığı : **190^{0}C**
Uygulanan Test Yükü (kg) : **5**
Kesme Zaman Aralığı (sn) : **120**
Kesilen Parçaların Kütleleri (gr)

1.Parça = 0,1802
2.Parça = 0,1814
3.Parça = 0,1830
4.Parça = 0,1709
5.Parça = 0,1757
6.Parça = 0,1818
7.Parça = 0,1855

Kütlesel Erime Akış Oranı – MFR	0,90	±	0,03	gr/10 dak
Rapor edilen ölçüm belirsizliği, genişletilmiş belirsizlik olup bileşik belirsizlikten kapsam faktörü k=2 kullanılarak elde edilmiştir. Güvenilirlik düzeyi %95'tir.				

Tel:0(216) 646 01 87 (3 hat) Faks: 0(216) 646 18 62 e-mail: ugetam@ugetam.com.tr
www.ugetam.com.tr

Form no: LTR-42-01
Yayın Tarihi: 14.08.2008 - Rev. No: 01/29.06.09

Figure B.22: Official material test result, test: T10-217, page: 15/23.

TÜRKAK
TÜRK AKREDİTASYON KURUMU
TURKISH ACCREDITATION AGENCY
tarafından akredite edilmiş

UGETAM TEST LABORATUVARI

Çamlık Mah. Yahya Kemal Beyatlı Cad. No:1
34906 Kurtköy-Pendik / İSTANBUL

Deney Raporu
Testing Report

AB-0094-T
T10-217
10-10

T10-217-03-04 YOĞUNLUK TAYİNİ

Test metot standardı adı : **TS EN ISO 1183-1-Plastikler-Yoğunluk ve Bağıl Yoğunluk *Tayini (Plastics – Methods for Determining the density and relative density of non-cellular plastics)***

Numune Formu (şekli) : **1 – 2gr. Kübik Şekil**
Şartlandırma Ortamı : **Hava, Min.2 saat 23°C ± 2°C , %50 ± %10 Bağıl Nem**
Test Sıcaklığı ve doğruluğu : **23°C ± 2°C (Daldırma sıvısının sıcaklığı)**

Ölçülen numune yoğunlukları (g/cm3) :

Parça = 0,9401
Parça = 0,9402
Parça = 0,9404

Ortalama Yoğunluk ($\rho_{s,23^0C}$):	**0,940**	±	**0,0005**	g/cm^3

Rapor edilen ölçüm belirsizliği, genişletilmiş belirsizlik olup bileşik belirsizlikten kapsam faktörü k=2 kullanılarak elde edilmiştir. Güvenilirlik düzeyi %95'tir.

T10-217-03-05 OKSİDASYON İNDÜKSİYON SÜRESİ (OIT)

Test metodu : **TS EN 728-Oksidasyon İndüksiyon Süresinin Tayini *(Determination of the oxidation induction time)***
Atıf Yapılan Standartlar : TS 1148 ISO 293, TS EN ISO 1133:2006

Numunelerin boru veya ekleme parçasının çeperlerinden alındığı yerler : **DIŞ –ORTA – İÇ YÜZEYLER**
Deney parçasının kütlesi (mg) : **16,7 – 14,8 –15,8**
Deney Sıcaklığı (°C) : **200**
Kullanılan DSC cihazının markası, türü, modeli, imalat yeri, seri numarası : **Perkin Elmer JADE, İntercooler, USA, SN: 520A6092505**

Her bir numunenin OIT değeri (dak)

Oksidasyon İndüksiyon Süresi – OIT (dak)				**Belirsizlik (dak)**	
Dış Yüzey	OIT	>	**25**	±	**2,5**
Orta Yüzey	OIT	>	**25**	±	**2,5**
İç Yüzey	OIT	>	**25**	±	**2,5**

Rapor edilen ölçüm belirsizliği, genişletilmiş belirsizlik olup bileşik belirsizlikten kapsam faktörü k=2 kullanılarak elde edilmiştir. Güvenilirlik düzeyi %95'tir.

Figure B.23: Official material test result, test: T10-217, page: 16/23.

TÜRKAK
TÜRK AKREDİTASYON KURUMU
TURKISH ACCREDITATION AGENCY
tarafından akredite edilmiş

UGETAM TEST LABORATUVARI

Çamlık Mah. Yahya Kemal Beyatlı Cad. No:1
34906 Kurtköy-Pendik / İSTANBUL

Deney Raporu
Testing Report

AB-0094-T
T10-217
10-10

T10-217-03-06 -YAVAŞ ÇATLAK İLERLEMESİNE MUKAVEMET (NOTCH: e> 5 mm)

Test metodu : **TS EN ISO 13479-Çentikli borular üzerinde çatlak ilerlemesi deneyi** ***(Test method for slow crack growth on notched pipes -notch test)***
Atıf Yapılan Standartlar : TS EN 1167-1:2006

Örneklerin Tanımı : **FIRAT PE80 SDR11 DN125x11,4 SDR11 LOT:129 EKİM 05**

Çakı çapı, diş sayısı, çakı açısı : **D=168,8 mm, 20 diş, 60^0**
Çakı Dönme hızı (devir/dakika) : **700 dev/dakika**
Çakı İlerleme (travers) Hızı (mm/dakika) : **150 mm/dakika**
Basınç altındaki deney süresi (veya hasarlanma süresi) (saat) : **165**
Deney Basıncı (bar) : **8**

Test Numunesindeki çentik ölçüleri

Çentik tabanındaki et kalınlığı (mm)	**9,3**
Çentik Derinliği	**2,10**
% Çentik Derinliği	**18**

Hasarlanmış çentiğin konumu : **Hasar Yok**
Uç kapakları arasındaki en küçük serbest uzunluk (Lo=3xdn±5mm) : **Lo= 375**
Test Ortamı : **Su içinde –Su ile**
Test başlıklarının tipi : **A tipi**
Test edilen numune sayısı : **3**
Test parçalarının termo tank içindeki vaziyeti : **Dikey**

Uygulanan Deney Basıncı – P (bar)	**8**	±	**0,38**	**bar**

Rapor edilen ölçüm belirsizliği, genişletilmiş belirsizlik olup bileşik belirsizlikten kapsam faktörü k=2 kullanılarak elde edilmiştir. Güvenilirlik düzeyi %95'tir.

Tel:0(216) 646 01 87 (3 hat) Faks: 0(216) 646 18 62
www.ugetam.com.tr e-mail: ugetam@ugetam.com.tr

Form no: LTR-42-01
Yayın Tarihi: 14.08.2008 - Rev. No: 01/29.06.09

Figure B.24: Official material test result, test: T10-217, page: 17/23.

TÜRKAK
TÜRK AKREDİTASYON KURUMU
TURKISH ACCREDITATION AGENCY
tarafından akredite edilmiş

UGETAM TEST LABORATUVARI

Çamlık Mah. Yahya Kemal Beyatlı Cad. No:1
34906 Kurtköy-Pendik / İSTANBUL

Deney Raporu
Testing Report

AB-0094-T
T10-217
10-10

T10-217-03-07 BOYUTSAL KARARLILIK

Test metodu : **TS EN ISO 2505-Termoplastik Borular – Boyca Eski Halini Alabilme Özelliğinin Tayini**
(Thermoplastics pipes - Longitudinal reversion - Test method and parameters (ISO 2505:2005)

Nominal Boyutları	: d_n= 125 e_n= 11,4
Şartlandırma Ortamı, süresi	: **Hava, 23°C ± 2°C, min. 6 saat**
Test Sıcaklığı ve doğruluğu	: **110°C ± 2°C**
Testin Süresi (saat)	: **120 dak**
Test Ortamı	: **Etüv (Hava)**
Test edilen numune sayısı	: **3**
Test parçalarının etüv içindeki vaziyeti	: **Yatay-Askı**

Her parçanın boyca değişikliği (%):

$$R_L = \frac{(L_0 - L)}{L_0} \times 100$$

1.Parça:	L_0=	100,00	L=	98,60	ΔL=	1,40	R_L=	1,40
2.Parça:	L_0=	100,00	L=	98,53	ΔL=	1,47	R_L=	1,47
3.Parça:	L_0=	100,00	L=	98,54	ΔL=	1,46	R_L=	1,46

L_0 : Test numunesinin etüve konmadan önceki boyu (mm), L : Test numunesinin etüvden alındıktan sonraki boyu (mm)

Ortalama boyca değişim – $R_{L,m}$ (%)	**1,44**	±	**0,12**	%
Rapor edilen ölçüm belirsizliği, genişletilmiş belirsizlik olup bileşik belirsizlikten kapsam faktörü k=2 kullanılarak elde edilmiştir. Güvenilirlik düzeyi %95'tir.				

Tel:0(216) 646 01 87 (3 hat) Faks: 0(216) 646 18 62
www.ugetam.com.tr e-mail: ugetam@ugetam.com.tr

Form no: LTR-42-01
Yayın Tarihi: 14.08.2008 - Rev. No: 01/29.06.09

Figure B.25: Official material test result, test: T10-217, page: 18/23.

TÜRKAK
TÜRK AKREDİTASYON KURUMU
TURKISH ACCREDITATION AGENCY
tarafından akredite edilmiş

UGETAM TEST LABORATUVARI

Çamlık Mah. Yahya Kemal Beyatlı Cad. No:1
34906 Kurtköy-Pendik / İSTANBUL

Deney Raporu
Testing Report

AB-0094-T
T10-217
10-10

4. **NUMUNE : T10 - 217 – 04:**

Marka	: **FIRAT PLASTIK**	Renk	: **SARI**
Örneklerin Tanımı (Lot, Seri No, Üretim Tarihi v.s.)	: **İ.T. EKİM 05 LOT:129**	Nominal Boyutları	: d_n= 125 e_n= 11,4
Malzeme Tipi (PE 80, PE 100 v.s.)	: **PE 100**	Markalama	: **FIRAT PE100 GAZ 4 SDR11 SINIF C DN125x11,4 SDR11 LOT:129 EKİM 05**
SDR / PN	: **SDR11**	İlave açıklama	: **15m Derinlik**

T10-217-04-01 HİDROSTATİK İÇ BASINCA MUKAVEMET

Test metodu : **TS EN ISO 1167-1-Sabit sıcaklık altında iç basınca dayanımın tayini. (Determination of resistance to internal pressure at constant temparature)**
Atıf Yapılan Standartlar : TS EN ISO 1167-2, TS EN ISO 3126

Nominal Boyutları : d_n= 125 e_n= 11,4
Test Sıcaklığı ve doğruluğu : 80 ^{0}C ± 1^{0}C
Test Cihazının Tanımı : **SCITEQ-HAMMEL-2000: Hidrostatik test ünitesi:9742-01571 – Termo Tank:15377, 17748**

Uygulanan Çevresel Gerilme – σ	5,4	±	0,13	Mpa
Rapor edilen ölçüm belirsizliği, genişletilmiş belirsizlik olup bileşik belirsizlikten kapsam faktörü k=2 kullanılarak elde edilmiştir. Güvenilirlik düzeyi %95'tir.				

Testin Süresi (saat)	: 165
Test Numunesinin Ölçülen Boyutları	
Ortalama dış çap (mm)	: d_e = 125
Minimum et kalınlığı (mm)	: e_{min}= 11,4
Test numunesinin toplam boyu (mm)	: L= 575
Test numunesinin serbest uzunluğu (mm)	: L_0 = 375
Uygulanan test basıncı (bar)	**: P = (20 x σ) / (SDR-1) = 10,80**
Test Ortamı	: Su içinde –Su ile
Numunelerin şartlandırma sıcaklık ve süresi	: 80^{0}C – 6 Saat
Test başlıklarının tipi	: A tipi
Test edilen numune sayısı	: 1
Test parçalarının termo tank içindeki vaziyeti	: Dikey
Test basıncına gelme zamanı (30 sn – 1 dk.)	: 60sn.
Varsa hasarın tipi (yumuşak veya kırılgan)	: Hasar Yok

Tel:0(216) 646 01 87 (3 hat) Faks: 0(216) 646 18 62
www.ugetam.com.tr e-mail: ugetam@ugetam.com.tr
Form no: LTR-42-01
Yayın Tarihi: 14.08.2008 - Rev No: 01/29.06.09

Figure B.26: Official material test result, test: T10-217, page: 19/23.

TÜRKAK
TÜRK AKREDİTASYON KURUMU
TURKISH ACCREDITATION AGENCY
tarafından akredite edilmiş

UGETAM TEST LABORATUVARI

Çamlık Mah. Yahya Kemal Beyatlı Cad. No:1
34906 Kurtköy-Pendik / İSTANBUL

Deney Raporu
Testing Report

AB-0094-T
T10-217
10-10

T10-217-04-02 KOPMA UZAMASI (ÇEKME ÖZELLİKLERİNİN TAYİNİ)

Test metodu: **TS EN ISO 6259 – 1: Çekme Özelliklerinin Tayini (Determination of tensile properties – Part 1 : General test method)**
ISO 6259 – 3 : **Thermoplastics pipes – Determination of tensile properties – Part 3 : Polyolefin pipes**

Test numunesi tipi ve hazırlanma şekli : **Tip1 – Kaşık Numune / Makinede İşlenmiş**
Test Sıcaklığı (^{0}C) : **23 ^{0}C ± 2^{0}C**
Test numunesi sayısı (adet) : **5**
Çekme hızı (mm/dakika) : **50**
Uzama ölçer ve boyut ölçer tipi : **Elektronik uzama ölçer (S.N: 159948) ve Dijital kumpas**

Test numune No	Kalınlık (mm) a_0	Genişlik (mm) b_0	Kesit Alanı (mm^2) S_0	Baş. Ölçme Uzunluğu (mm) L_0	Akma gerilmesi (MPa) σ_Y	Akma Uzaması (%) ε_Y	Maksimm Çekme Gerilmesi (Mpa) σ_M	Kopma gerilmesi (MPa) σ_B	Kopma Uzaması (%) ε_B	Elastiklik Modülü (MPa) E_t
1.	12,15	9,80	119,08	50,00	20,74	11,26	20,74	9,26	583,27	1007,77
2.	11,55	9,71	112,19	50,00	20,87	12,34	20,87	16,20	597,33	852,15
3.	11,51	9,69	111,60	50,00	21,78	9,70	21,78	16,81	586,15	928,29
4.	11,71	9,71	113,70	50,00	5,37	0,39	21,08	16,59	588,79	882,96
5.	11,66	9,86	114,93	50,00	20,65	11,17	20,65	16,19	592,70	959,19
ORT.	11,72	9,76	114,30	50,00	**17,88**	**8,97**	**21,02**	**15,01**	**589,65**	**926,07**
Std. Sapma	-	-	-	-	**7,01**	**4,89**	**0,45**	**3,23**	**5,52**	**61,44**
Belirsizlik	-	-	-	-	**0,33**	**0,10**	**0,39**	**0,28**	**6,82**	**40,60**

Ölçüm Belirsizliği ± (MPa) (k=2, %95 Güvenilirlik Seviyesinde)

T10-217-04-03 KÜTLESEL ERİME AKIŞ HIZI (MFR)

Test metot standardı adı : **TS EN ISO 1133- Metot A -Plastikler – Termoplastiklerin erime kütle –akış oranı (MFR) nın tayini *(Plastics – Determination of the melt mass-flow rate (MFR) of thermoplastics)***
Şartlandırma Ortamı : **23^{0}C ± 2^{0}C**
Test Sıcaklığı : **190^{0}C**
Uygulanan Test Yükü (kg) : **5**
Kesme Zaman Aralığı (sn) : **240**
Kesilen Parçaların Kütleleri (gr)

1.Parça = 0,0930
2.Parça = 0,0919
3.Parça = 0,0914
4.Parça = 0,0911

Kütlesel Erime Akış Oranı – MFR	**0,23**	±	**0,01**	**gr/10 dak**

Rapor edilen ölçüm belirsizliği, genişletilmiş belirsizlik olup bileşik belirsizlikten kapsam faktörü k=2 kullanılarak elde edilmiştir. Güvenilirlik düzeyi %95'tir.

Tel:0(216) 646 01 87 (3 hat) Faks: 0(216) 646 18 62
www.ugetam.com.tr e-mail: ugetam@ugetam.com.tr

Form no: LTR-42-01
Yayın Tarihi: 14.08.2008 - Rev. No: 01/29.06.09

Figure B.27: Official material test result, test: T10-217, page: 20/23.

TÜRKAK
TÜRK AKREDİTASYON KURUMU
TURKISH ACCREDITATION AGENCY
tarafından akredite edilmiş

UGETAM TEST LABORATUVARI

Çamlık Mah. Yahya Kemal Beyatlı Cad. No:1
34906 Kurtköy-Pendik / İSTANBUL

Deney Raporu
Testing Report

AB-0094-T
T10-217
10-10

T10-217-04-04 YOĞUNLUK TAYİNİ

Test metot standardı adı : **TS EN ISO 1183-1-Plastikler-Yoğunluk ve Bağıl Yoğunluk** ***Tayini*** ***(Plastics – Methods for Determining the density and relative density of non-cellular plastics)***

Numune Formu (şekli) : **1 – 2gr. Kübik Şekil**
Şartlandırma Ortamı : **Hava, Min.2 saat 23^{0}C ± 2^{0}C , %50 ± %10 Bağıl Nem**
Test Sıcaklığı ve doğruluğu : **23^{0}C ± 2^{0}C (Daldırma sıvısının sıcaklığı)**

Ölçülen numune yoğunlukları (g/cm3) :

Parça = 0,9614
Parça = 0,9612
Parça = 0,9615

Ortalama Yoğunluk ($\rho_{s,23^0C}$):	**0,961**	±	**0,0006**	g/cm^3
Rapor edilen ölçüm belirsizliği, genişletilmiş belirsizlik olup bileşik belirsizlikten kapsam faktörü k=2 kullanılarak elde edilmiştir. Güvenilirlik düzeyi %95'tir.				

T10-217-04-05 OKSİDASYON İNDÜKSİYON SÜRESİ (OIT)

Test metodu : **TS EN 728-Oksidasyon İndüksiyon Süresinin Tayini** ***(Determination of the oxidation induction time)***
Atıf Yapılan Standartlar : TS 1148 ISO 293, TS EN ISO 1133:2006

Numunelerin boru veya ekleme parçasının çeperlerinden alındığı yerler : **DIŞ –ORTA – İÇ YÜZEYLER**
Deney parçasının kütlesi (mg) : **14,4 – 16,9 –16,7**
Deney Sıcaklığı (^{0}C) : **200**
Kullanılan DSC cihazının markası, türü, modeli, imalat yeri, seri numarası : **Perkin Elmer JADE, İntercooler, USA, SN: 520A6092505**

Her bir numunenin OIT değeri (dak)

Oksidasyon İndüksiyon Süresi – OIT (dak)			**Belirsizlik (dak)**	
Dış Yüzey	OIT >	**25**	±	**2,5**
Orta Yüzey	OIT >	**25**	±	**2,5**
İç Yüzey	OIT >	**25**	±	**2,5**

Rapor edilen ölçüm belirsizliği, genişletilmiş belirsizlik olup bileşik belirsizlikten kapsam faktörü k=2 kullanılarak elde edilmiştir. Güvenilirlik düzeyi %95'tir.

Figure B.28: Official material test result, test: T10-217, page: 21/23.

TÜRKAK
TÜRK AKREDİTASYON KURUMU
TURKISH ACCREDITATION AGENCY
tarafından akredite edilmiş

UGETAM TEST LABORATUVARI

Çamlık Mah. Yahya Kemal Beyatlı Cad. No:1
34906 Kurtköy-Pendik / İSTANBUL

Deney Raporu
Testing Report

AB-0094-T
T10-217
10-10

Sayfa: 22/23

T10-217-04-06 -YAVAŞ ÇATLAK İLERLEMESİNE MUKAVEMET (NOTCH: e> 5 mm)

Test metodu : **TS EN ISO 13479-Çentikli borular üzerinde çatlak ilerlemesi deneyi** ***(Test method for slow crack growth on notched pipes -notch test)***
Atıf Yapılan Standartlar : TS EN 1167-1:2006

Örneklerin Tanımı : **FIRAT PE100 SDR11 DN125x11,4 SDR11 LOT:129 EKİM 05**

Çakı çapı, diş sayısı, çakı açısı : **D=168,8 mm, 20 diş, 60^0**
Çakı Dönme hızı (devir/dakika) : **700 dev/dakika**
Çakı İlerleme (travers) Hızı (mm/dakika) : **150 mm/dakika**
Basınç altındaki deney süresi (veya hasarlanma süresi) (saat) : **165**
Deney Basıncı (bar) : **8**

Test Numunesindeki çentik ölçüleri

Çentik tabanındaki et kalınlığı (mm)	**9,3**
Çentik Derinliği	**2,10**
% Çentik Derinliği	**18**

Hasarlanmış çentiğin konumu : **Hasar Yok**
Uç kapakları arasındaki en küçük serbest uzunluk (Lo=3xdn±5mm) : **Lo= 250**
Test Ortamı : **Su içinde –Su ile**
Test başlıklarının tipi : **A tipi**
Test edilen numune sayısı : **3**
Test parçalarının termo tank içindeki vaziyeti : **Dikey**

Uygulanan Deney Basıncı – P (bar)	**9,20**	±	**0,44**	**bar**

Rapor edilen ölçüm belirsizliği, genişletilmiş belirsizlik olup bileşik belirsizlikten kapsam faktörü k=2 kullanılarak elde edilmiştir. Güvenilirlik düzeyi %95'tir.

Tel:0(216) 646 01 87 (3 hat) Faks: 0(216) 646 18 62
www.ugetam.com.tr e-mail: ugetam@ugetam.com.tr

Form no: LTR-42-01
Yayın Tarihi: 14.08.2008 - Rev. No: 01/29.06.09

Figure B.29: Official material test result, test: T10-217, page: 22/23.

TÜRKAK
TÜRK AKREDİTASYON KURUMU
TURKISH ACCREDITATION AGENCY
tarafından akredite edilmiş

UGETAM TEST LABORATUVARI

Çamlık Mah. Yahya Kemal Beyatlı Cad. No:1
34906 Kurtköy-Pendik / İSTANBUL

Deney Raporu
Testing Report

AB-0094-T
T10-217
10-10

T10-217-04-07 BOYUTSAL KARARLILIK

Test metodu : **TS EN ISO 2505-Termoplastik Borular – Boyca Eski Halini Alabilme Özelliğinin Tayini**
(Thermoplastics pipes - Longitudinal reversion - Test method and parameters (ISO 2505:2005)

Nominal Boyutları	: d_n= 125 e_n= 11,4
Şartlandırma Ortamı, süresi	: Hava, 23^{0}C ± 2^{0}C, min. 6 saat
Test Sıcaklığı ve doğruluğu	: 110^{0}C ± 2^{0}C
Testin Süresi (saat)	: 120 dak
Test Ortamı	: Etüv (Hava)
Test edilen numune sayısı	: 3
Test parçalarının etüv içindeki vaziyeti	: Yatay-Askı

Her parçanın boyca değişikliği (%):

$$R_L = \frac{(L_0 - L)}{L_0} \times 100$$

1.Parça:	L_0=	100,00	L=	99,11	ΔL=	0,89	R_L=	0,89
2.Parça:	L_0=	100,00	L=	99,07	ΔL=	0,93	R_L=	0,93
3.Parça:	L_0=	100,00	L=	98,92	ΔL=	1,08	R_L=	1,08

L_0 : Test numunesinin etüve konmadan önceki boyu (mm), L : Test numunesinin etüvden alındıktan sonraki boyu (mm)

Ortalama boyca değişim – $R_{L,m}$ (%)	**0,97**	±	**0,08**	%
Rapor edilen ölçüm belirsizliği, genişletilmiş belirsizlik olup bileşik belirsizlikten kapsam faktörü k=2 kullanılarak elde edilmiştir. Güvenilirlik düzeyi %95'tir.				

Tel:0(216) 646 01 87 (3 hat) Faks: 0(216) 646 18 62
www.ugetam.com.tr e-mail: ugetam@ugetam.com.tr

Form no: LTR-42-01
Yayın Tarihi: 14.08.2008 - Rev. No: 01/29.06.09

Figure B.30: Official material test result, test: T10-217, page: 23/23.

APPENDIX C: Input Parameters and Results of Numerical Models

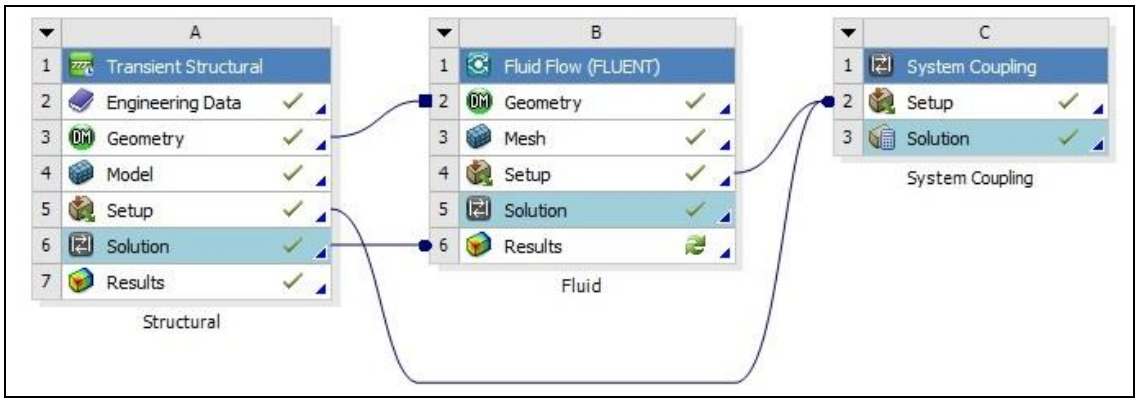

Figure C.1: System Coupling Procedure.

Files

	A	B	C	D	E	
1	Name	Cell ID	Size	Type	Date Modified	
2	test1.wbpj		248 KB	ANSYS Project File	02.10.2013 17:12:56	C:\Users\ugur\Desk
3	EngineeringData.xml	A2	20 KB	Engineering Data File	02.10.2013 17:12:54	C:\Users\ugur\Desk
4	SYS.agdb	A3,B2	1 MB	Geometry File	11.09.2013 15:58:16	C:\Users\ugur\Desk
5	material.engd	A2	20 KB	Engineering Data File	11.09.2013 15:22:45	C:\Users\ugur\Desk
6	SYS.engd	A4	20 KB	Engineering Data File	11.09.2013 15:22:45	C:\Users\ugur\Desk
7	SYS.mechdb	A4	38 KB	Mechanical Database File	02.10.2013 16:18:08	C:\Users\ugur\Desk
8	FFF.msh	B3,B4	436 KB	Fluent Mesh File	11.09.2013 16:03:41	C:\Users\ugur\Desk
9	FFF.mshdb	B3	179 KB	Mesh Database File	11.09.2013 16:03:58	C:\Users\ugur\Desk
10	FFF.set	B4	20 KB	FLUENT Model File	02.10.2013 15:49:30	C:\Users\ugur\Desk
11	scInput.sci	C3	7 KB	Default File	02.10.2013 16:09:18	C:\Users\ugur\Desk
12	FFF-3-00000.cas.gz	B	174 KB	FLUENT Case File	02.10.2013 16:09:45	C:\Users\ugur\Desk
13	FFF-3-00100.dat.gz	B5	227 7 KB	FLUENT Data File	02.10.2013 16:18:05	C:\Users\ugur\Desk
14	file.rst	A6	17 MB	ANSYS Result File	02.10.2013 16:18:05	C:\Users\ugur\Desk
15	FFF-3-00098.dat.gz	B	227 KB	FLUENT Data File	02.10.2013 16:17:52	C:\Users\ugur\Desk
16	FFF-3-00100.cas.gz	B5	181 KB	FLUENT Case File	02.10.2013 16:18:04	C:\Users\ugur\Desk
17	FFF-3-00096.dat.gz	B	227 KB	FLUENT Data File	02.10.2013 16:17:43	C:\Users\ugur\Desk
18	FFF-3-00098.cas.gz	B	181 KB	FLUENT Case File	02.10.2013 16:17:52	C:\Users\ugur\Desk
19	FFF-3-00095.dat.gz	B	227 KB	FLUENT Data File	02.10.2013 16:17:38	C:\Users\ugur\Desk
20	FFF-3-00096.cas.gz	B	182 KB	FLUENT Case File	02.10.2013 16:17:42	C:\Users\ugur\Desk
21	FFF-3-00094.dat.gz	B	227 KB	FLUENT Data File	02.10.2013 16:17:33	C:\Users\ugur\Desk
22	FFF-3-00095.cas.gz	B	183 KB	FLUENT Case File	02.10.2013 16:17:37	C:\Users\ugur\Desk

Figure C.2: Numerical Model ANSYS File Structure.

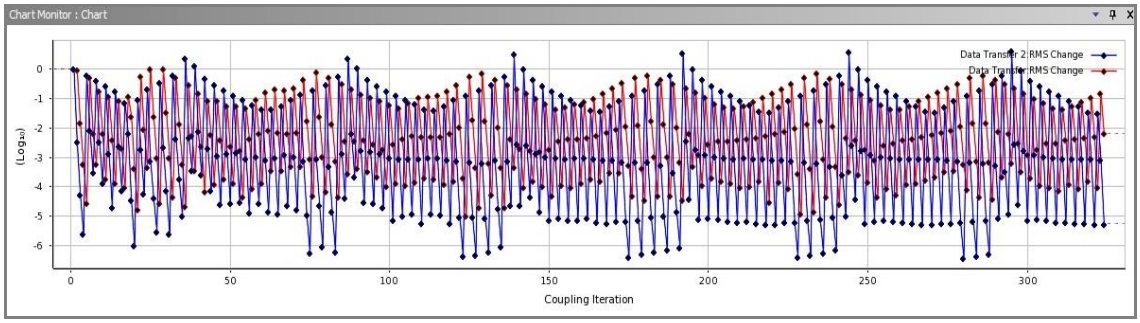

Figure C.3: Coupling Iteration.

```
Exchanging Data... done.

COUPLING STEP = 1        COUPLING ITERATION = 1

Updating solution at time level N... done.

Updating mesh at time level N...
Laplace mesh smoothing...
  iter         lms-u         lms-v         lms-w
     1   1.0000e+00    3.6361e-02    1.6882e-06
     2   3.7437e-02    2.3910e-03    6.1274e-08
     3   1.3511e-03    5.1859e-05    4.9768e-09
     4   5.4196e-05    3.5076e-06    6.3494e-11
done.
  iter continuity x-velocity y-velocity z-velocity     time/iter
     1 1.0000e+00 3.6789e-02 2.5803e-03 0.0000e+00  0:00:04    4
     2 6.1610e-01 1.8739e-02 6.6077e-03 0.0000e+00  0:00:03    3
     3 3.4367e-01 5.7175e-03 3.1464e-03 0.0000e+00  0:00:02    2
     4 2.0487e-01 2.6784e-03 1.5565e-03 0.0000e+00  0:00:01    1
     5 1.1924e-01 1.4167e-03 8.7286e-04 0.0000e+00  0:00:00    0
Flow time = 0.10000000149011611s, time step = 1

Exchanging Data... done.

COUPLING STEP = 1        COUPLING ITERATION = 2
  iter continuity x-velocity y-velocity z-velocity     time/iter
     5 1.1924e-01 1.4167e-03 8.7286e-04 0.0000e+00  0:00:04    5

Updating mesh at iteration...
Laplace mesh smoothing...
  iter         lms-u         lms-v         lms-w
     1   1.0000e+00    3.6369e-02    1.4104e-06
     2   3.7770e-02    2.3978e-03    9.6481e-08
     3   1.4866e-03    5.3077e-05    1.4876e-09
     4   7.5582e-05    3.7849e-06    3.2613e-11
done.
     6 6.4804e-02 8.2691e-04 5.0774e-04 6.6115e-11  0:00:02    4
     7 3.7481e-02 4.0407e-04 2.7359e-04 3.5026e-11  0:00:01    3
     8 2.1123e-02 2.2409e-04 1.5125e-04 3.0115e-11  0:00:01    2
     9 1.1959e-02 1.2583e-04 8.4145e-05 2.6792e-11  0:00:00    1
    10 6.7332e-03 7.1170e-05 4.6727e-05 1.8634e-11  0:00:00    0
Flow time = 0.1s, time step = 1

Exchanging Data... done.

COUPLING STEP = 1        COUPLING ITERATION = 3
  iter continuity x-velocity y-velocity z-velocity     time/iter
    10 6.7332e-03 7.1170e-05 4.6727e-05 1.8634e-11  0:00:02    5

Updating mesh at iteration...
Laplace mesh smoothing...
  iter         lms-u         lms-v         lms-w
     1   1.0000e+00    3.6368e-02    1.7524e-06
     2   3.7764e-02    2.3977e-03    7.8748e-08
     3   1.4863e-03    5.3073e-05    1.2004e-09
     4   7.5641e-05    3.7814e-06    2.9026e-11
done.
    11 3.8677e-03 4.1659e-05 2.6613e-05 2.5284e-11  0:00:01    4
    12 2.1797e-03 2.2994e-05 1.4964e-05 1.7932e-11  0:00:01    3
    13 1.2149e-03 1.2975e-05 8.3592e-06 1.8446e-11  0:00:01    2
!   14 solution is converged
    14 6.7745e-04 7.3347e-06 4.7191e-06 1.7993e-11  0:00:00    1
Flow time = 0.1s, time step = 1

Exchanging Data... done.

COUPLING STEP = 1        COUPLING ITERATION = 4
  iter continuity x-velocity y-velocity z-velocity     time/iter
!   14 solution is converged
    14 6.7745e-04 7.3347e-06 4.7191e-06 1.7993e-11  0:00:01    5

Updating mesh at iteration...
Laplace mesh smoothing...
  iter         lms-u         lms-v         lms-w
     1   1.0000e+00    3.6369e-02    1.7409e-06
     2   3.7764e-02    2.3977e-03    7.7297e-08
     3   1.4863e-03    5.3073e-05    1.1762e-09
     4   7.5616e-05    3.7806e-06    2.8322e-11
done.
!   15 solution is converged
    15 3.8161e-04 4.1766e-06 2.7699e-06 2.0752e-11  0:00:01    4
Flow time = 0.1s, time step = 1

Exchanging Data... done.
```

Figure C.4: Sample part from Fluent's "Solution.trn" file.

```
================================================================================
================================================================================
+============================================================================+
|                                                                            |
|                    ANSYS System Coupling Service                           |
|                    Version 14.0,  Copyright 2011                           |
|                 (Build Info. - 14:42:13, Oct 25 2011)                      |
|                                                                            |
+============================================================================+
================================================================================
================================================================================


================================================================================
+============================================================================+
|                                                                            |
|                  Summary of System Coupling Setup                          |
|                                                                            |
+============================================================================+
================================================================================

+============================================================================+
|                       Analysis Information                                 |
+============================================================================+

General :
  Analysis Type          = Transient
  Unit System            = MKS

Initialization :
  Option                 = Program Controlled
                           (Starting from step/time equal to zero.)

Step :
  Option                 = Step Size
  Size                   = 0.1
  Minimum Iterations     = 1
  Maximum Iterations     = 20

Duration :
  Option                 = End Time
  Time                   = 10

+============================================================================+
|               Coupling Participant Information (2)                        |
+============================================================================+

+----------------------------------------------------------------------------+
| Participant: Structural                                                    |
+----------------------------------------------------------------------------+

General :
  Unit System            = MKS_STANDARD
  Type                   = CoSimulation
  Name                   = Solution

Summary of Coupling Regions (1)
Region : Fluid Solid Interface
  Internal Name          = FSIN_1
  Type                   = Surface

Summary of Coupling Variables (2)
Variable : Force
  Internal Name          = FORC
  Physical Type          = Force
Variable : Incremental Displacement
  Internal Name          = INCD
  Physical Type          = Length

Summary of Base Units (9)
  Angle                  = radian
  ChemicalAmount         = mol
  Current                = A
  Length                 = m
  Luminance              = cd
  Mass                   = kg
  SolidAngle             = sr
  Temperature            = C
  Time                   = s


+----------------------------------------------------------------------------+
| Participant: Fluid                                                         |
+----------------------------------------------------------------------------+

General :
  Unit System            = SI
```

Figure C.5: Sample part from System Coupling file.

Properties of Outline Row 3: Polyethylene

	A	B	C	D	E
1	Property	Value	Unit		
2	Density	950	kg m^-3		
3	Isotropic Secant Coefficient of Thermal Expansion				
4	Coefficient of Thermal Expansion	0.00023	C^-1		
5	Reference Temperature	22	C		
6	Isotropic Elasticity				
7	Derive from	Young's Modulus...			
8	Young's Modulus	1.1E+09	Pa		
9	Poisson's Ratio	0.42			
10	Bulk Modulus	2.2917E+09	Pa		
11	Shear Modulus	3.8732E+08	Pa		
12	Tensile Yield Strength	2.5E+07	Pa		
13	Compressive Yield Strength	0	Pa		
14	Tensile Ultimate Strength	3.3E+07	Pa		
15	Compressive Ultimate Strength	0	Pa		

Figure C.6 Material properties for pipe structure.

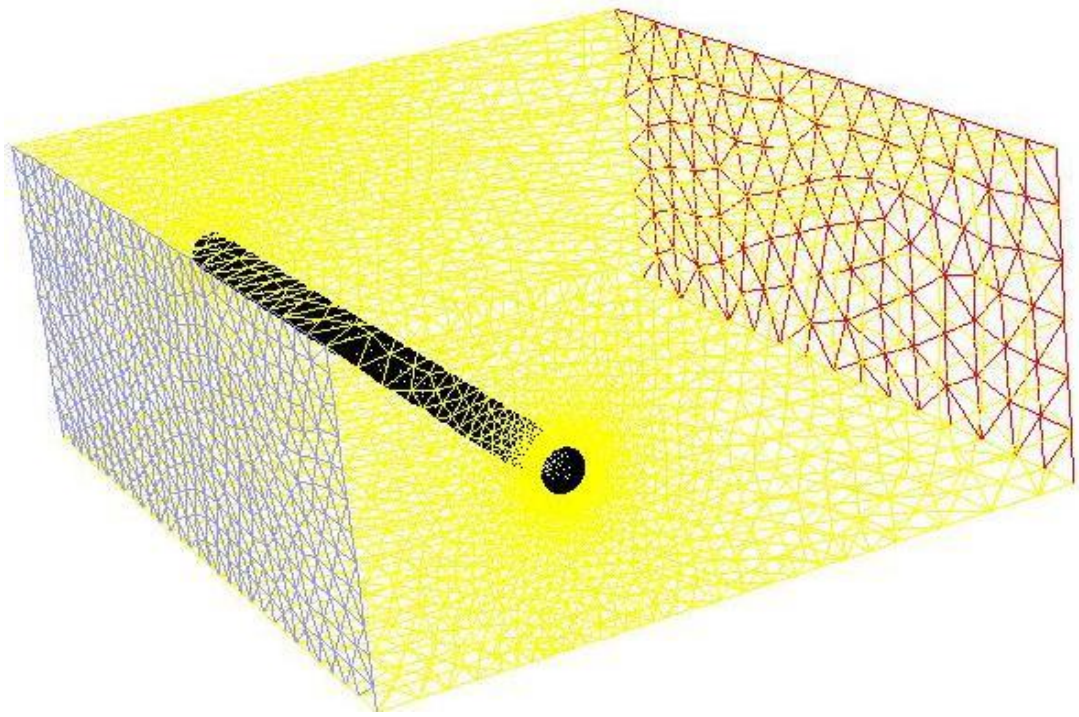

Figure C.7 Defined mesh structure.

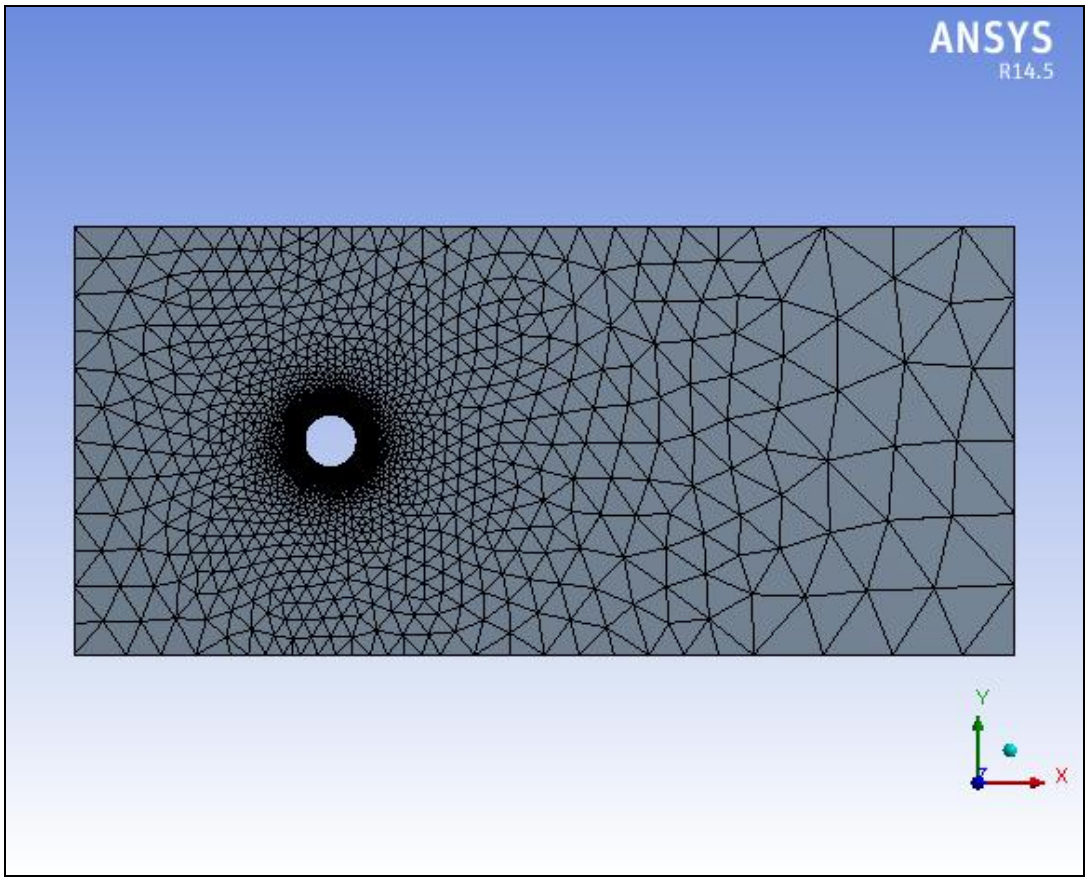

Figure C.8 Defined mesh structure (2D view).

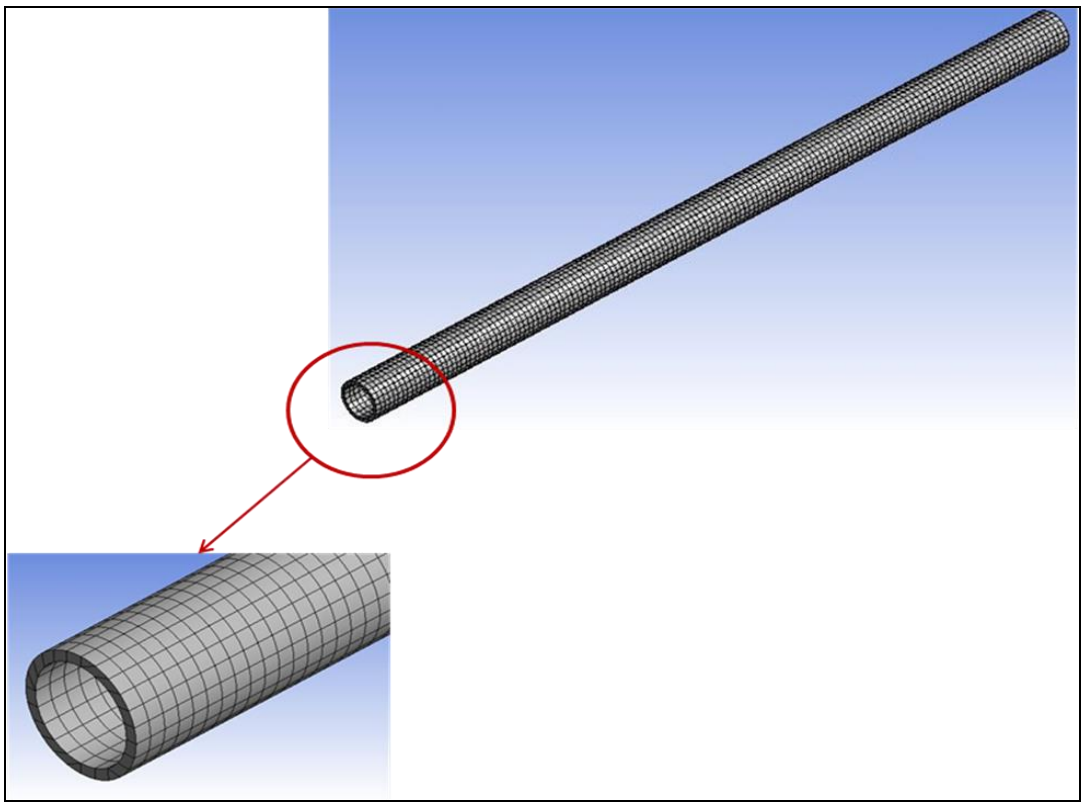

Figure C.9 Mesh structure for pipe element.

APPENDIX D: Numerical Model Results and Diagrams

Below are the results from numerical models and their visual representations.

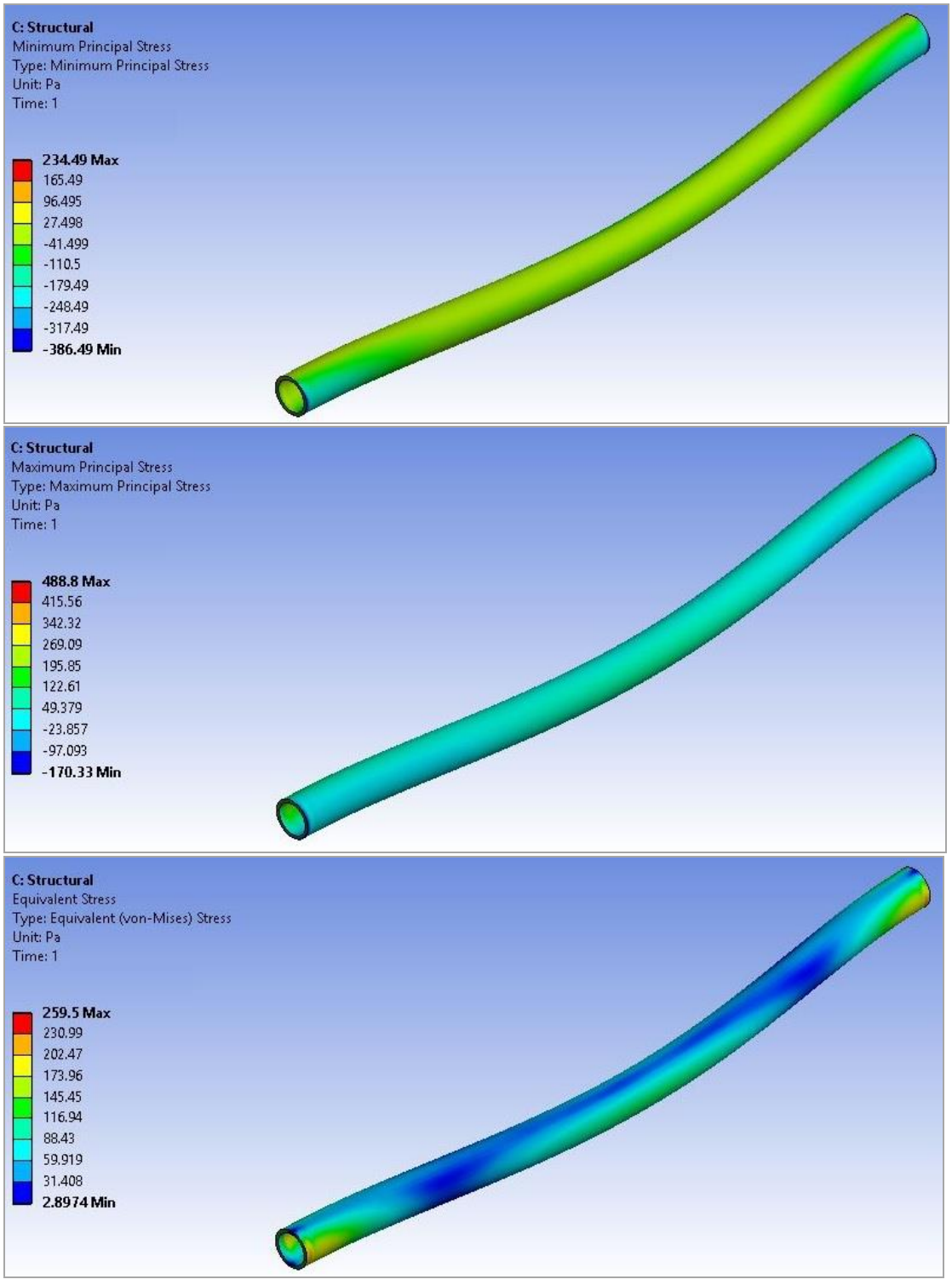

Figure D.1: Results for pipe element.

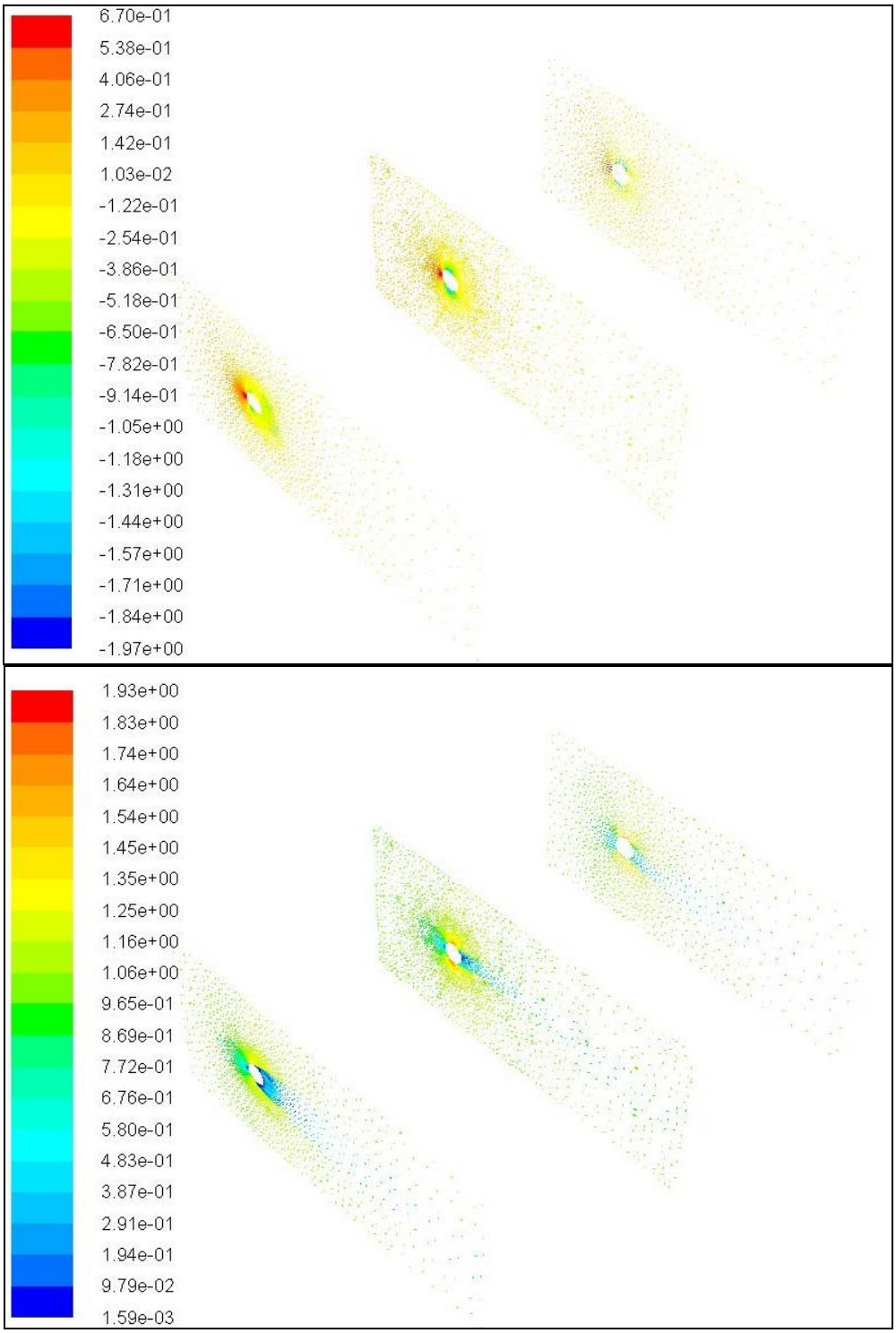

Figure D.2: Flow characteristics around the pipe in near supports and in the middle of span (Velocity vectors colored by velocity magnitude (m/s)).

CURRICULUM VITAE

Name Surname: Uğur Çalışkan

Place and Date of Birth: Diyarbakır – 25-05-1980

Address: Istanbul-Turkey

E-Mail: caliskan_ugur@yahoo.com

B.Sc.: Yildiz Technical University - Civil Engineering (1999-2004)

M.Sc.: Istanbul Technical University - Hydraulic and Water Resources Engineering (2004-2007)

Professional Experience and Rewards:

2009 ~ ENET Engineering, Civil Engineer (Design Engineer, MSc)

2005 ~ 2008 EMAY International Engineering, Civil Engineer

List of Publications and Patents:

Publications/Presentations On The Thesis

▪ **Caliskan, U.** and Avci, I (2014). Investigation and Analysis of Undersea Natural Gas PE Pipelines Against Steady Current Effects, EEST Part A, Energy Science and Research, 32(1), 625-632.